Assessment of steel-concrete shear connector system with resin injected bolts

Master's Thesis

Alkyoni Sarri

Faculty of Civil Engineering and Geosciences

Delft University of Technology

April 2019, Delft

TU Delft

Assessment of steel-concrete composite shear connector system with resin injected bolts

By

Alkyoni Sarri

in partial fulfilment of the requirements for the degree of

Master of Science

in Civil Engineering

at the Delft University of Technology,

to be defended publicly on Tuesday April 9, 2019 at 11:00 AM.

Supervisor:	Prof.dr.	M. Veljkovic	TU Delft
Thesis committee:	Dr.ir.	R. Abspoel	TU Delft
	Ir.	M.P. (Martin) Nijgh	TU Delft
	Ir.	Lagendijk	TU Delft

TU Delft

Preface

This thesis is made as a completion of my master degree in Structural Engineering at the faculty of Civil Engineering and Geosciences at Delft University of Technology, the Netherlands.

The members of my assessment committee that guided me through my research work consist of professor dr. M. Veljkovic, dr. ir. R. Abspoel, ir. M.P. Nijgh, ir. P. Lagendijk from Delft University of Technology. I would like to express my gratitude to my assessment committee members, especially my supervisor ir. M.P. Nijgh, for their professional guidance, valuable support and critical comments throughout my thesis period that contributed to the completion of my thesis.

I would also like to thank the laboratory staff that helped me with the execution of my experiments.

Finally, I would like to thank my family and friends for being helpful, supportive and for inspiring me to follow my dreams and never give up during my master period.

Abstract

The building and construction sector play a key role in achieving a sustainable development. In European countries, buildings are responsible for 40-45% of energy consumption, leading to significant amounts of CO_2 emissions. The implementation of reusable structures lead to less waste and harmful emissions to the environment. The main purpose of this thesis is to analyse and evaluate the use of a new type of demountable shear connectors, resin injected bolts, in steel-concrete composite structures through push-out tests.

Steel-concrete composite structures are commonly used in flooring systems of offices, car parks and bridge decks throughout the world. The most widely used shear connectors are welded headed studs. Even though they are inexpensive and extended research has been conducted about their application, welded headed studs do not allow for the demountability and reusability of the structural components.

An innovative type of shear connector consists of a coupler and a bolt which are embedded in the prefabricated concrete deck. The assembly of the concrete deck with the flange of the steel section which has oversized holes is achieved through resin injected bolts. Resin injected bolts are bolts in which the cavity formed by the clearance between the bolt and the hole is filled up with resin. Large hole clearances allow for fabrication tolerances and lead to a faster execution.

Push-out tests were conducted in the laboratory in order to examine resin injected bolts in terms of shear capacity, stiffness and ductility. Two different test configurations were created, one with resin injected bolts and the other one with reinforced resin injected bolts. For each configuration three specimens were tested which were nominally identical, one was loaded until failure using displacement control and the other two were loaded initially in force-controlled load cycles and then until failure. The results obtained from the experiments are compared with the results from researches conducted on other types of demountable shear connectors.

FEA models were developed with the same geometry, materials and loading as in experiments using the ABAQUS software and push-out test were performed in order to check the validity of the experimental work. In addition, a parametric study was conducted using FEA in order to evaluate the influence of certain parameters on shear resistance and stiffness. The parameters considered are: the concrete strength class, the bolt diameter, the bolt strength class, the embedded bolt height, the hole diameter of the steel section, the effect of the L-angle profile and the injection material.

Contents

List of Figures

List of Tables

1 Introduction

1.1 Problem definition

Steel-concrete composite structures are widely used throughout the world. Composite construction using steel and concrete started in the 1920s and in 1950s was mostly used for bridges and in multi-storey buildings [38]. The main advantage of composite structures is that the properties of each material can be combined to form one unit which has a better performance than its separate parts. In case of steel-concrete structures, concrete behaves well in compression and steel in tension, so their combination leads to a highly efficient design. Moreover, at high temperatures concrete provides corrosion protection and thermal insulation to the steel and also restrains slender steel parts from local or lateral torsional buckling. In case of composite behaviour, load capacity and stiffness increase. Steel-concrete composite action is mostly applied in multi-storey buildings and bridges where steel beams are combined with concrete floor slabs and concrete decks in multi-storey buildings and bridges respectively.

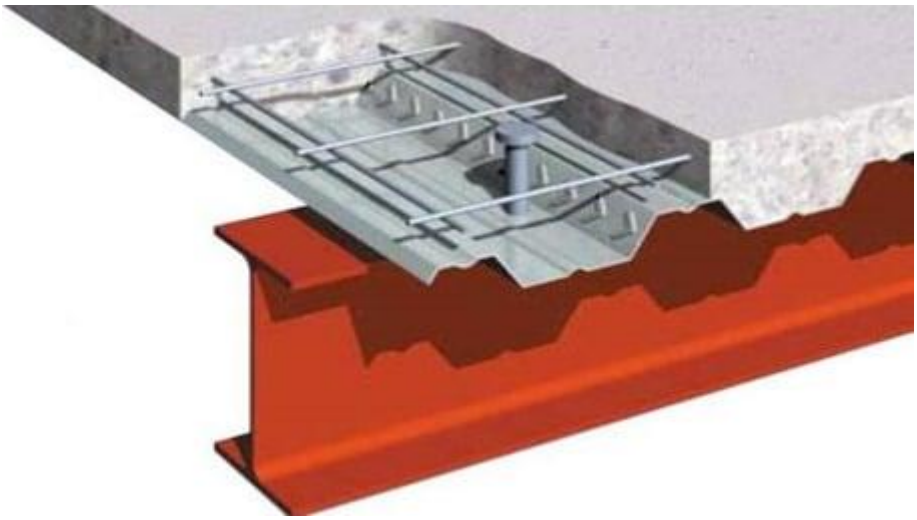

Figure 1.1: Steel-concrete shear connection [32]

The longitudinal shear force in steel-concrete interface is transferred through shear connectors. The shear connectors allow the transfer of forces between steel and concrete and resist vertical uplift forces at their interface. There are many different types of shear connectors but the most used ones are welded headed studs. A reason why studs are widely used is that extended research about their application has been conducted and many design rules in many codes can be found.

A disadvantage of welded headed studs is that demountability and reusability of the structural components is very difficult. The main reason of this is that studs are welded to the steel beam and embedded in concrete. So the separation of the steel beam from the concrete slab and the reusability of the parts is not possible.

In recent years there is an international interest in circular economy, an economy in which materials and products can be reused. This leads to less waste and harmful emissions to the

environment. The construction industry is responsible for the highest percentage of total waste in the world [9]. Recycling and reusability of the structural components after their working life instead of disposal is of high importance. Although many efforts have been made regarding the recycling of construction materials, reusability is considered more beneficial because less energy usage is required compared to recycling.

Research for possible reuse of components and deconstruction techniques in the construction domain have been carried out in order to reduce the economic and environmental costs. Therefore, an extended research on demountable shear connectors instead of welded headed studs as shear connectors has been conducted the last years in order to investigate their structural behaviour and possibilities of reusability of the components. There are many different types of demountable bolted shear connectors some of which are depicted in figure 1.2. These type of shear connectors are analysed in Chapter 2.

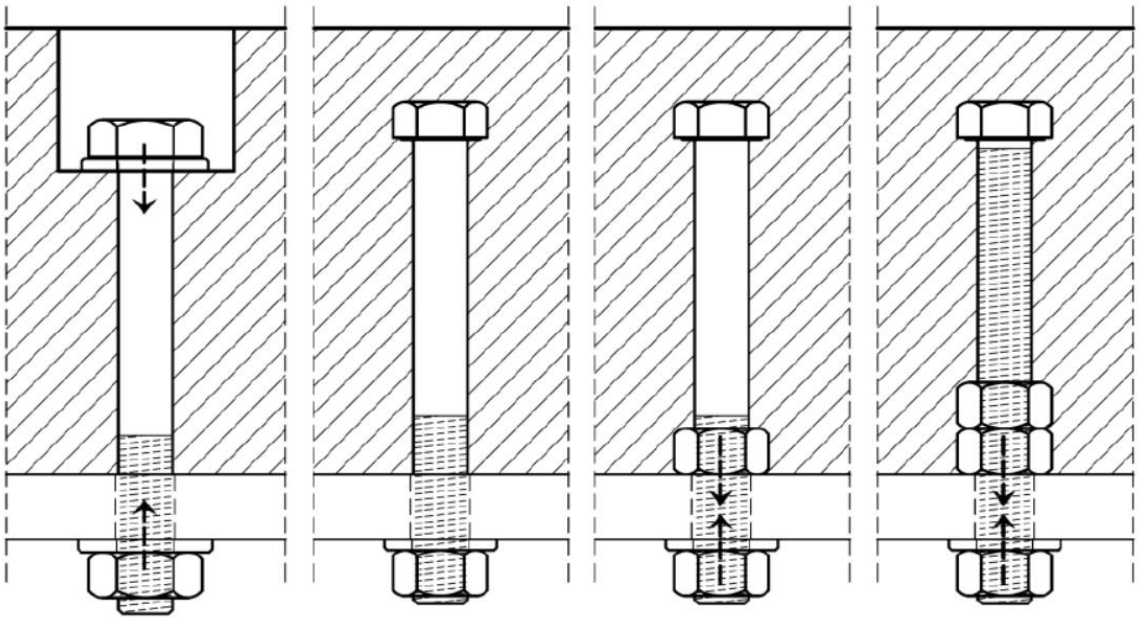

a) Friction grip bolts b) Bolts without embedded nut c) Single embedded nut bolt d) Double embedded nut bolt

Figure 1.2: Demountable bolted shear connectors [42]

1.2 Research questions

The main aim of this thesis is to investigate the behaviour of an innovative type of demountable shear connector, resin injected bolts, in composite structures. The following research questions will be answered in this thesis:

- What is the behaviour of the shear connector system with resin injected bolts in terms of shear capacity and stiffness?
- What are the failure modes of the shear connector system with resin injected bolts?
- How does different parameters influence the behaviour of the shear connector system?

- Concrete strength class
- Bolt diameter
- Bolt strength class
- Embedded bolt height
- Hole diameter of the steel section
- Detailing of the deck
- Injection material

1.3 Methodology of the research

Literature study is performed to present current state of the art on demountable shear connectors and resin injected bolts.

Experimental work is performed, the push-out tests, in order to examine the behaviour of resin injected bolts in terms of shear capacity, ductility and stiffness. These results are compared with the results derived from other types of shear connectors.

Finite element models of push-out tests are built, validated and compared with the experimental push-out tests.

A parametric study is conducted in order to examine the influence of different parameters on the behaviour of the shear connector system.

1.4 Outline of the thesis

This thesis is organized in seven chapters:

Chapter 1 provides a general introduction of the topic and presents the research objectives and methodology of the thesis.

Chapter 2 presents the state of the art for various demountable shear connectors and focuses on resin injected bolted connections.

Chapter 3 describes the experimental set-up and procedure and presents the results of the push-out tests under static loading. These results are compared with the results derived from the experimental work conducted on other types of shear connectors.

Chapter 4 presents the results of push-out tests of Finite Element models. The models have the same geometry, properties and loading conditions as the experimental specimens. The results are compared with the results of the push-out tests conducted in the lab.

Chapter 5 presents the results of a parametric study conducted in order to examine the influence of concrete strength class, bolt strength class, bolt diameter, embedded bolt height, hole diameter of the steel section, detailing of the deck and injection material on the behaviour of the shear connection with resin injected bolts.

Chapter 6 provides the main conclusions of the research conducted and recommendations for future work.

2 Literature review

Steel-concrete composite action permits the steel section and the concrete slab to act more efficiently compared to the non-composite condition. The composite action is achieved by the means of mechanical shear connectors that allow the transfer of forces and resist the vertical separation at the interface of the two materials. Welded headed studs shear connectors have been developed in the past but the need for reusability and demountability of the structural components has led to the research of new types of shear connectors. In this section, the outcomes of the research on demountable shear connectors are presented and attention is paid on resin injected bolts.

2.1 Push-out procedure

Eurocode 4 Annex B provides a detailed procedure for performing push-out tests in order to examine the shear capacity of welded shear connectors [17]. However, this procedure described in Eurocode 4 is for welded headed studs in solid slabs made of concrete. Push-out tests are used instead of full scale tests as they have lower cost and require less time. The specimen consists of two reinforced concrete slabs and a steal section connected with welded headed studs. The concrete slabs should be cast in the horizontal position and cured in open air. The specimen is loaded in increments up to 40% of the expected failure load and then is loaded in 25 cycles of 40% of the expected failure load. The specimen layout is depicted in figure 2.1.

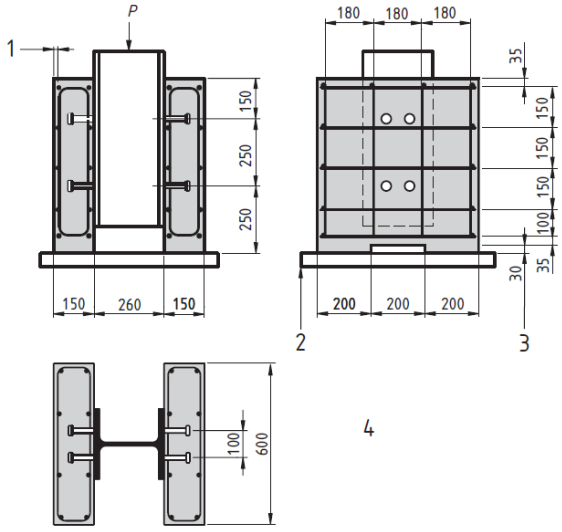

Key

1 cover 15 mm

2 bedded in mortar or gypsum

3 recess optional

4 reinforcement: ribbed bars ϕ 10 mm resulting in a high bond with $450 \leq f_{sk} \leq 550$ N/mm^2
steel section: HE 260 B or 254 x 254 x 89 kg. UC

Figure 2.1: Push-out test layout according to Eurocode 4 [17]

The characteristic resistance is taken as the minimum failure load per shear connector with a reduction of 10%. Ductility is also important in composite structures. The ductility of a shear connector can be derived from push-out tests and it depends on the slip capacity in the steel section-concrete slab interface. The slip capacity is the maximum slip that corresponds to the characteristic resistance and is depicted in figure 2.2. The characteristic slip capacity is equal to the slip capacity reduced by 10%. According to Eurocode, in order to consider a shear connector as ductile the slip to failure should be larger than 6 mm. In case slip to failure is smaller than 6 mm the shear connector is considered as brittle.

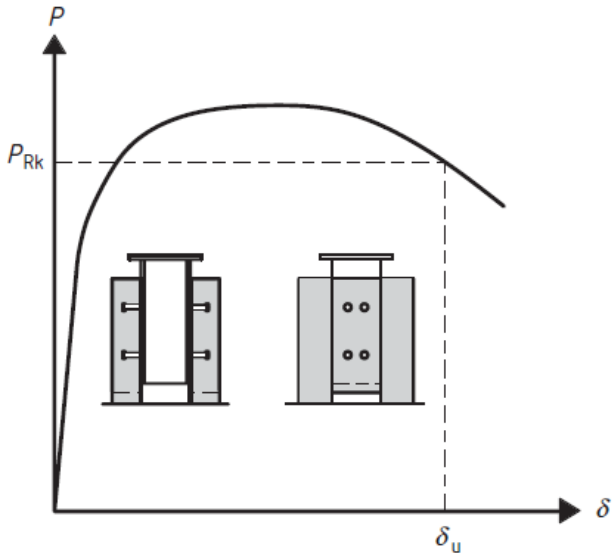

Figure 2.2: Slip capacity determination according to Eurocode 4 [17]

2.2 Welded headed studs

Welded headed studs are the most commonly used shear connectors in construction industry. One of the reasons is the large availability of design rules in design codes. These shear connectors are welded to the steel section with a stud welding system before casting the concrete slabs in order to provide shear connection in terms of strength and fatigue. A typical welded headed stud is depicted in figure 2.3.

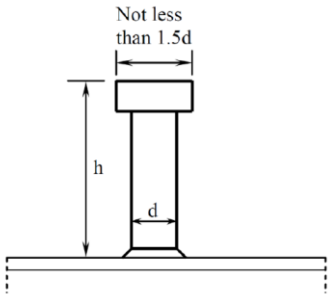

Figure 2.3: Welded headed stud layout [46]

Eurocode 4 Annex B provides a detailed procedure for performing push-out tests in order to examine the behaviour of welded headed studs [17]. According to Eurocode 4 the design

resistance of welded headed studs is the minimum value of the equations 2.1 and 2.2, related to concrete cone failure and shear failure of the bolt, respectively.

$$P_{Rd} = 0.8 \cdot f_u \cdot \frac{\pi . d^2}{4} \cdot \frac{1}{\gamma_v} \quad (2.1)$$

$$P_{Rd} = 0.29 \cdot \alpha \cdot d^2 \cdot \sqrt{f_{ck} \cdot E_{cm}} \cdot \frac{1}{\gamma_v} \quad (2.2)$$

With $\alpha = 0.2 \cdot (\frac{h_{sc}}{d} + 1)$ for $3 \leq h_{sc}$ and $\alpha = 1$ for $h_{sc}/d > 4$

d: the diameter of the shank of the shear connector (mm), $16 \leq d \leq 25$ mm

f_u: the ultimate tensile strength of the material of the shear connector (N/mm^2), $f_u \leq 500$ N/mm^2

f_{ck}: the characteristic cylinder compressive strength of the concrete at the age considered of density more than 1750 kg/m^3

h_{sc}: the overall height of the shear connector (mm)

γ_v: the partial safety factor, γ_v = 1.25

A comprehensive experimental study on welded headed studs using push-out tests was performed by Ollgaard (1971) [38]. He performed a series of push-out tests using 48 specimens with welded headed studs with diameters of 16 and 19 mm embedded in a solid slab made of concrete. The ultimate strength of welded headed studs under static load was evaluated in the testing and it was concluded that the ultimate strength depends on the compressive strength and modulus of elasticity of concrete.

The research results on push-out tests performed the past few decades on welded headed studs was summarized by Pallares and Hajjar (2010) [39]. Nowadays, due to the large database of experimental results, the research on welded headed studs is performed using Finite Element Analysis. Lam and El-Lobody in 2005 developed a model using FEA in order to examine the behaviour of welded headed studs using different headed stud heights and concrete strengths [30].

2.3 Demountable shear connectors

2.3.1 Friction grip bolts

Friction grip bolts transfer the shear forces in the concrete slab-steel flange interface through friction. The friction in the steel-concrete interface is achieved by preloading of the bolt through the thickness of the concrete slab. This leads to high compression stresses on the concrete slab, so helical reinforcement is used around the bolt hole to strengthen the slab. This type of shear connectors is very beneficial in preventing fatigue effects due to repeated loading. Moreover, their construction is easy and they provide high rigidity. However, long term effects such as shrinkage and creep need to be taken into account at serviceability limit state. Friction grip bolts are high strength bolts with grade from 8.8 to 10.9 and standard diameter.

The first experimental attempt to examine the performance of bolted shear connectors in steel-concrete structures was made by Dallam (1968) [11]. Dallam performed push-out tests in order to investigate the performance of high strength friction grip bolts. High strength grip bolts ASTM A325 and A449 with diameters 12.7 15.9 and 19.1 mm and height above the flange h_{sc}=102 mm were used in the tests. The test set-up is depicted in figure 2.4.a. Four bolts were erected over the steel profile with the use of wire springs as depicted in figure 2.4.b. The concrete was poured over the steel profile and after hardening, the nuts were tightened from below the slab.

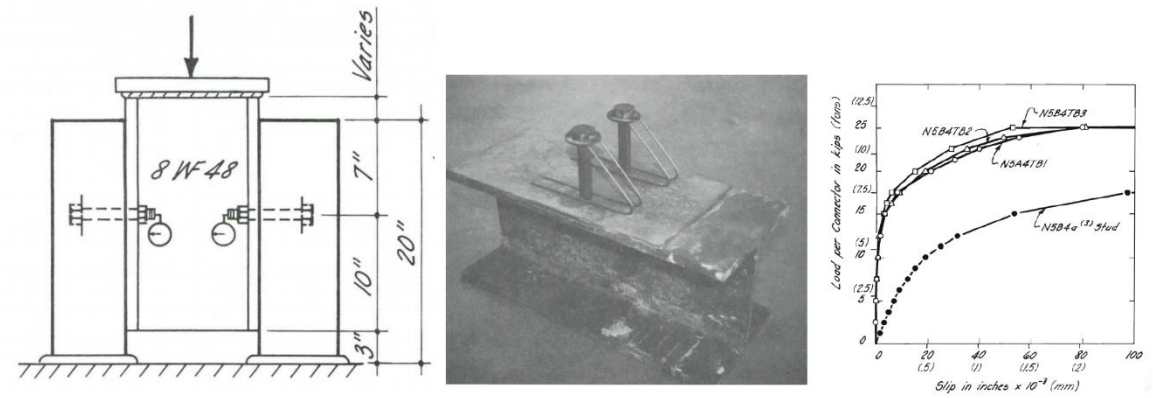

a) Test set-up b) Installation of bolts c) Force-slip curve

Figure 2.4: Friction grip bolts push out test (Dallam 1968) [11]

The force per shear connector-slip curve for the bolts ASTM A449 with diameter d=15.9 mm is depicted in figure 2.4.c and compared with the curve of welded headed studs with the same diameter. At the serviceability limit stage the slip is zero and the ultimate shear strenght is nearly double of that of welded headed studs.

The behaviour of friction grip bolts in composite structures was also investigated by Marshall (1971) with the performance of push-out tests [33]. He conducted 11 tests with friction grip bolts of diameter d=16 mm. The concrete slabs were casted either in situ or they were prefabricated and their cube strength varied from 36 to 50 MPa. Before the tests the bolts were preloaded in order to achieve a friction coefficient of 0.45. The test set-up is depicted in figure 2.5.a.

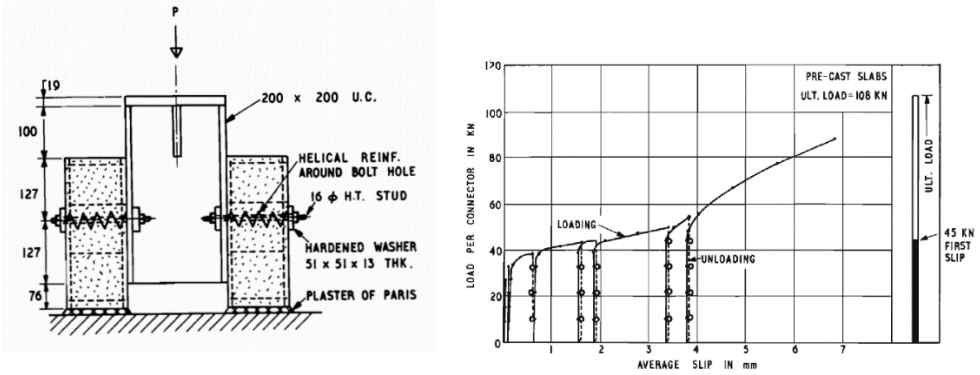

a) Test set-up b) Force-slip curve

Figure 2.5: Friction grip bolts push out test (Marshall 1971) [33]

The force per shear connector-slip curve of one of the specimens with precast concrete slabs is depicted in figure 2.5.b. The failure mode of all tests was shear failure of the bolts except one that the failure mode was crushing of concrete. However, after the test in the area of the base of the connector the concrete was crushed in all specimens. The ultimate load per shear connector varies from 100 to 122 kN and the average is 114 kN. The slip in steel-concrete interface varies from 41 to 63 mm and the average is 50.2 mm which indicates a very ductile behavior according to Eurocode.

The behaviour of friction grip bolts as post installed shear connectors in existing non-composite bridges was examined by Kwon (2008) who performed single bolt shear tests under static and fatigue loading [27]. The specimens consisted of a steel plate with thickness of 25.4 mm that represents the top flange of a steel beam being on top of a concrete block that represents the concrete bridge deck as depicted in figure 2.6.a. ASTM A325 friction grip bolts were used in the push-out tests with diameter d=22 mm and height above the flange h_{sc}=127 mm as depicted in figure 2.6.b. The bolts were preloaded with a force of 175 kN.

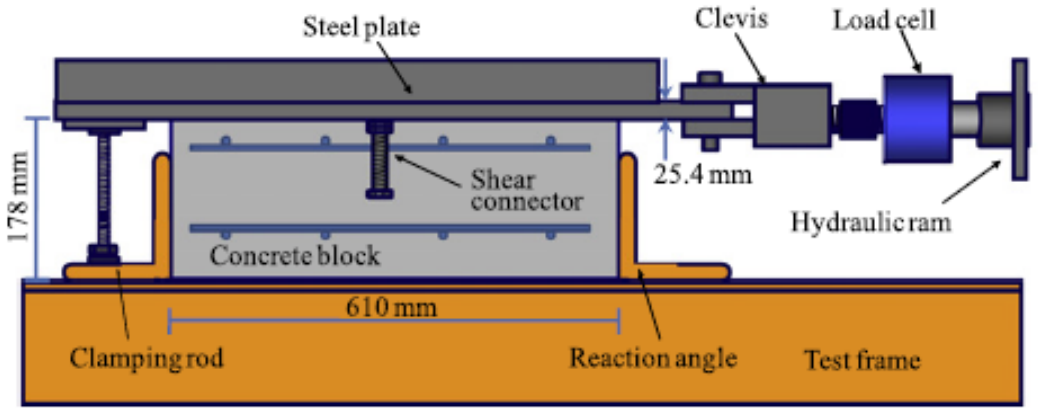

a) Test set-up

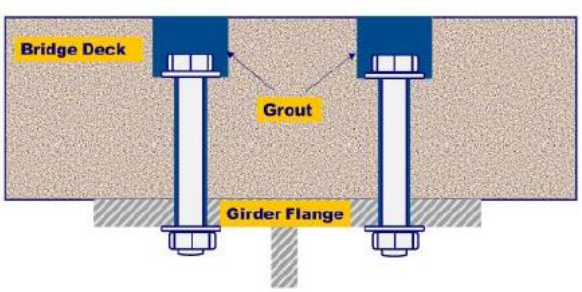

b) Shear connection layout

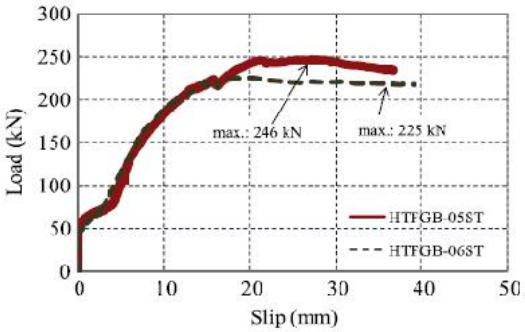

c) Force-slip curve

Figure 2.6: Friction grip bolts push out test (Kwon 2008) [27]

Two specimens were tested. The force per shear connector-slip curve obtained by the test is depicted in figure 2.6.c. The average ultimate strength per shear connector is 235 kN and the average ultimate slip is 37.9 mm. The stiffness is high at low levels of load because the shear is transferred through friction under loading. One of the specimens failed due to fracture of the bolt while the other one failed due to crushing of concrete. From Kwon's research it can be

concluded that ASTM A325 friction grip bolts is a reliable solution to convert a non-composite bridge into a composite one.

Two push-out tests according to Eurocode 4 Annex B using friction grip bolts M20 of grade 8.8 were conducted by Lee and Bradford (2013) [31]. The bolds were preloaded with a force of 145 kN. Geopolymer concrete was used as it leads to less CO_2 emissions to the environment with concrete strength of 48 MPa at 90 days. The specimen set-up is depicted in figure 2.7.a.

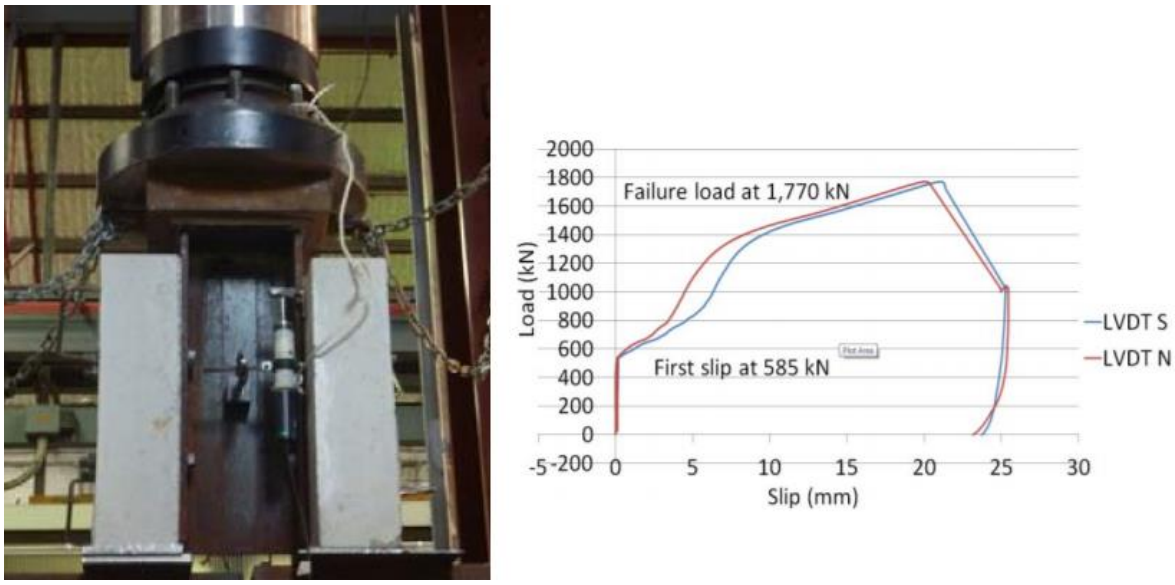

a) Test set-up b) Force-slip curve

Figure 2.7: Friction grip bolts push out test (Lee and Bradford 2013) [31]

Force-slip curve of the one push-out test is depicted in figure 2.7.b. The failure mode of both specimens was fracture of the bolts. There were no apparent cracks in concrete after the test. The ultimate force per shear connector is 207.6 kN. The average ultimate slip to failure is 20 mm which indicates a very ductile behaviour of the bolts.

2.3.2 Bolts with embedded nuts

Embedded bolted shear connectors can have one or two nuts and their behaviour as shear connectors is similar. The shear forces are transferred by the shear in the thread of the bolt and bearing in hole. The embedded nut increases the stiffness compared to the use of bolts without embedded nut.

The use of bolts with single embedded nut as shear connectors in rehabilitation work of existing bridges and other structures was investigated by Dedic and Klaiber (1984) [12]. They performed four push-out tests using ASTM A325 strength bolts with embedded nut and diameter d=19 mm as depicted in figure 2.8.a.

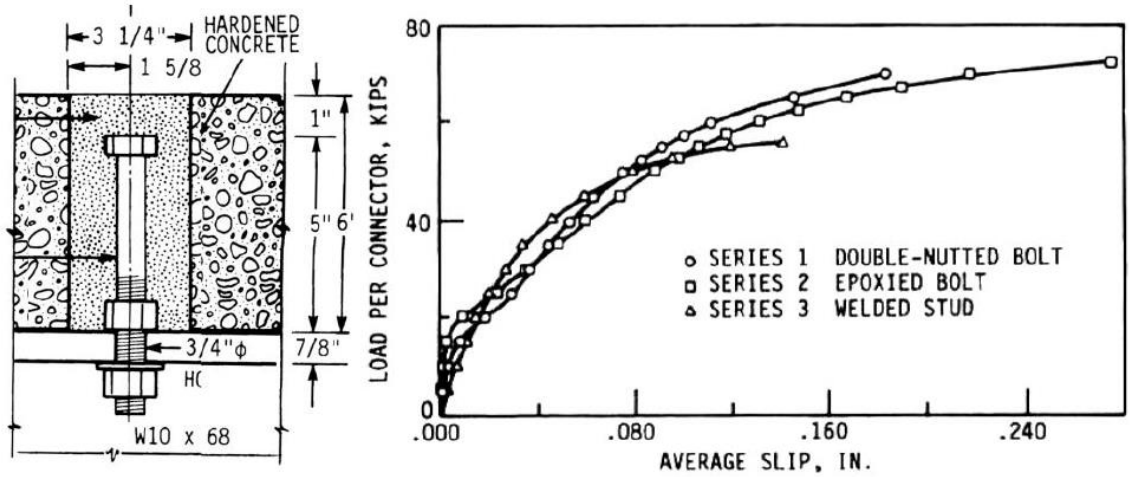

a) Shear connection layout b) Force-slip curve

Figure 2.8: Single embedded nut bolts push-out test (Dedic and Klaiber 1984) [12]

The force per shear connector-slip curve is depicted in figure 2.8.b. All specimen failed due to shear failure of the bolts. The average ultimate shear force was 152.1 kN. Compared to welded headed studs, bolted shear connectors with single embedded nut have a similar behaviour in terms of shear resistance and force-slip behaviour.

The behaviour of bolted shear connectors with double embedded nuts in existing non-composite bridges was investigated by Kwon (2008) [27]. The bolts used in the push-out tests had diameter d=22 mm and height above the flange h_{sc}=127 mm. The specimens consisted of a steel plate with a thickness of 25.4 mm placed on top of a concrete block. The bolts were installed in the concrete blocks in a way to represent real construction conditions. Firstly, a hole with diameter of 57 mm was drilled in concrete with the use of a rotary drilled hummer. A hole with diameter of 57 mm was also drilled in steel plate with the use of a portable drill. The shear connector was placed on the plate with a single nut below and two nuts above the plate. The bolts were preloaded with a force of 175 kN. Lastly the concrete block was placed above the steel plate and the hole was filled with grout. The shear connection layout is depicted in figure 2.9.a.

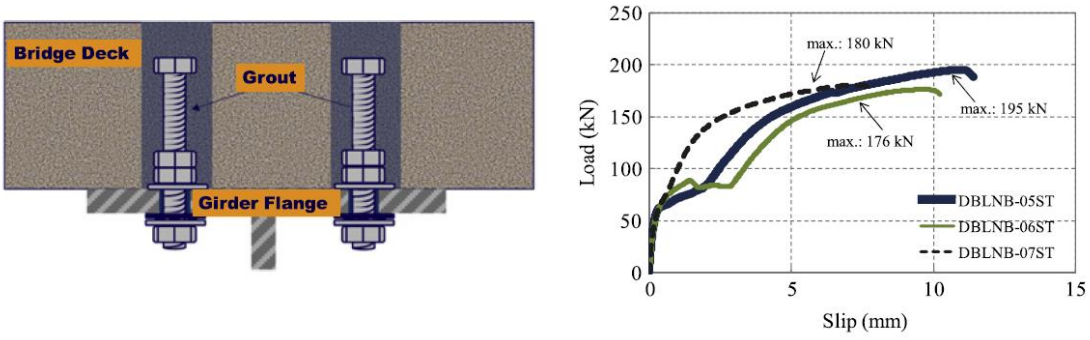

a) Shear connection layout b) Force-slip curve

Figure 2.9: Double embedded nut bolts push-out test (Kwon 2008) [27]

The force per shear connector-slip curve is depicted in figure 2.9.b. All specimens failed due to shear failure of the bolts. The average ultimate strength was 183 kN and the average ultimate slip was 9.9 mm. In the elastic region the stiffness was high because of the embedded nuts in concrete that led to an increase of the bearing surface between bolts and concrete.

Lee and Bradford (2013) conducted two push-out tests according to Eurocode 4 Annex B using bolts M20 of grade 8.8 with single embedded nut and height above the flange h_{sc}=135 mm [31]. The test set-up is depicted in figure 2.10.a. The bolds were preloaded with a force of 130 kN. Geopolymer concrete was used with concrete strength of 48 MPa at 90 days.

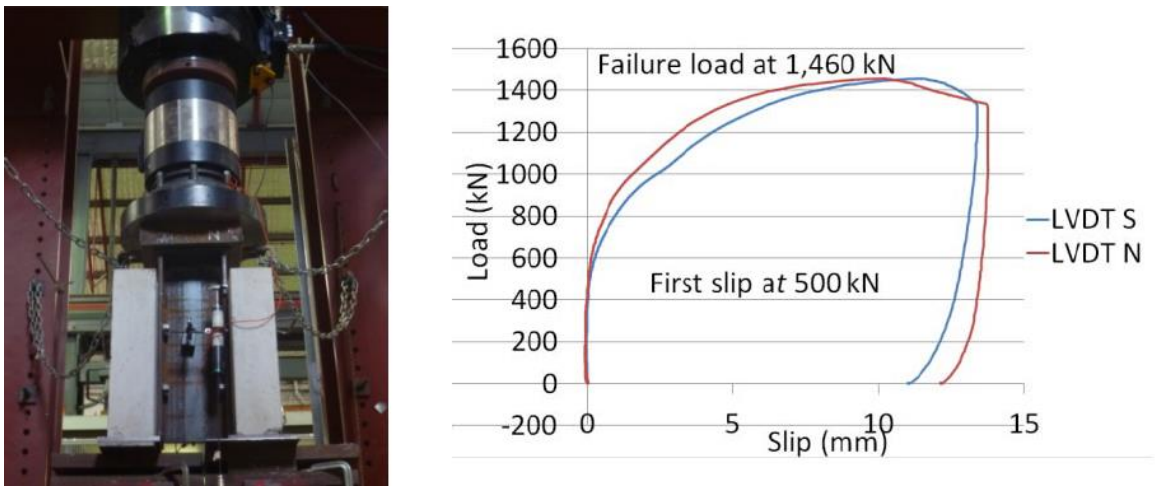

a) Test set-up b) Force-slip curve

Figure 2.10: Single embedded nut bolts push-out test (Lee and Bradford 2013) [31]

Force-slip curve of the one push-out test is depicted in figure 2.10.b. The failure mode of both specimens was shear failure of the bolt and concrete shear cracks. The average ultimate strength is 177.5 kN and the average ultimate slip is 11 mm.

Push-out tests in order to examine the behaviour of bolted shear connectors were conducted also by Pavlovic (2013) and a comparison was made with welded headed studs [42]. The specimens were consisted of steel section type I, prefabricated concrete slabs with standard reinforcement layout and the shear connectors. He used bolted shear connectors with single embedded nut with diameters M16 and M24, grade 8.8 and height above the flange h_{sc}=105 mm. The test set-up is depicted in figure 2.11.a. The properties of the materials used in the push-out tests were determined by tests. The results for the welded headed studs were obtained from push-out tests conducted by Spremic according to which the bolt diameter was d=16 mm and the height above the flange h_{sc}=100 mm. The tests were executed according to Eurocode 4-Annex B and the resulted force-slip curves are shown in figure 2.11.b.

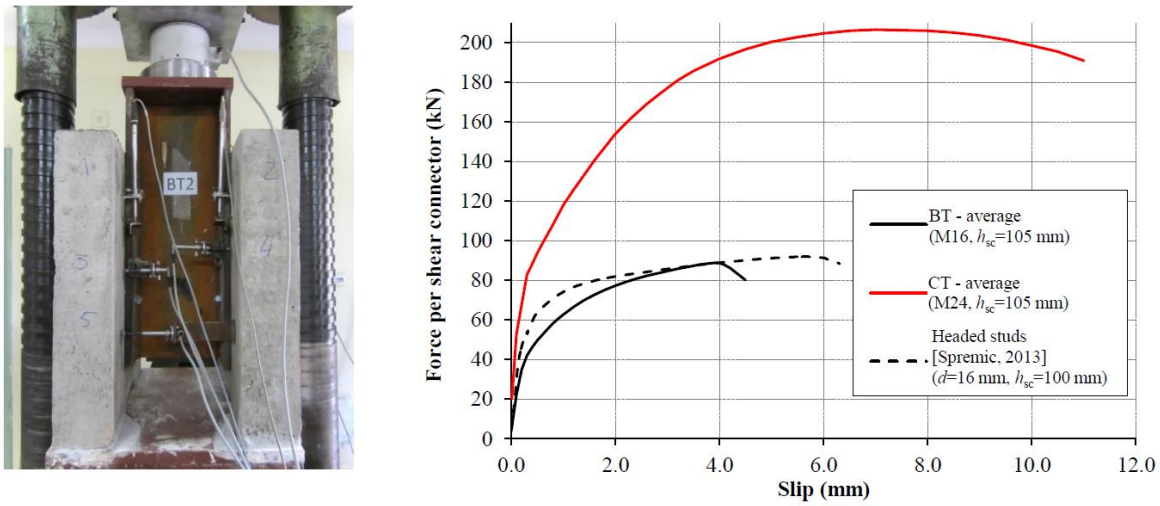

a) Test set-up b) Force-slip curve

Figure 2.11: Single embedded nut bolts push-out test (Pavlovic 2013) [42]

All the specimens with bolts M16 failed due to fracture of the bolts at the steel flange-concrete interface and not significant cracking of concrete was observed. In this case the ultimate slip is 4.5 mm, so bolted shear connectors M16 with single embedded nut have a brittle behaviour according to Eurocode 4-1-1 because the slip is smaller than 6 mm. All the specimen with bolts M24 failed due to concrete crushing. In case of bolted shear connectors M24 with single embedded nut the slip is 13.4 mm, which is higher than 6 mm so they have a ductile behaviour.

M16 bolted shear connectors with single embedded nut achieved 95% of the shear resistance of welded headed studs under static loading. However, M16 bolted shear connectors with single embedded nut achieved only 50% of the stiffness of welded headed studs. Moreover, it was concluded that the bolt preloading force F_p and the number of embedded nuts does not influence neither the ductility nor the shear resistance of the shear connection.

A parametric study was also conducted in order to examine the influence of certain parameters on the shear resistance and ductility of the bolted shear connection. It was concluded that the bolt diameter, the concrete strength and the height of the shear connector had the most significant influence on resistance and ductility.

2.3.3 Bolts without embedded nuts

Push-out tests similar to the test set-up described in Eurocode 4-Annex B were conducted by Lam (2013) in order to investigate the behaviour of demountable shear connectors without embedded nut and compared the results to welded headed studs [28]. The test set-up consisted of a steel beam with short length connected to two concrete slabs with dimensions 300*300*150 mm. Four shear connectors were used to connect the concrete slabs to the steel beam. The bolts' layout is depicted in figure 2.12.a. Eight push-out tests were performed with different concrete strengths and bolt diameters.

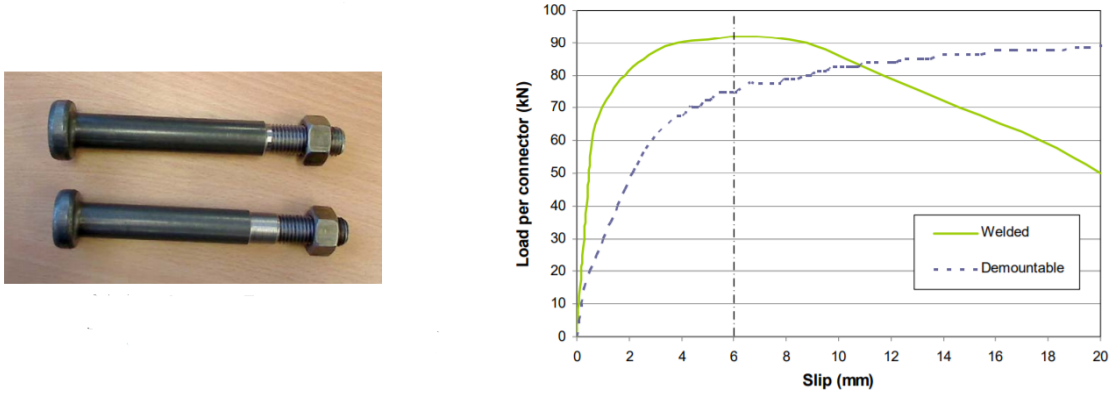

a) Bolts layout b) Force-slip curve

Figure 2.12: Bolts without embedded nut push-out test (Lam 2013) [28]

Two types of failure modes were observed: fracture of the demountable shear connector and crushing of concrete. The force per shear connector-slip curve received from one of the tests, in which the bolt diameter is 19 mm and the concrete cubic strength is 29.9 MPa, is depicted in figure 2.12.b and a comparison is made to welded headed studs. The failure mode of this specimen is concrete crushing, the maximum strength per shear connector is 92.7 kN and the slip at maximum load is 9 mm. It can be concluded that the demountable shear connectors have shear resistance 16% lower than welded headed studs. Moreover, they are more ductile but they have lower stiffness.

2.4 Resin injected bolts

2.4.1 Resin injected bolts' layout

Resin injected bolts are considered a reliable and not expensive solution for repair and strengthening of existing structures as well as for the construction of new structures. They are widely used in the Netherlands since 1970 for the repair of old bridges, for new railway bridges and for other applications [8]. All these years of application, resin injected bolts have a good performance and the continuity of their research is necessary. Extensive research about resin injected bolts has been carried out in the Stevin Laboratory of Technical University of Delft.

Resin injected bolts are bolts in which the cavity formed by the clearance between the bolt and the hole is filled up with resin. The clearance of the bolt is injected with resin through a small hole in the bolt's head. When the resin is fully cured, the connection is slip resistant. They are used in connections where slip is not allowed. Large hole clearances lead to a faster erection and subsequently to demountable structures. However, excessive hole clearances reduce the stiffness of the composite structure because of the initial slip between steel beam and the concrete decks. By using resin injected bolts, the slip and also the vertical displacement of the composite structure is restricted. The transfer of the shear load is achieved through shear and bearing of the bolt.

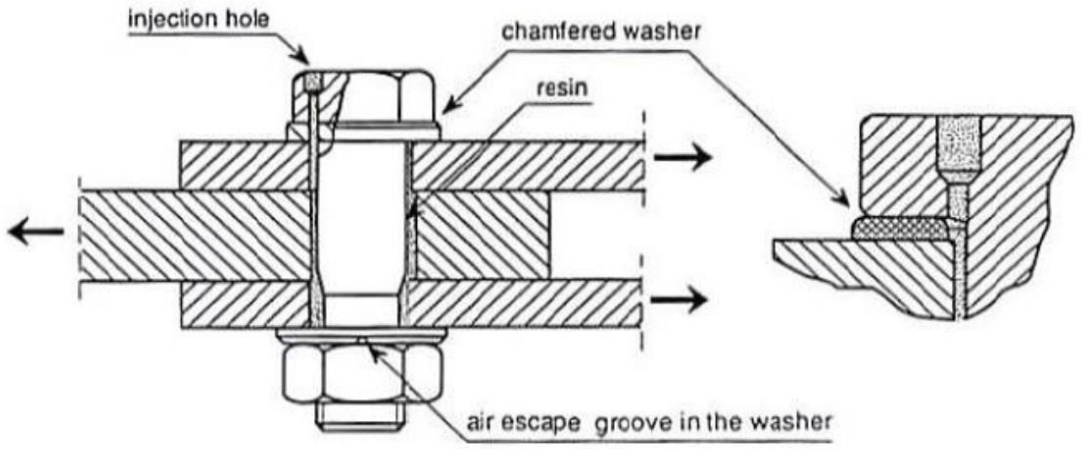

Figure 2.13: Injection bolt layout [8]

2.4.2 Advantages of resin injected bolts

Compared to other bolted connectors, resin injected bolts have many advantages. First of all, resin injected bolts are considered a very successful solution for connections with low slip factor. That is the reason why they are widely used for the repair of riveted connections. The application of new rivets is not possible due to the fact that this connection is not used anymore and there is lack of equipment and skilled workers. A characteristic example is the Schlossbrucke bridge in Oranienburg near Berlin, in which riveted connection successfully was replaced by injected bolted connection. Fitted bolts could also be used as they have a similar behaviour to resin injected bolts but they are more expensive. Moreover, they provide very good resistance in bearing and also prohibit internal corrosion as the cavity is filled up with resin. Last but not least, bolt tightening doesn't need to be controlled to achieve slip resistance due to the presence of resin. That is an advantage of resin injected bolts over high friction grip bolts.

2.4.3 Regulations on resin injected bolts

Calculation rules for the design resistance of the connections with resin injected bolts can be found in EN1993-1-8 [16] while executional information on the bolt detailing and the bolt hole can be found in EN 1090-2 [14].

2.4.4 Costs of resin injected bolts

The cost of a connection with resin injected bolts consists of the following expenses:

- The purchase of the bolts, the nuts and the washers

- the drilling of the hole in the bolts for the resin injection and the preparation of special washers
- the purchase, preparation and injection of the resin
- the equipment needed for the injection

A variety of aspects like the overall number of bolts of the connection, the accessibility of the bolts and the bolt dimensions influence the cost of injection per bolt. There are bolt suppliers that provide injection bolts and washers ready to use. However, the adaptation of the bolts and washers can also be carried out in workshops. Usually, the time needed for the injection of one bolt varies between 1 and 2 minutes [8].

When the resin is cured, the bolts cannot be untightened or removed. So when the connection is about to be demounted some measures should be taken in advance to face the difficulties. For example, a mould release agent could be used to avoid the bonding of the resin to the bolt and the wall of the hole. Materials that can be used as mould release agents are Teflon-based products, wax-based products and silicon-based products [35].

2.4.5 Components of resin injected bolts

- **Bolts**

Bolts of class 8.8 or 10.9, preloaded or non-preloaded can be used in connections with resin injected bolts. A hole is drilled in the head of the bolt through which the resin is injected with an injection device. The position and dimensions of the hole are indicated in figure 2.14. Resin injected bolts can be manufactured from normal bolts with some adaptations to enable the resin injection. If preloaded bolts are used, tightening should be carried out before the resin injection.

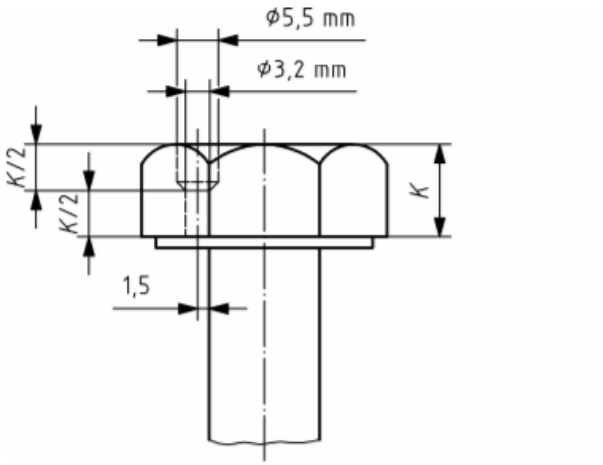

Figure 2.14: Resin injection hole layout [14]

- **Washers**

In case of connections with resin injected bolts, two washers are used: one under the bold head and one under the nut. A special washer is used under the bold head with inner diameter at least 5 mm larger than the bolt diameter. The one side is machined and is installed towards the head of the bolt. The space that is created facilitates the flow of resin between the bolt and

the steel member. The washer under the nut has an air escape groove with smooth and round edges that facilitates the escape of air during the injection of resin. This washer should be installed with the groove towards the nut.

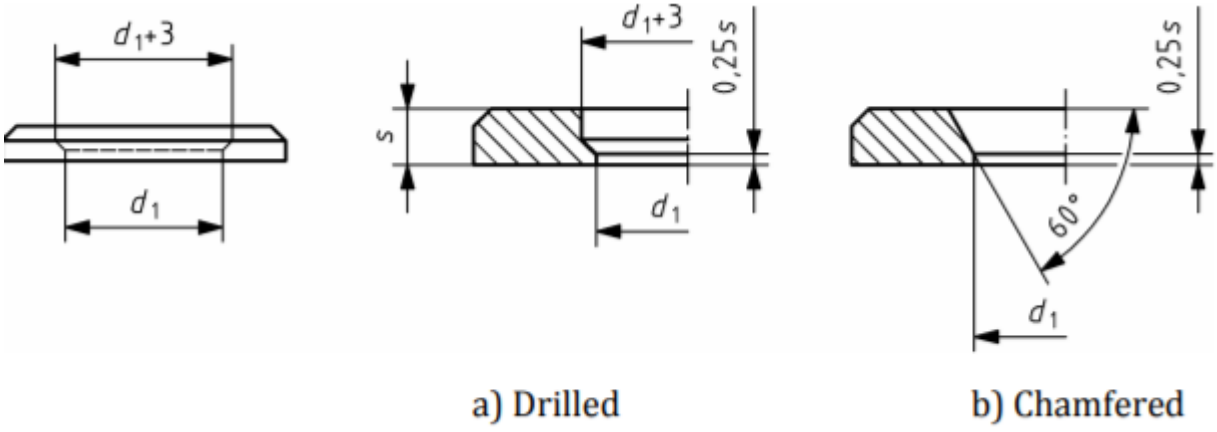

Figure 2.15: Washers' layout [14]

- **Resin**

A two component resin is used with a potlife at least 15 min at ambient temperature. The viscosity of the resin should be such that the cavities of the connection will be filled sufficiently. If there are not available data, a series of tests should be carried out in order to determine the suitable resin temperature and curing time. The temperature of the resin should be in the range of 15-25°C. If the temperature in the atmosphere is very low the resin and sometimes the steel components need to be preheated. One of the most widely used two component epoxy resins in resin injected bolted connections is Araldite/RenGel SW 404 which is combined with hardening agent Ren HY 2404.

2.4.6 Static design resistance of a resin injected bolted connection

The static resistance of a resin injected bolted connection depends on the shear connection category. In case of Category A: bearing type, non-preloaded shear connection with bolts from class 4.6 up to and including class 10.9, the static design resistance is the smallest of the design shear resistance of the bolt $F_{v,Rd}$ and the design bearing resistance of the resin $F_{b,Rd,resin}$ as shown in equation 2.3 [16]:

$$F_{Rd,A} = \min (F_{vRd} , F_{b,Rd,resin}) \quad (2.3)$$

In case of Category B: slip-resistant at Serviceability Limit State and Category C: slip-resistant at Ultimate Limit State, preloaded shear connection with bolts class 8.8 or 10.9, the static design resistance should not exceed the smallest of the design shear resistance of the bolt $F_{v,}Rd$, the design bearing resistance of the resin $F_{b,Rd,resin}$ plus the design slip resistance of the bolt $F_{s,Rd}$ and the design bearing resistance $F_{b,Rd}$ as shown in equation 2.4 [16] :

$$F_{Rd,B} = F_{Rd,C} = \min (F_{vRd} , F_{b,Rd,resin} + F_{s,Rd} , F_{b,Rd}) \quad (2.4)$$

The design bearing resistance of the resin $F_{b,Rd,resin}$ is calculated according to the following equation:

$$F_{b,Rd,resin} = \frac{k_t \cdot k_s \cdot d \cdot t_{b,resin} \cdot \beta \cdot f_{b,resin}}{\gamma_{M4}} \quad (2.5)$$

Where:

k_t: for SLS is equal to 1.0 and for ULS is equal to 1.2

k_s: is equal to 1.0 for holes with normal clearances or 1.0-0.1 m for oversized holes

m: is the difference expressed in mm between the normal and oversized hole dimensions. In case of short slotted holes m is equal to half the difference between the hole length and width

$t_{b,resin}$: is the resin effective bearing thickness and is given in Table 2.1

β: is a coefficient which depends on the thickness ratio of the connected plates and is given in Table 2.1

$f_{b,resin}$: is the bearing strength of the resin calculated according to Annex G of EN 1090-2

Table 2.1: Values of β and $t_{b,resin}$ [16]

t_1/t_2	β	$t_{b,resin}$
≥2,0	1,0	min($2t_2$;1,5d)
1,0≤ t_1/t_2≤ 2,0	1,66-0.33(t_1/t_2)	min(t_1;1,5d)
≤ 1,0	1,33	min(t_1;1,5d)

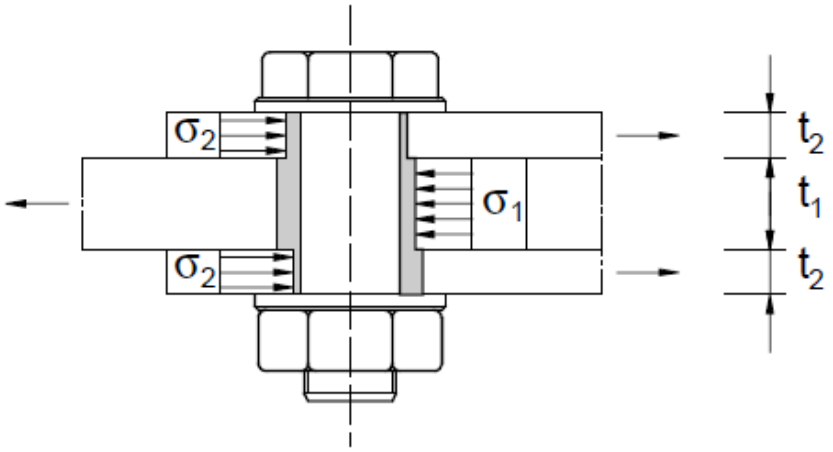

Figure 2.16: t_1 and t_2 definition [16]

2.4.7 Research on resin injected bolts

Push-out tests were performed in the laboratory of steel and composite structures at the University of Luxembourg in order to examine the behaviour of resin injected bolts with embedded coupler and provide the potential of reusing the structural components [26]. The tests were not executed as described in Eurocode 4-Annex B, a slightly different set-up was chosen. The dimensions and layout of the tests are shown in figure 2.17.a. The specimens were consisted of steel section type I, four prefabricated concrete decks with standard reinforcement layout and L-angle and the resin injected bolts with embedded coupler. The holes in steel flanges are oversized to allow for the demountability of the structural components. The embedded coupler system consists of the embedded bolt, the embedded bolt coupler and a removable bolt positioned below as depicted in figure 2.17.b.

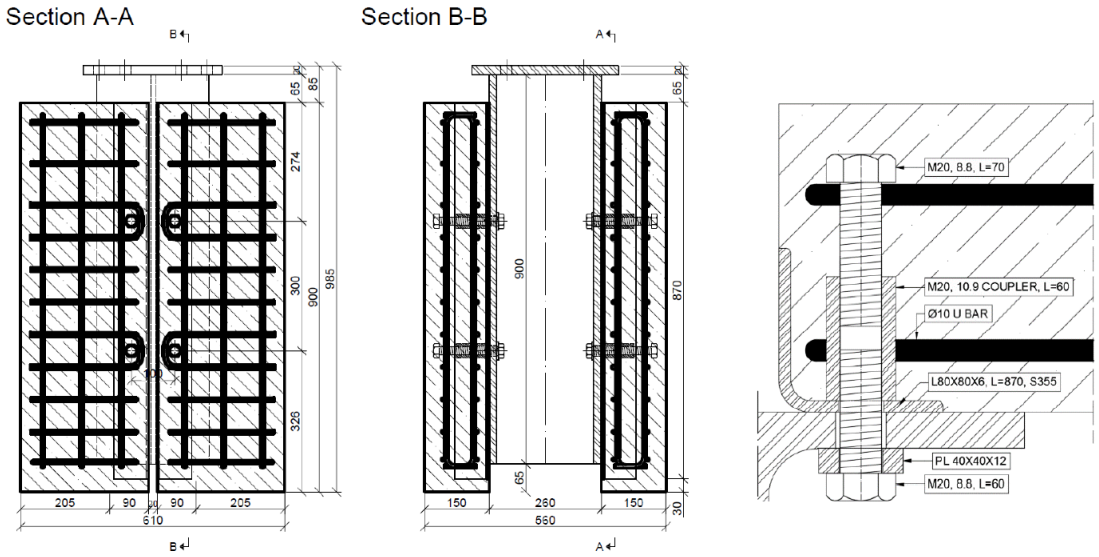

a) Dimensions of the specimens b) The coupler system layout

Figure 2.17: Specimens' dimensions (University of Luxemburg) [26]

The steel section is HEB260 with steel grade S355. The embedded coupler is grade 10.9 while the bolts are grade 8.8 with diameter M20. A lower bolt grade was selected in order to get damaged before the coupler and allow for reusability. Concrete decks are class C35/45 and the reinforcement is grade B500. The bolt holes in the flanges of the steel part had a diameter of 24 mm.

The specimens were placed into a mortar bedding. A hydraulic jack with a load capacity of 1000 kN was used. During the test, the force in the jack and the displacements were constantly monitored. The test setup is depicted in figure 2.18.a. The first experiment was conducted without cycles in order to receive the failure load. The second and third test included 25 load cycles between 5% and 40% of the failure load received in the first experiment. In the third experiment, additionally to the 25 cycles, unloading-reloading cycles were also performed in order to find the actual stiffness at large displacements. During the first test, at the load level of 500 kN the specimen was unloaded and the 4 out of the 8 bolts were removed because the bolts had overstrength so the 1000 kN capacity of the hydraulic jack could not lead to failure. The second and third test were also conducted with 4 bolts.

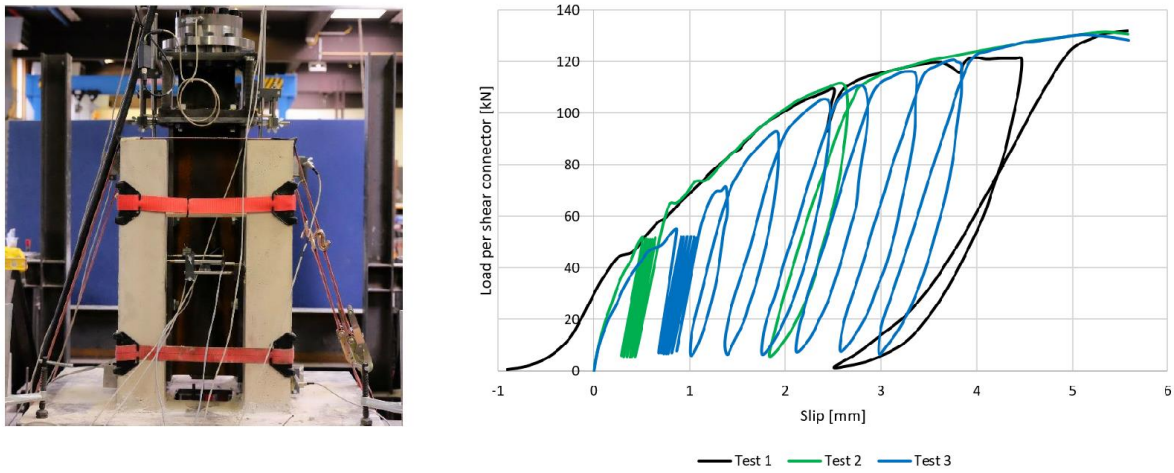

a) Test set-up b) Force-slip curve

Figure 2.18: Resin injected bolt push-out test (University of Luxemburg) [26]

The results of the tests are shown in figure 2.18.b. The shear connector failed due to shear failure of the bolt and no concrete damage and damage of the embedded parts was observed. The average ultimate slip is 5.53 mm, so resin injected bolts M20 with embedded coupler have a brittle behaviour according to Eurocode 4-1-1. The average ultimate failure load per shear connector of the three push-out tests is 131 kN.

3 Experimental work

Reusability of the structural components in the construction industry protects the natural environment, saves resources and conserves energy. TU Delft, among other universities, participates in a research project named 'REDUCE' (Reuse and demountability using steel structures and the circular economy) that aims to provide technical solutions, tools and guidance in the design of demountable and reusable structures. This led to the investigation of push-out tests with an innovative type of shear connectors, resin injected bolts, within a national network organization specialized in materials research named Material innovation institute (M2i). This chapter describes the experimental work that was performed to investigate the feasibility of resin injected bolts as shear connectors. This section includes the description of the specimens, their assembly, the test set-up and finally the test results. The test results are compared with the results obtained from the research on other types of demountable shear connectors and welded headed studs.

3.1 Description of the specimens

Demountable injected bolt-coupler system was used to connect the steel section with the concrete decks and achieve composite action in push-out tests. This system consists of an embedded coupler, an embedded bolt and a removable bolt as depicted in figure 3.2. A hole is drilled in the head of the removable bolt for the injection of resin. The steel section has oversized holes d_1=32 mm which allow for an easier assembly process. With the injection procedure, the cavity formed by the clearance between the bolt and the hole is filled up with resin.

A total of 6 push out tests were conducted and two different test configurations were created, one with resin injected bolts and the other one with reinforced resin injected bolts. For each configuration three specimens were tested which were identical with each other. Each specimen consisted of a steel section type I and four prefabricated concrete decks connected with eight shear connectors. The basic test parameters are presented in table 3.1.

Table 3.1: Experimental push-out test parameters

Test	Shear connector system	Shear connection bolts	Steel section hole diameter d1 (mm)	Number of shear connectors
R1	Coupler system	Resin injected bolts	32	8
R2				
R3				
SRR1	Coupler system	Reinforced resin injected bolts	32	8
SRR2				
SRR3				

Full-scale tests have been performed in TU Delft laboratory in order to investigate the feasibility of construction of a demountable steel-concrete composite car park the shear resistance of which is achieved through resin injected bolts [19]. Further to this research, push-out test are performed in order to investigate resin injected bolts as shear connectors in the composite car park. The test set-up was similar to that described in Eurocode 4 Annex B. One difference is that HE260A steel sections were used instead of HE260B because in the beam test for the car park the thickness of the flange of the steel section was 12 mm and H260A sections have steel flange thickness 12.5 mm and this value is closer to 12 mm compared to H260B sections which have steel flange thickness 17.5 mm. Another difference from Eurocode is that the distance of the shear connectors was 300 mm instead of 250 mm because also in beam tests the distance of shear connectors was 300 mm. Moreover, the dimensions of the concrete decks were 860*300*120 mm instead of 650*300*150 mm as in beam tests the concrete thickness was 120 mm. Last but not least, reinforcement bars Ø8 were used instead of Ø10 same as in the push-out tests with resin injected bolts that performed in the University of Luxemburg [26]. The detailed layout and the dimensions of the specimens are depicted in figure 3.1. The cross section A-A' of the specimen is depicted in figure 3.2.

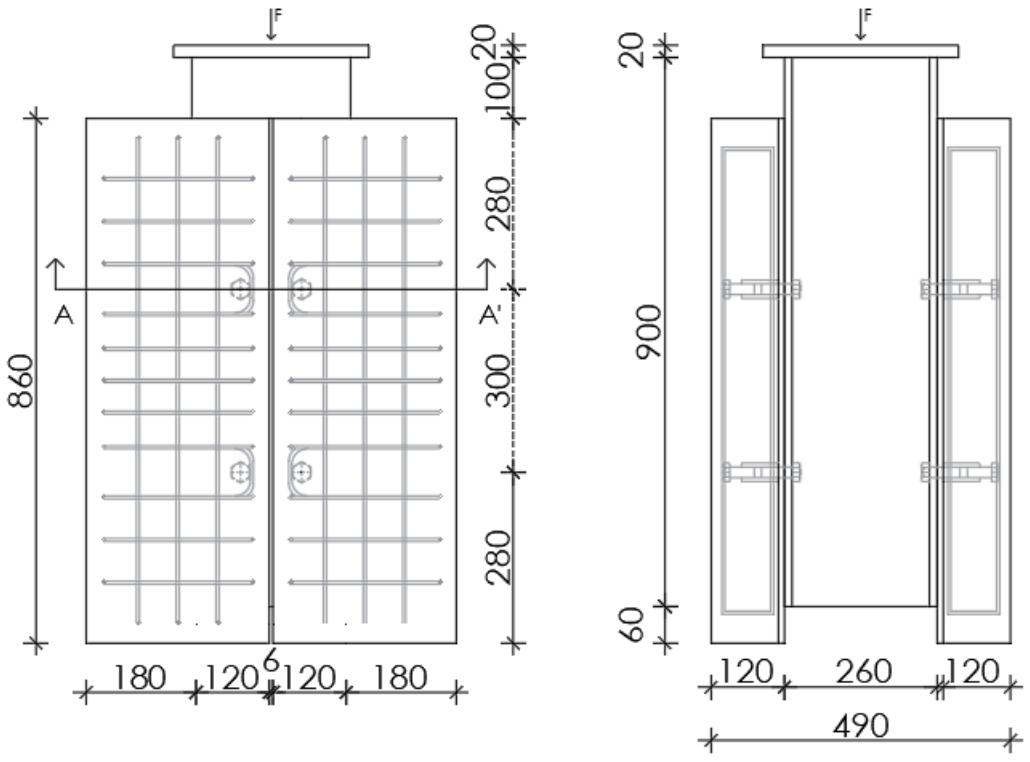

a) Front view b) Side view

Figure 3.1: Dimensions of the specimens

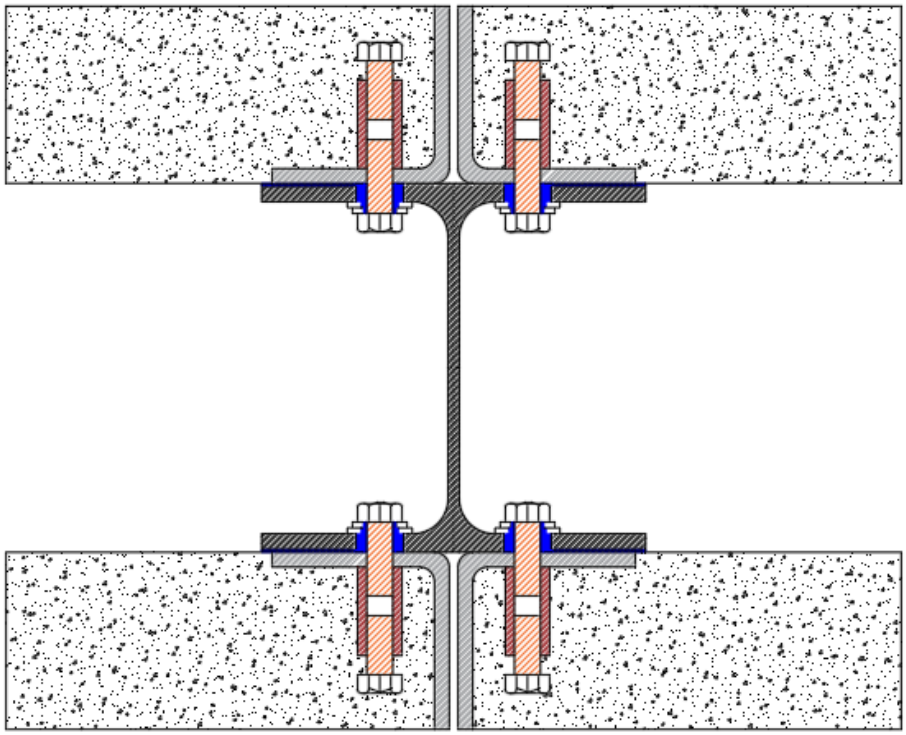

Figure 3.2: Cross section A-A' of the specimen

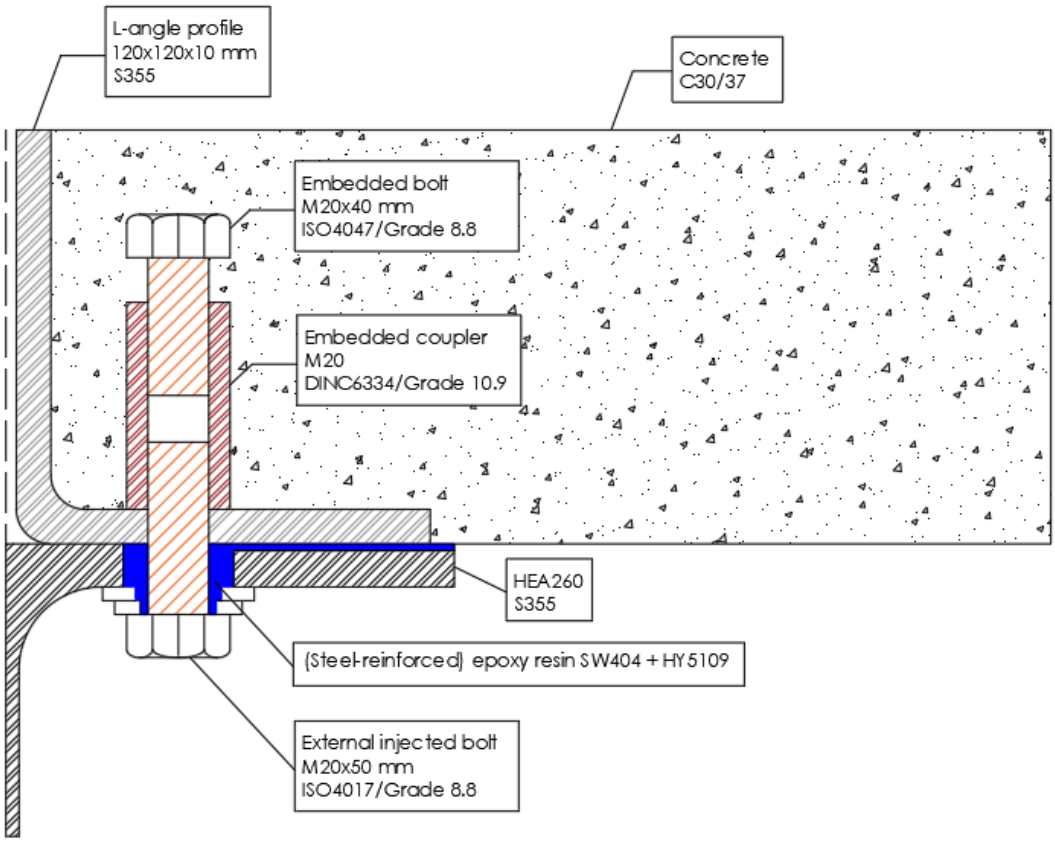

Figure 3.3: Details of cross section A-A'

The steel sections were HE260A with oversized holes of diameter d_1=32 mm, length of 900 mm and steel grade S355. Air grooves are constructed in the flanges of the steel section for the escape of the air during the injection process. The concrete decks were prefabricated with embedded reinforcement, coupler, bolt and L-angle. The dimensions of the concrete decks were 860*300*120 mm. The L-angle profiles have dimension 120*120*10 mm and steel grade S355. Two layers of Ø8/75 reinforcement was applied with material grade of B500B. The concrete strength was C30/37. The bolts were grade 8.8 and had a diameter of d=20 mm according to ISO4017/DIN933. The length of the coupler was equal to 60 mm according to DIN6334. A hole was drilled in the head of the bolt for the injection of the resin. Special washers were used which facilitate the resin injection.

3.2 Assembly of the specimens

Hydraulic oil was applied to the specimens before their connection and a release agent was sprayed to them in order to prevent adhesion and allow for an easy separation of the components after the test. Shell Tellus S2V oil was used which is a fluid which provides protection and performance. ACMOS 82-2405 released agent was used which is an aerosol spray for sliding effect improvement. The hydraulic oil and release agent used are depicted in figures 3.4.a and 3.4.b respectively.

a) Hydrauic oil	b) Release agent	c) Hardener	d) Resin
Shell Tellus S2V	ACMOS 82-2405	REN HY 5159	RenGel SW 404

Figure 3.4: Materials used during the experiments

The prefabricated concrete decks were placed on the flanges of the steel section as depicted in figure 3.5.a and when the hole of the concrete deck was aligned with the hole of the steel section, the bolts with two special washers were placed in the hole as depicted in figure 3.5.b.

a) Position of concrete decks

b) Position of bolts

Figure 3.5: Phases of the assembly procedure

The next step of the assembly is the injection of the resin. The resin RenGel SW 404 and the hardener REN HY 5159 which are depicted in figures 3.4.d and 3.4.c respectively were used in a mixing ratio 8:1. Although according to the manufacturer the resin is completely cured after 24 hours, research on the resin that conducted in TU Delft have shown that the strength and stiffness are developed after 3-4 hours [23]. When the resin and the hardener were mixed, they were put in a plastic caulk tube. Then the mixture was injected through the hole in the bold head with the use of a hand-operated caulking gun as depicted in figure 3.6.

a) Plastic caulk tube

b) Hand-operated caulking gun

Figure 3.6: Resin injection procedure items used

The injection was completed when the resin came out of the escape groove. Due to the time needed for the curing of resin, the bolts on the one flange were injected the one day and the bolts on the other flange the following day. In case of reinforced resin injected bolts, small steel particles S330 filled the oversized hole before the injection of resin. The steel shots had a diameter of 1 mm.

It is important to be mentioned that in case of specimens with resin injected bolts, the resin injection was executed upwards as depicted in figure 3.7.a while in case of specimens with reinforced resin injected bolts, the resin injection was executed downwards as depicted in figure 3.7.b.

a) Upwards b) Downwards

Figure 3.7: Resin injection procedure

3.3 Test set-up

When the resin was cured, the specimens were positioned in the testing frame with hydraulic jack. A steel section was used between the specimen and the hydraulic jack for the even distribution of the force. The specimens were placed on fast setting time gypsum in order to achieve alignment as the specimens were not completely aligned and to provide protection of concrete. The gypsum was put in a bucket with water in a ratio of 1.5:1 and the mixture was mixed with a driller until it was homogenised. With the use of a controller the specimens were lifted up and two PVC parts with gypsum were placed under the specimen. Afterwards the specimen was lowered until the layer of gypsum was 1 cm.

a) PVC parts

b) Mixing of gypsum

c) Placement of the PVCs under the specimen

d) Hardening of gypsum

Figure 3.8: Placement of the specimen on a fast setting time gypsum

In each specimen 10 LVDTs (Linear Variable Displacement Transducers) were positioned: 8 that measured the longitudinal slip between the steel section and the concrete decks (4 on each side) and 2 that measured the horizontal displacement between the steel section and the concrete decks (only on one side). The sensors were connected to steel profiles 60*60*5 mm, through magnets, which were glued to the steel section with a silicon gun. Before the L-profiles were glued to the steel section, the surfaces were cleaned with acetone. For the vertical displacements, aluminium cube profiles were glued with the silicon gun on concrete below the L-profiles. The sensors' edges were in touch with the cube profiles in order to measure the vertical displacements. For the measurement of the horizontal displacements, 2 small PVC parts were glued in concrete and the sensor edges were in touch with them.

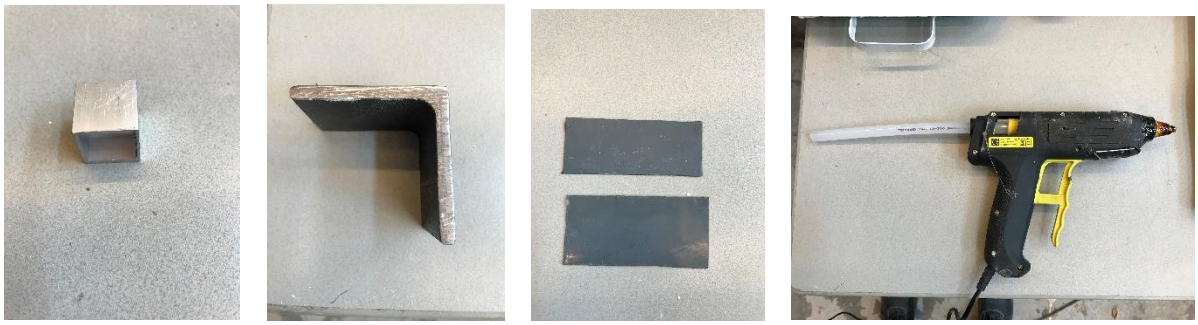

a) Cube profiles b) L-profiles c) PVC parts d) Silicon gun

Figure 3.9: Sensors' preparation

The completed test set-up is depicted in figure 3.10.

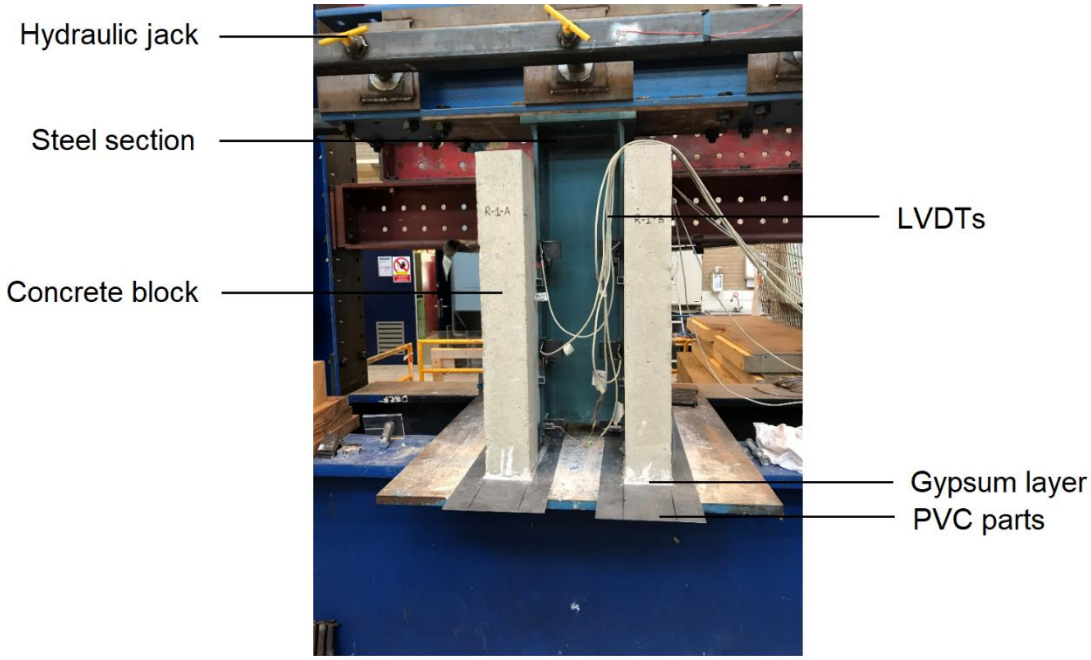

Figure 3.10: Complete set-up

For each of the two test configurations, three static push-out tests were conducted. In the first test, the specimen was loaded until failure using displacement control at a speed of 1 mm/min. In the second test, the specimen was loaded in 25 force-controlled load cycles of 40% of the failure load from the first experiment with loading and unloading rate of 6 kN/s and then after the 25th load cycle was loaded until failure using displacement control at a speed of 1 mm/min. Finally, in the third test the specimen was loaded in 25 force-controlled load cycles as in the second one and after the 25th load cycle using displacement control it was loaded 0.5 mm further than during the 25th cycle and then unloaded until the force was equal to zero. This process was continued until the force between subsequent cycles was nearly identical. Then the specimen was loaded until failure. The loading regime is depicted in figure 3.11.

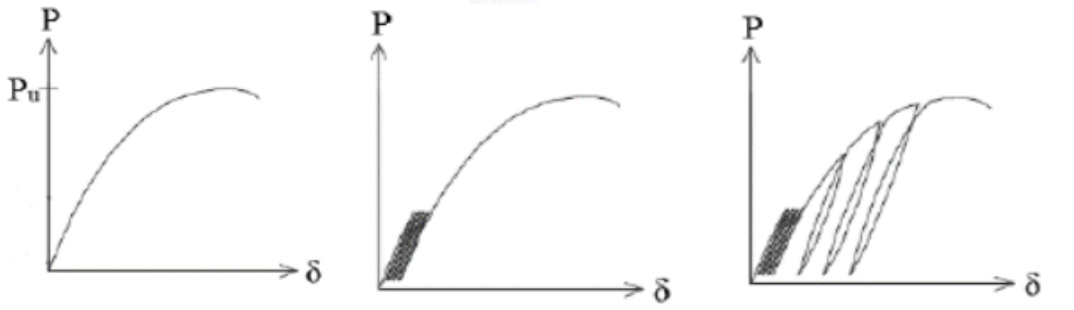

a) First test b) Second test c) Third test

Figure 3.11: Loading regime of push-out tests [26]

3.4 Test results

3.4.1 Test R1

The specimen R1 was loaded until failure with constant displacement rate at a speed of 1mm/min. The force-slip curve for each of the 8 bolts and the average force-slip curve are depicted in figure 3.12.

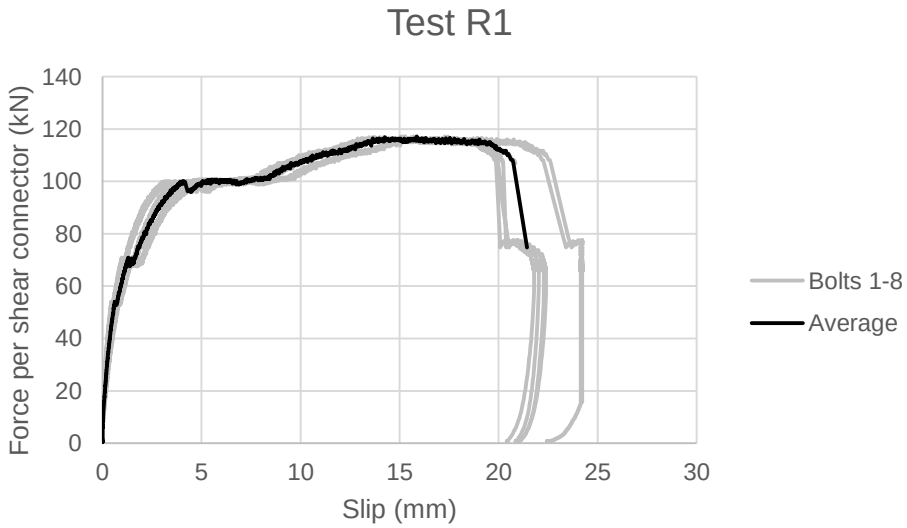

Figure 3.12: Force-slip curve of shear connectors of test R1

Concrete failure preceded shear failure of the bolts since significant cracks were observed in concrete during the test as depicted in figure 3.13. The maximum force per shear connector is 117.2 kN and the slip at 90% of the maximum force is 20.6 mm, which indicates that the shear connectors behaved in very ductile manner as according to Eurocode the limit of ductile behaviour is 6 mm.

Figure 3.13: Concrete cracks during test R1

3.4.2 Test R2

The specimen R2 was loaded in 25 force-controlled load cycles of 40% of the expected failure load 100 kN from test R1 with loading and unloading rate of 6 kN/s and then after the 25th load cycle was loaded until failure as in test R1. The force-slip curve for each of the 8 bolts and the average force-slip curve are depicted in figure 3.14.

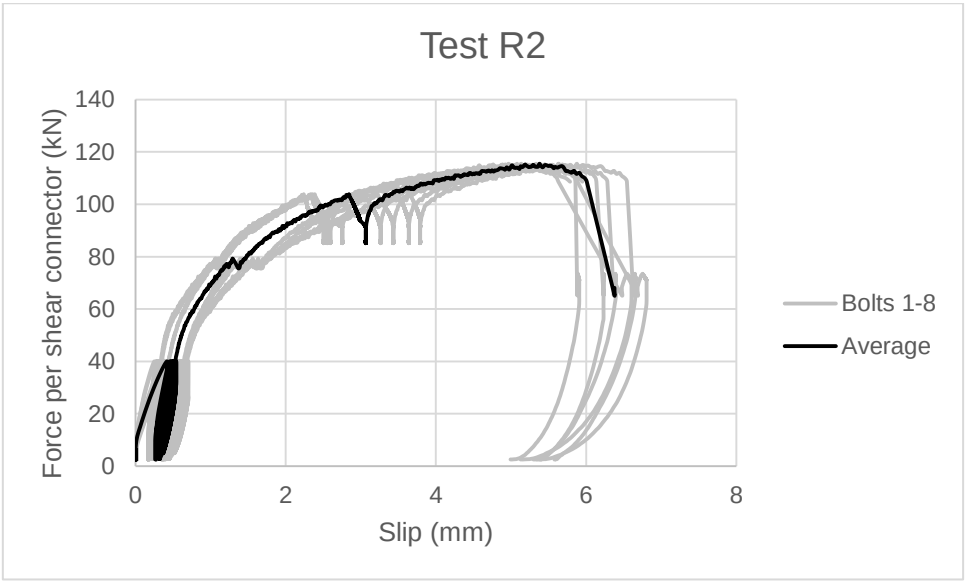

Figure 3.14: Force-slip curve of shear connectors of test R2

The failure mode was shear failure of the bolts. In contrast with test R1, no cracks were observed in concrete. The maximum force per shear connector is 115.5 kN and the slip at 90% of the maximum force is 5.9 mm which is in the limit of ductile behaviour according to Eurocode.

3.4.3 Test R3

The specimen R3 was loaded initially in 25 force-controlled load cycles as in test R2 and after the 25th load cycle using displacement control it was loaded 0.5 mm further than during the 25th cycle and then unloaded until the force was equal to zero. This process was continued until the force between subsequent cycles was nearly identical. Then the specimen was loaded until failure. The force-slip curve for each of the 8 bolts and the average force-slip are depicted in figure 3.15.

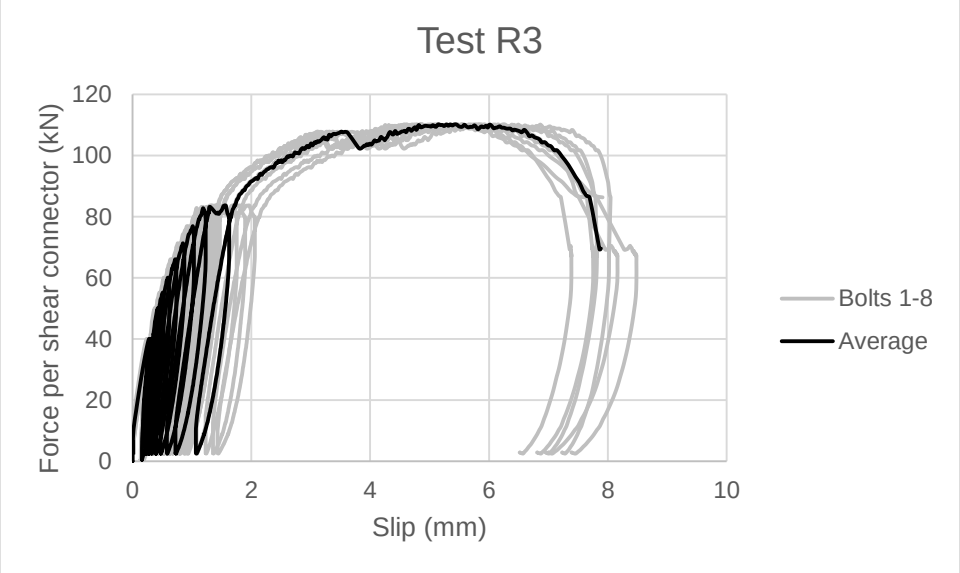

Figure 3.15: Force-slip curve of shear connectors of test R3

The failure mode was shear failure of the bolts. As in test R2, no cracks were observed in concrete. The maximum force per shear connector is 110.2 kN and the slip at 90% of the maximum force is 7.3 mm, higher than 6 mm so the shear connector behaved in a ductile manner.

3.4.4 Test SRR1

Same loading procedure was followed for test SRR1 with reinforced resin injected bolts as in test R1. The force-slip curve for each of the 8 bolts and the average force-slip curve are depicted in figure 3.16.

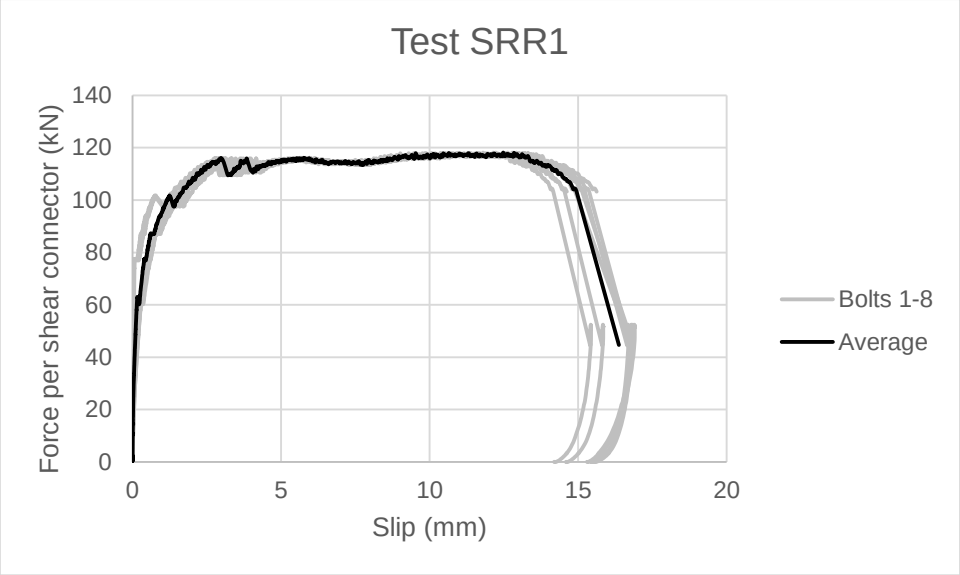

Figure 3.16: Force-slip curve of shear connectors of test SRR1

As in test R1, concrete failure preceded shear failure of the bolts since significant cracks were observed in concrete during the test as depicted in figure 3.17. The maximum force per shear connector is 118.2 kN and the slip at 90% of the maximum force is 14.7 mm, which indicates that the shear connectors behaved in a ductile manner according to Eurocode.

Figure 3.17: Concrete cracks during test SRR1

3.4.5 Test SRR2

Same loading procedure was followed as in test R2. The force-slip curve for each of the 8 bolts and the average force-slip curve are depicted in figure 3.18.

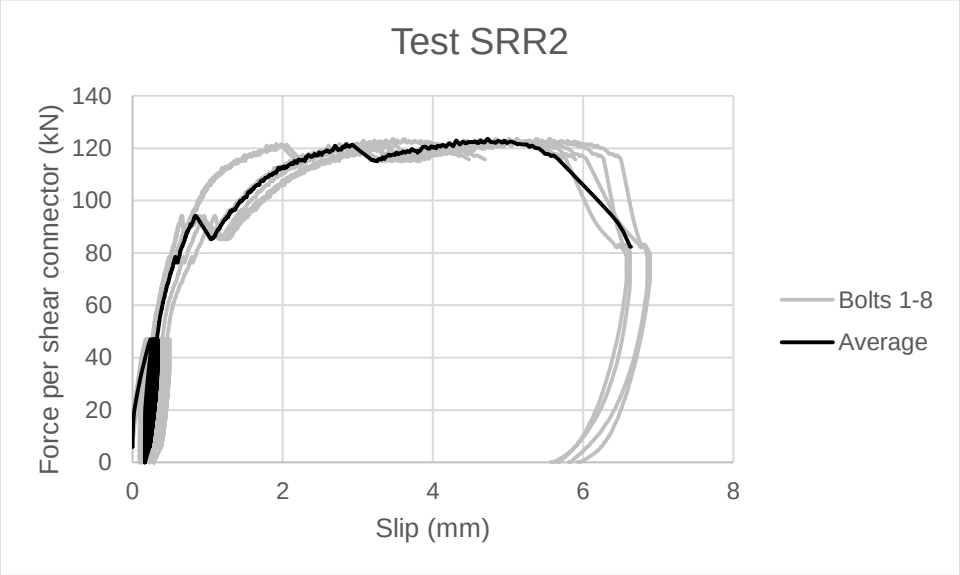

Figure 3.18: Force-slip curve of shear connectors of test SRR2

The failure mode was shear failure of the bolts. In contrast with test SRR1, no cracks were observed in concrete. The maximum force per shear connector is 123.6 kN and the slip at 90% of the maximum force is 5.6 mm which is in the limit of ductile behaviour according to Eurocode.

3.4.6 Test SRR3

Due to the leakage of resin that was observed around the hole of the steel section when the specimens were demounted, before the application of load in test SRR3, the bolts were untightened and a small gap was created in steel-concrete interface. The gap in steel-concrete interface was created with the machine depicted in figure 3.19.

Figure 3.19: Creation of gap in steel-concrete interface

Same loading procedure was followed as in test R3. The force-slip curve for each of the 8 bolts and the average force-slip curve are depicted in figure 3.20.

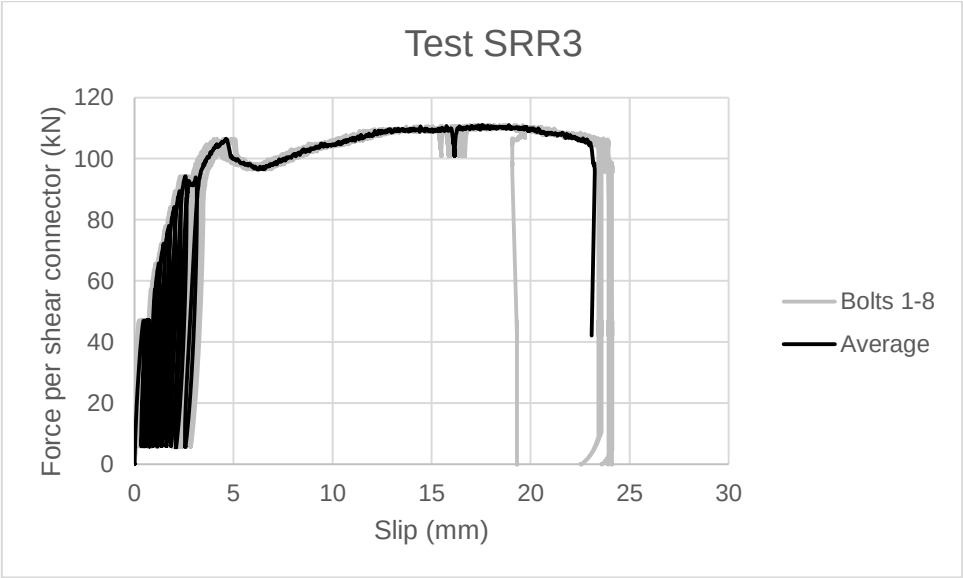

Figure 3.20: Force-slip curve of shear connectors of test SRR3

The failure mode was shear failure of the bolts. As in test SRR2, no cracks were observed in concrete. The maximum force per shear connector is 111 kN and the slip at 90% of the maximum force is 23.1 mm, higher than 6 mm so the shear connectors behaved in a very ductile manner.

3.5 Demounting of the specimens

After performing the push-out tests, the specimens were demounted with the use of the suitable equipment. In most of the experiments, the specimens failed due to shear failure of

the bolts. In the push-out tests when the specimens were subjected to loading, one of the four concrete decks broke off and the bolts failed due to shear as it can be seen in figure 3.21. The resin in steel section hole that is depicted in figure 3.21 remained intact after the experiments. A possible reason is that the resin is confined and there is no space for expansion.

Figure 3.21: Specimen failed due to shear failure of the bolts

After separation of the L-angle profile and the concrete deck, adhesion of the concrete on the L-angle profile was observed in most of the specimens as depicted in figure 3.22.a. Moreover, as it can be seen in figure 3.22.b, leakage of resin around the hole in the steel section was also observed after demounting of the specimens especially in the specimens with reinforced resin injected bolts. The reason why this happened is the resin injection procedure. The specimens with reinforced resin injected bolts, during the resin injection procedure, were horizontal and the resin was injected downwards which led to leakage of the resin.

a) Adhesion b) Leakage of resin

Figure 3.22: Specimens after demounting

It is important to be mentioned that the steel section was not damaged and reused in other push-out tests, proving the demountability and reusability of the system.

3.6 Summarization of the results

The force-slip curves from the six push-out tests that performed in the lab are depicted in figure 3.23 and the results in table 3.2.

Table 3.2: Results of the push-out tests

Test	Max force per shear connector (kN)	Slip at 90% of the max force (mm)	Failure mode
R1	117,2	20,6	concrete failure
R2	115,5	5,9	shear failure of the bolts
R3	110,2	7,3	shear failure of the bolts
SRR1	118,2	14,7	concrete failure
SRR2	123,6	5,6	shear failure of the bolts
SRR3	111,0	23,1	shear failure of the bolts

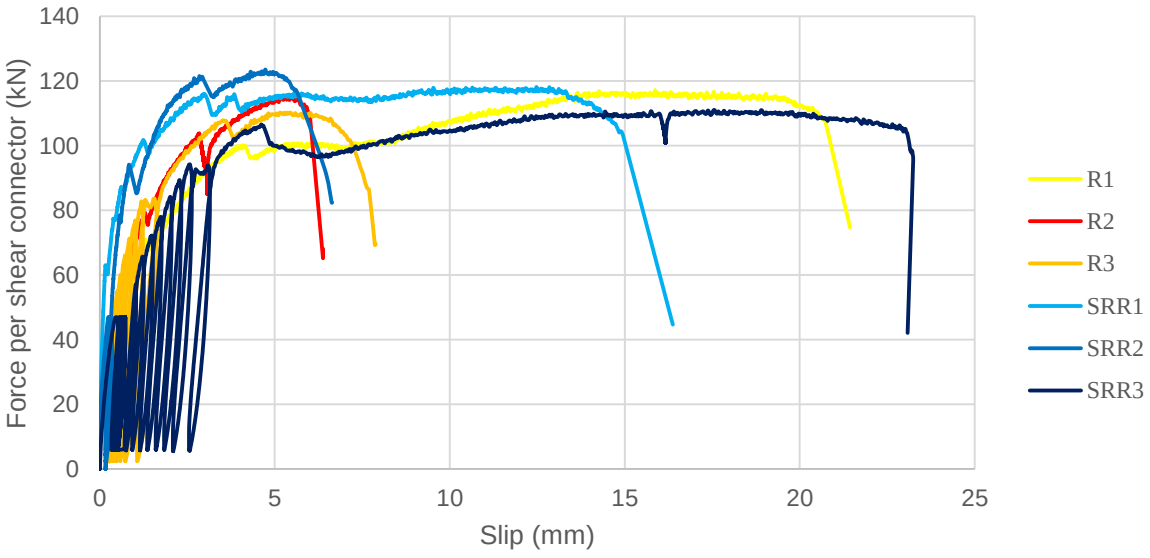

Figure 3.23: Force-slip curve of all the tests

In test SRR3 the slip at 90% of the maximum force is much larger than in other experiments which failed due to shear failure of the bolts. Moreover, due to the gap that created in the steel-concrete interface, concrete was slightly damaged before the experiment. For these reasons, the results of test SRR3 are not considered valid and are not included in the final results.

The shear capacities of the specimens did not differ significantly, the average maximum force per shear connector derived from tests R1, R2, R3, SRR1 and SRR2 is 116.9 kN.

The shear connectors in tests R1 and SRR1, which failed due to concrete failure, behaved in a very ductile manner while in tests R2, R3 and SRR2, which failed due to shear failure of the bolts, the slip was very close to the limit for a ductile behaviour according to Eurocode.

The second stiffness of specimens with resin injected bolts and reinforced resin injected bolts is calculated according to Eurocode 4 Annex B [17]. In case of reinforced resin injected bolts the second stiffness is higher than in case of resin injected bolts. In test SRR1 the second stiffness is 4.4 times higher than in test R1 as depicted in figure 3.24.

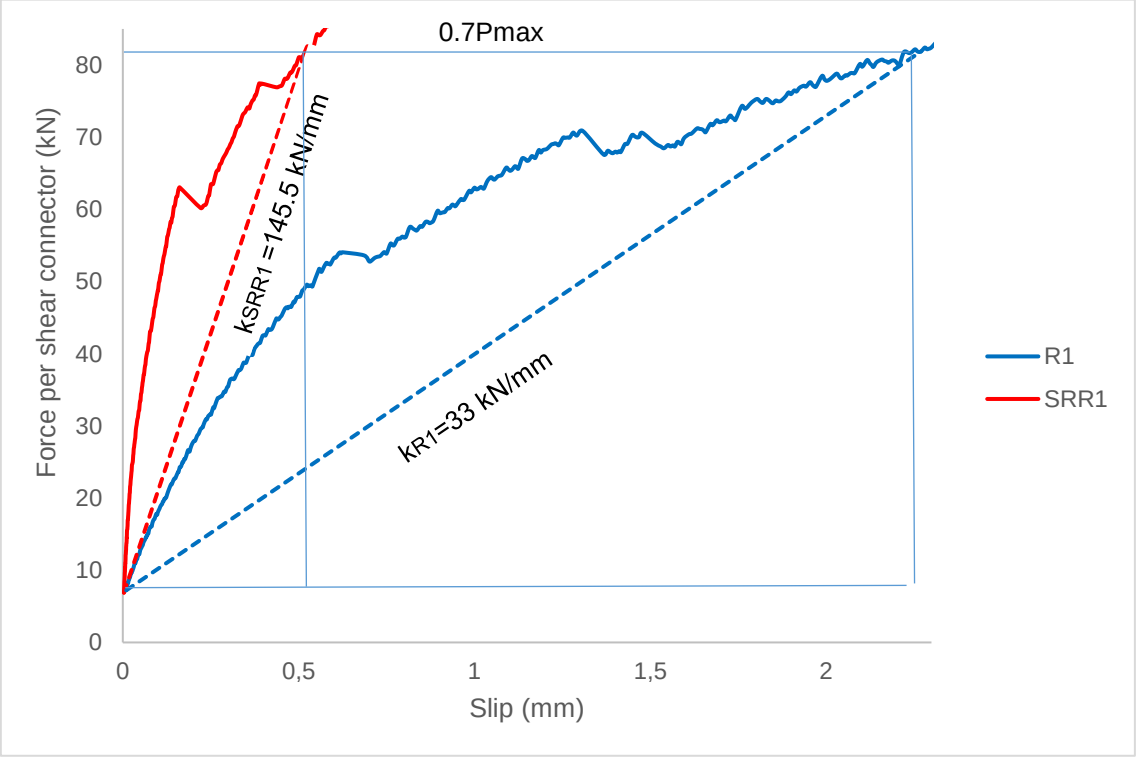

Figure 3.24: Shear connector second stiffness

Two failure modes were observed: concrete failure and shear failure of the bolts. Tests R1 and SRR1 which were loaded until failure failed due to concrete failure because many cracks were observed in concrete during the experiments while tests R2, R3 and SRR2 failed due to shear failure of the bolts and no cracks were observed in concrete. A possible reason is the type of loading. In case of cyclic loading, steady openings of cracks occur due to the cycles, so the energy is not released and no cracks occur in concrete.

The behaviour of resin injected bolts as shear connectors has also been examined in the University of Luxemburg. Three push-out tests were performed with the same loading regimes as in TU Delft. The force-slip curve obtained from the push-out test R1 conducted in the Stevin laboratory of TU Delft in which the specimen was loaded until failure is compared with the equivalent one obtained from the University of Luxemburg as depicted in figure 3.25.

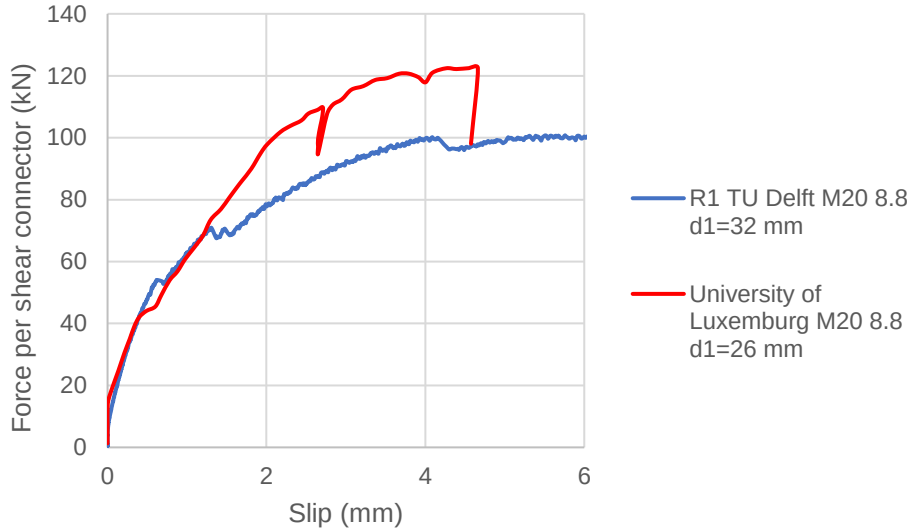

Figure 3.25: Comparison of push-out test R1 with the equivalent test conducted in the University of Luxemburg

The specimens had similar dimensions of the members and almost similar concrete cubic strength. In the University of Luxemburg steel sections HEB260 were used while in TU Delft HEA260. In both universities M20 bolts of bolt strength class 8.8 were used but in University of Luxemburg the diameter of the oversized holes of the steel section was equal to 26 mm while in TU Delft it was equal to 32 mm. The maximum average force per shear connector derived from the tests conducted in TU Delft is 88% of that derived from the tests conducted in the University of Luxemburg. The failure mode is different. In Luxemburg all specimens failed due to shear failure of the bolts while in TU Delft the specimen loaded until failure failed due to concrete failure while the other two due to shear failure of the bolts. Moreover, in TU Delft the shear connectors behaved in a very ductile manner in the specimen R1 which failed due to concrete failure and also in a ductile manner in the other two specimens according to Eurocode while the shear connectors in the University of Luxemburg behaved in a brittle manner in all tests.

3.7 Comparison with other types of shear connectors

A lot of research has been conducted in order to examine the behaviour of demountable shear connectors. The results derived from the push-out tests for the specimens with resin injected bolts are compared with the results derived from other researches on other type of shear connectors. In the following graph the force-slip curves obtained from push-out tests on friction grip bolts, single embedded nut bolts, without embedded nut bolts and welded headed studs are compared with the one obtained from the first push-out test with resin injected bolts that was loaded until failure where:

RB: resin bolts

FGB: friction grip bolts

SENB: single embedded nut bolts

WENB: without embedded nut bolts

WHS: welded headed studs

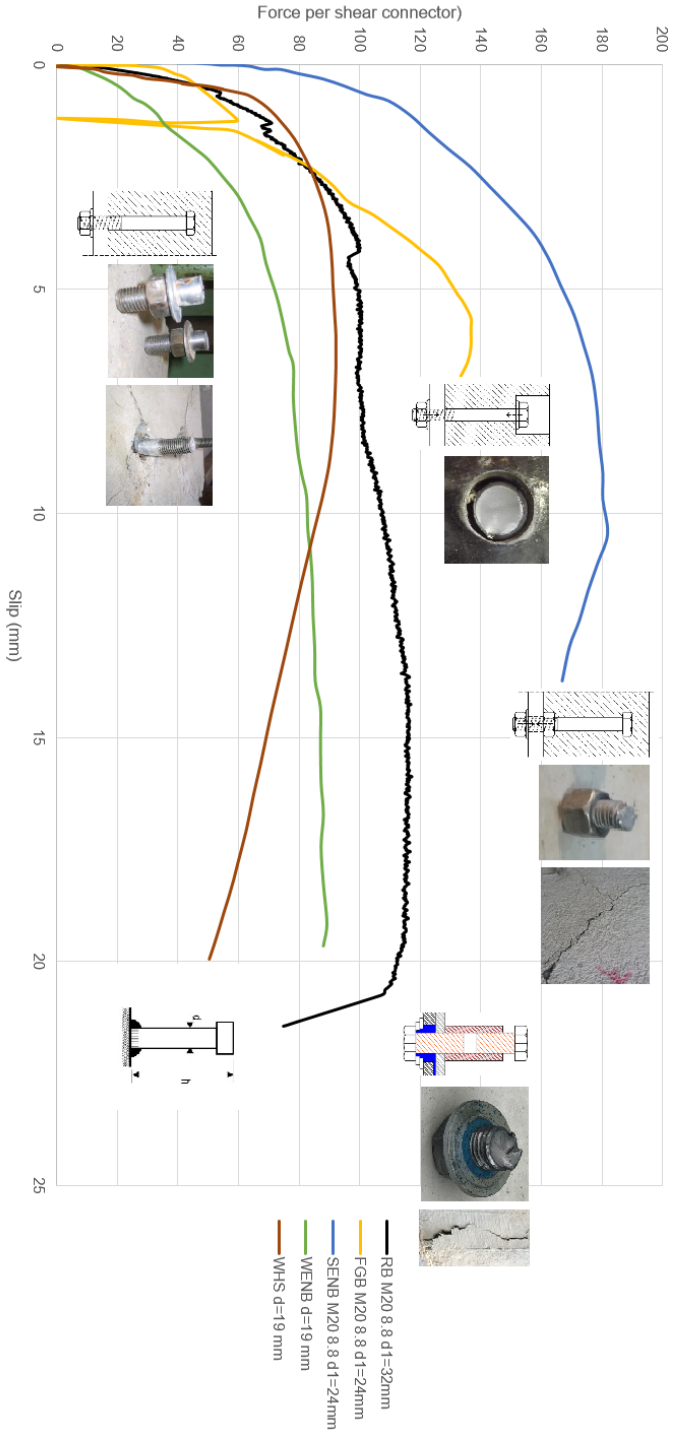

Figure 3.26: Comparison of push-out tests with other types of shear connectors [31], [28], [26]

Resin injected bolts have 82% and 65% of the friction grip bolts' and single embedded nut bolts' maximum force per shear connector respectively and lower stiffness. Marshall (1971) performed experiments and proved that the bolt preloading increases the capacity of the joint [32]. Friction grip bolts and single embedded nut bolts were preloaded before the experiments. Hence, the force per shear connector and stiffness are higher compared to other types of shear connectors. Bolts without embedded nut and welded headed studs have almost the same maximum force per shear connector which is 80% of that of resin injected bolts. However, welded headed studs have a higher initial stiffness than resin injected bolts while bolts without embedded nut have the lowest initial stiffness.

In all experiments the slip is higher than 6 mm so all the demountable shear connectors behave in a ductile manner except for the specimens with resin injected bolts, some of which had slip higher than 6 mm and some a little lower than 6 mm.

The failure mode was different. In cases of specimens with friction grip bolts the failure mode was shear failure of the connector. In case of specimens with bolts without embedded nut and welded headed stud the failure mode was crushing of concrete. All specimens had almost the same concrete cubic strength varied from 40 to 48 MPa except for concrete decks in specimens with bolts without embedded nut and welded headed studs which had lower concrete strength equal to 29.9 MPa. This explains the crushing of concrete in specimens with bolts without embedded nut and welded headed studs. In case of specimens with resin injected bolts and single embedded nut bolts, some specimens failed due to shear failure of the bolts and some others due to concrete failure.

3.8 Conclusions

Six push-out tests have been conducted in order to investigate the shear strength, the stiffness and ductility of resin injected bolts in steel-concrete composite structures. The following conclusions may be drawn:

1. The shear capacities of all specimens did not differ significantly, the average maximum force per shear connector is 116.9 kN.
2. Two failure modes were observed: concrete failure and shear failure of the bolts. Tests that were loaded until failure failed due to concrete failure because many cracks were observed in concrete during the experiment while tests under cyclic loading failed due to shear failure of the bolts and no cracks were observed in concrete.
3. The type of loading affected the failure mode. In case of cyclic loading, steady openings of cracks occur due to the cycles, so the energy is not released and no cracks occur in concrete.
4. In the specimens that failed due to concrete failure, the shear connectors behaved very ductile. In the specimens that failed due to shear failure of the bolts, the shear connectors behaved either ductile according to Eurocode as the slip was higher than 6 mm which is the limit for a ductile behaviour or brittle but the slip was close to the limit for a ductile behaviour.
5. The reinforcement in resin increases the second stiffness 341%.
6. Leakage of resin around the hole in the steel section was observed after demounting of the specimens. Hence, the resin injection procedure affected the final results.
7. Resin injected bolts have 82% and 65% of the friction grip bolts' and single embedded nut bolts' maximum force per shear connector respectively and lower stiffness.

8. Bolts without embedded nut and welded headed studs have almost the same maximum force per shear connector which is 80% of that of resin injected bolts. However, welded headed studs have a higher initial stiffness than resin injected bolts while bolts without embedded nut have lower stiffness.

4 Numerical Analysis

Although experiments in the lab provide more accurate and valuable results, it is a more expensive and time consuming process. The advances in computer technology has led to the existence of various sophisticated three-dimensional Finite Element Analysis softwares. So in order to check the validity of the push-out tests that conducted in the laboratory, Finite Element Models were developed with the use of the software ABAQUS/CAE 6.14-5. ABAQUS is an advanced Finite Element Analysis software that is widely used in civil engineering applications. The results of the Finite Element Analyses will be compared with the experimental work.

The description of the Finite Element models, same as the ones used in the experiments, is given in this section. The geometry, the properties, the boundary conditions, the meshing, the loading step and the results of the analysis of the models are presented below.

4.1 Geometry and assembly

The Finite Element models consisted of the same components as in push-out tests: steel sections, L-angle profiles, concrete slabs, reinforcement bars, washers, embedded couplers, embedded bolts and resin injected bolts. For simplification purposes, the threaded part of the bolt was omitted and the diameter d=17.66 mm of the non-threaded part of the bolt was considered. The embedded bolt, the embedded coupler and the reinforced resin injected bolt were merged into one part as depicted in figure 4.1.a. The reinforcement bars were modelled as cables inside the concrete as depicted in figure 4.1.b.

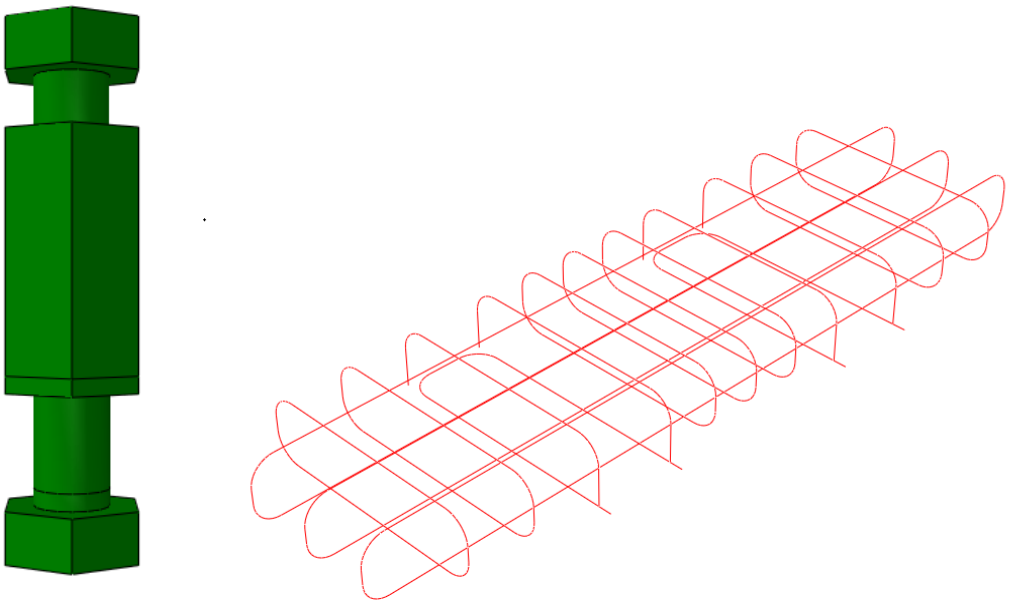

a) Bolt b) Reinforcement bars

Figure 4.1: Geometry of the bolts and the reinforcement bars

All parts were modelled separately and then assembled to create the final model. A quarter of the real specimen was modelled with double symmetry. The assembled model is depicted in figure 4.2 and the cross section of the shear connector system in figure 4.3.

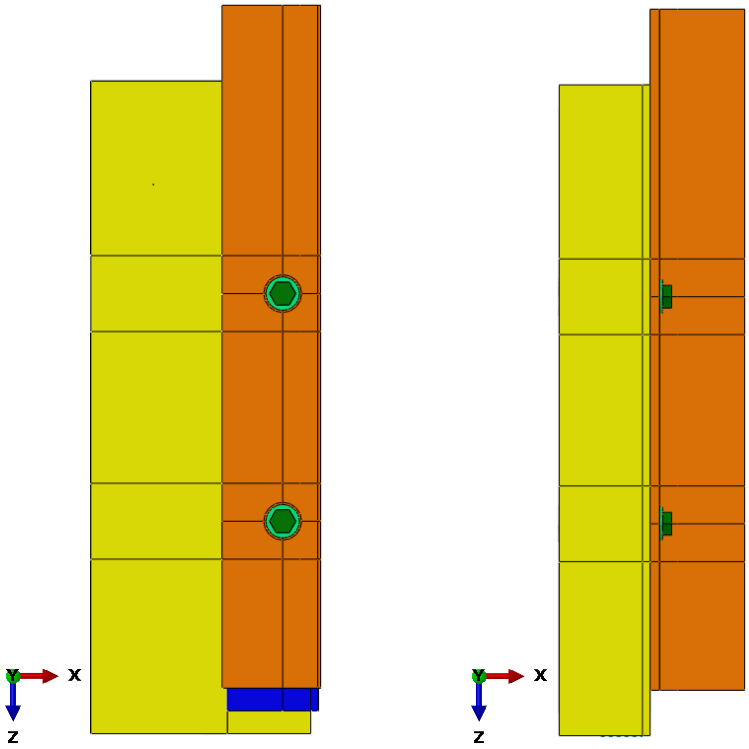

a) Front view b) Side view

Figure 4.2: Finite Element models geometry

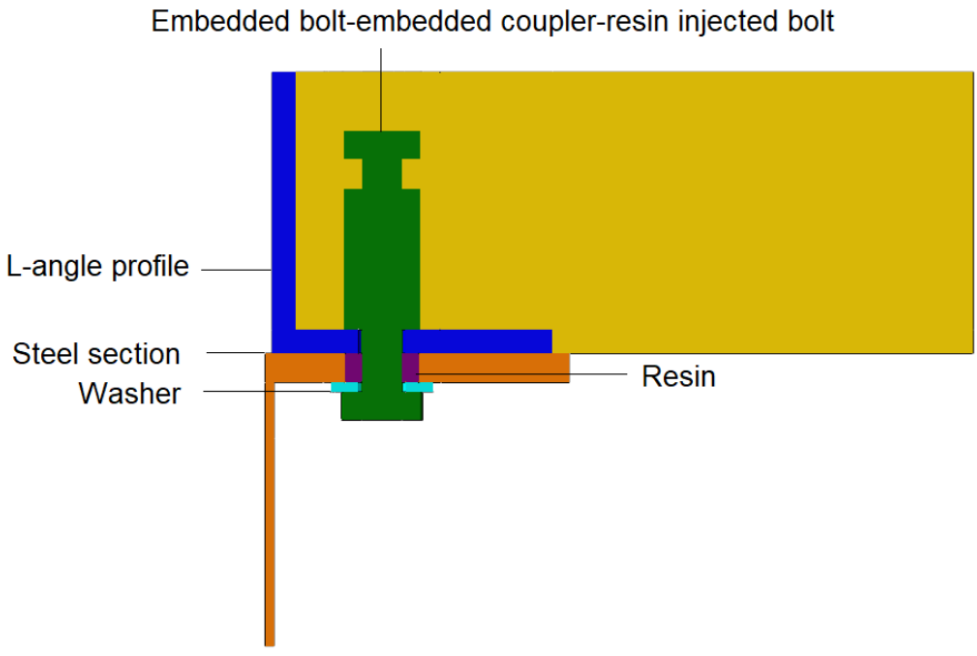

Figure 4.3: Cross section of shear connector system in Finite Element models

4.2 Boundary conditions and interactions

In order to save computational time, one quarter of the push-out test specimen was built. Symmetrical boundary conditions were applied in the steel section in x and y direction as depicted in figure 4.4. The bottom of the concrete deck was considered as fully fixed except for a lateral translation U_2 in order to simulate the concrete slab lying on the layer of gypsum [42]. The lateral restraint stiffness was calibrated to a value of 15 kN/mm in order to match the experimental results.

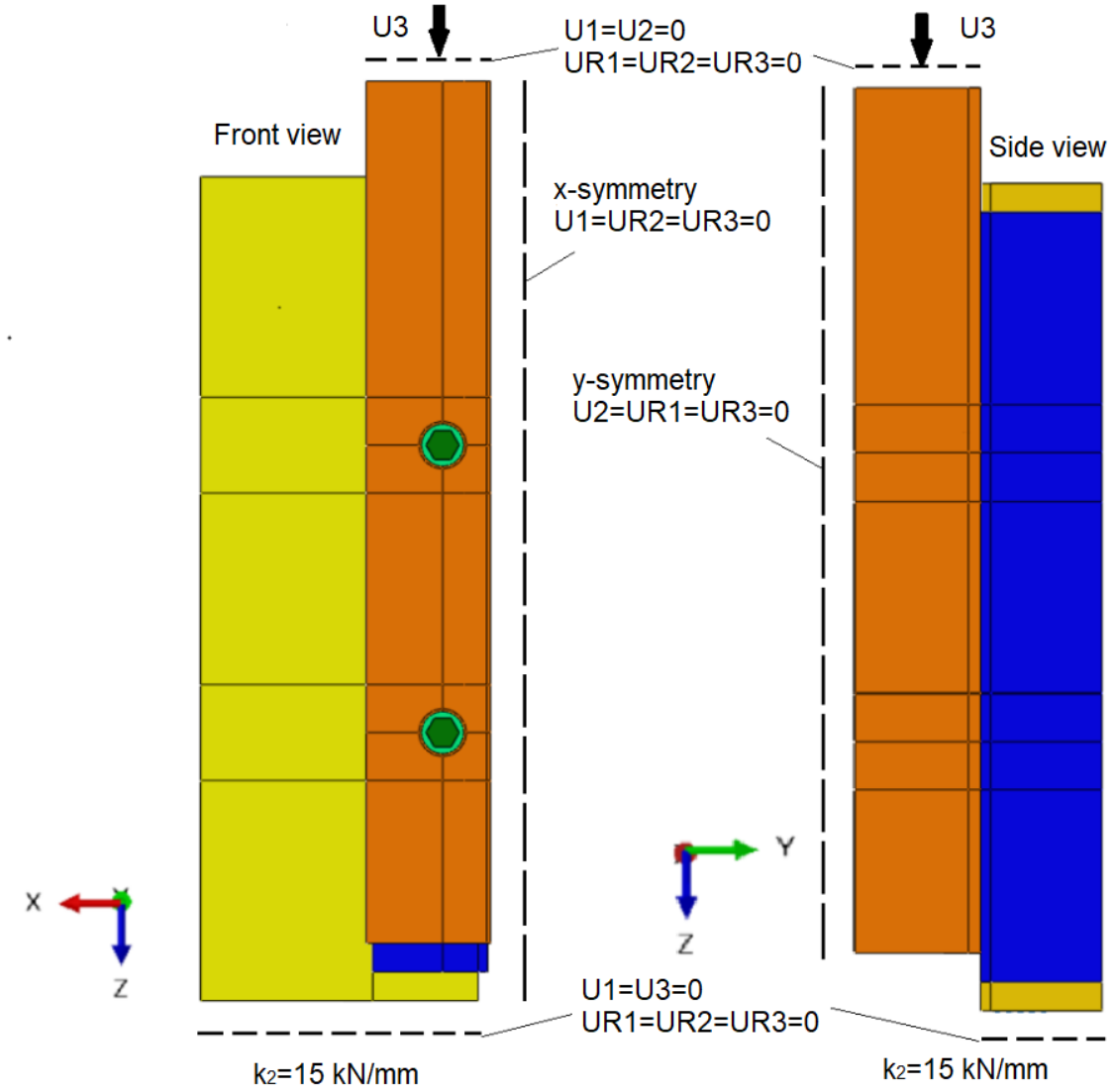

Figure 4.4: Boundary conditions

The general contact interaction with normal behaviour and tangential behaviour with friction coefficient 0.1 were chosen for all the surfaces of the model. Embedded region constraint was used to embed the reinforcement bars within the concrete. In experiments, the specimens were sprayed with a release agent in order to prevent adhesion and allow for an easy separation of the components. So the resin does not adhesively bond with any other part and general contact interaction was chosen for the interfaces of resin with the other parts.

4.3 Finite element mesh

Hexahedral solid brick 8-node elements with reduced integration (C3D8R) are generally used to mesh models because they lead to less computational run time. Due to complex geometry of the model, tetrahedron elements (C3D4) were used to mesh most of the parts. Hexahedral elements were used to mesh the steel section, the L-angle profile and the washers while tetrahedral elements were used to mesh the embedded bolt- embedded coupler- resin injected bolt part and the concrete deck.

Different mesh size was used for the parts in relation to their size and importance. The resin, the steel flange holes, the L-angle profile holes, the part of the bolt inside the holes and concrete areas near the bolts were meshed with element size 1.2 mm because in these regions higher deformations are expected to occur. The washers were meshed with element size 2 mm. In remote area, the concrete was meshed with 10 mm elements while the L-angle profile and the steel section with 5 mm elements. The reinforcement bars were also meshed with size 4 mm.

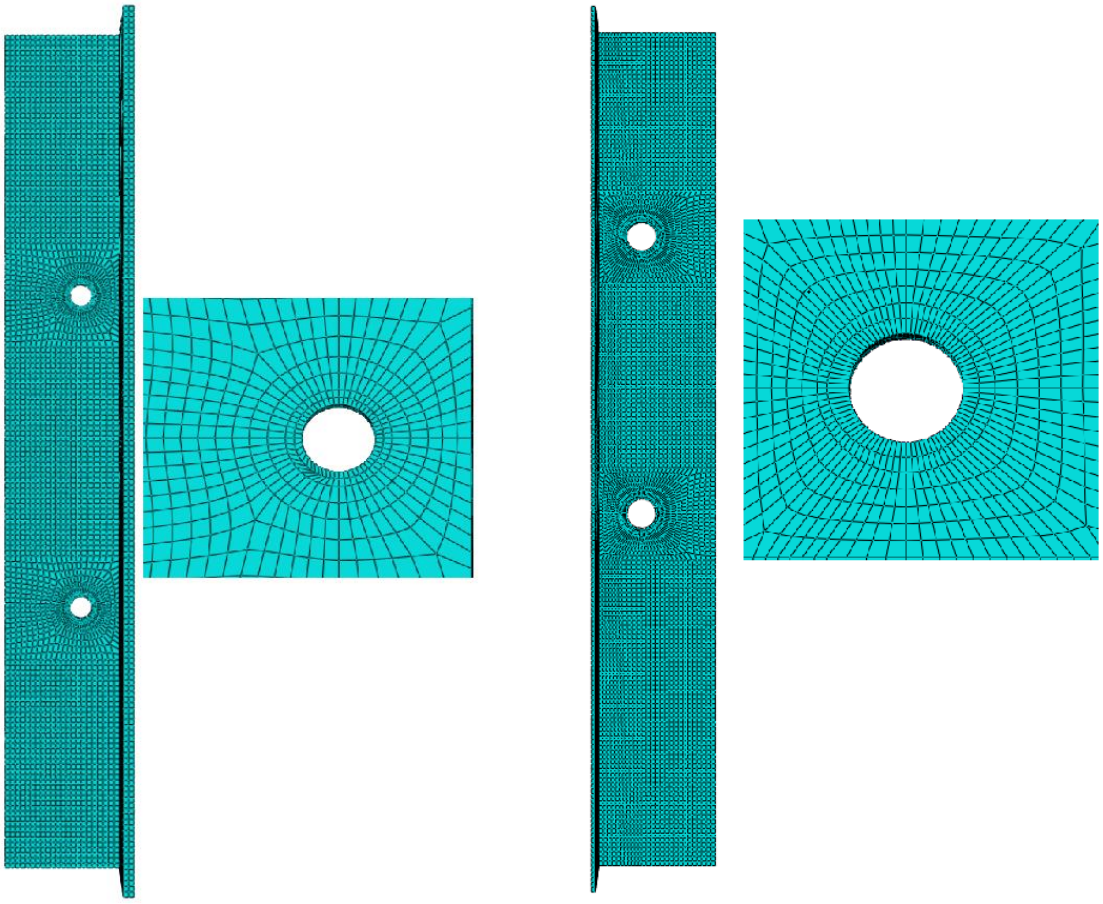

a) L-angle

b) Steel section

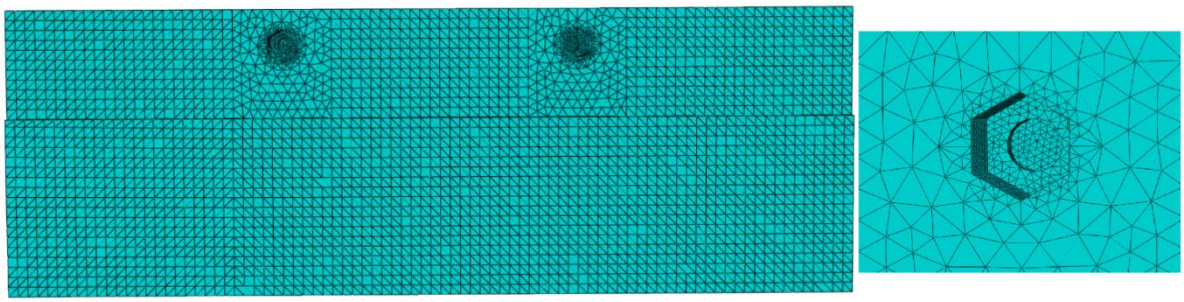

c) Concrete

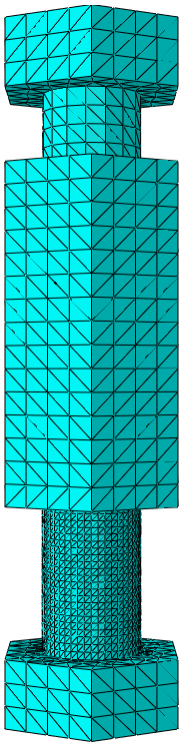

d) Embedded bolt-embedded coupler-resin injected bolt

Figure 4.5: Finite element model mesh

4.4 Properties and material models

Young modulus of elasticity E=210000 MPa and Poisson ratio v=0.3 were used for the steel section and the L-angle profile with a steel grade S355, the reinforcement bars and the bolts with grade 8.8. In experiments, the nominal class of concrete decks was C30/37 but when the cubic compressive strength was measured was equal to 48 MPa which matches the concrete strength class C40/50. For this reason, in FEA the concrete decks have strength category C40/50 with Young's modulus of elasticity E=33000 MPa and Poisson ratio v=0.2. Young modulus of elasticity E=5640 MPa and Poisson ratio v=0.3 were used for the resin while Young modulus of elasticity E=15200 MPa and Poisson ratio v=0.22 were used for the reinforced resin.

Five material damage models incorporating progressive damage behaviour have been used for the parts of the models which were derived from Pavlovic's doctoral dissertation [42]. The behaviour of the shear connection depends on the properties of the bolts and concrete material models and subsequently focus has been put on these material models.

Ductile and shear damage models were applied for the embedded bolt- embedded coupler-resin injected bolt part. In progressive damage it is assumed that different failure mechanisms develop simultaneously on a material. Material losses its load-carrying capacity and fails due to progressive degradation of the material stiffness. For the steel damage model the stress-strain curve was obtained from tensile test coupons. Three phases are distinguished as depicted in figure 4.6, in the first one (a-b) the material behaves linear elastically, in the second one (b-c) plastic yielding occurs and in the third one (c-d) the material ruptures. The onset of damage occurs at point c (damage initiation) and after point c the material losses its load bearing capacity (damage evolution). The ductile damage model was validated with tensile test coupons while the shear damage model with bolt shear tests.

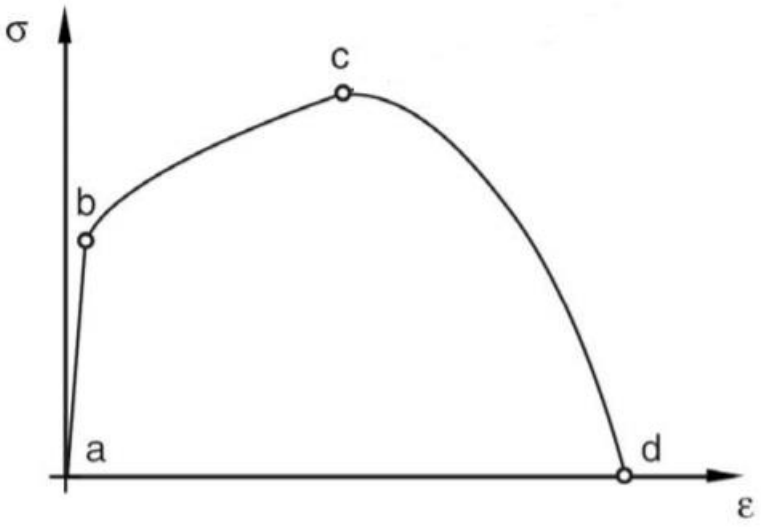

Figure 4.6: Ductile damage material model

Concrete damaged plasticity model was used in order to model the development of compressive crushing and tensile cracking in concrete. The behaviour of concrete in compression and tension was defined separately. Existing compressive stress-strain curve (EC2) has been used for the extraction of the corresponding damage curve. The parameters of the concrete damage model were calibrated according to mechanical properties of concrete from results of push-out tests. The behaviour of concrete in tension was derived in a similar way.

4.5 Loading step

Two models were run until failure. As in experiments, the models were loaded at the top surface of the steel section until failure using displacement control. A vertical displacement of

u_3=10 mm was applied on top of HEA260 and a time period of 900 seconds considered for the finite element step.

In order to avoid large inertia forces, a smooth amplitude was considered in all loading steps.

4.6 Analysis method

In order to avoid the convergence issues of the implicit static analysis, the dynamic explicit analysis was used to analyse the Finite Element models. ABAQUS/Explicit solves each problem as a wave propagation problem. The out-of-balance forces are propagated as wave stresses between the different neighbouring elements. The stable time increment is the minimum time needed for a dilatational wave to move across any element of the model. The stable time increment Δt depends on the characteristic length L_e of the element with the smallest size in the model and the dilatational wave speed c_d and is calculated according to the equation: $\Delta t = L_e/c_d$. The dilatational wave speed is equal to: $c_d = \sqrt{E/\rho}$ where E and ρ are the Young's modulus of elasticity and the current material density respectively. Mass scaling is used in order to increase the stable time increment. Mass scaling with time increment of 0.005 sec was adopted in analyses.

4.7 Validation of numerical results

A total of 2 push out tests were conducted using Finite Element Analysis. Two different test configurations were created, one with resin injected bolts and the other one with reinforced resin injected bolts, same as in the experiments. For each configuration one specimen was tested. The specimens was loaded until failure using displacement control. The basic test parameters are presented in table 4.1.

Table 4.1: FEA push-out test parameters

Test	Shear connector system	Shear connection bolts	Steel section hole diameter d1 (mm)	Number of shear connectors
FEA resin	Coupler system	Resin injected bolts	32	2
FEA reinforced resin	Coupler system	Reinforced resin injected bolts	32	2

The results of the Finite Element Analysis are compared with the results from the experiments presented in Chapter 3 in terms of shear capacity and stiffness. Due to the fact that the threaded part of the bolt was omitted and only the non-threaded part was considered in Finite Element Analysis, no comparison is made in terms of ductility.

4.7.1 Prediction for resin injected bolts

FEA force per shear connector-slip curve from push-out test for resin injected bolts M20 is shown in figure 4.7 and compared with the equivalent force-slip curves derived from the experiments.

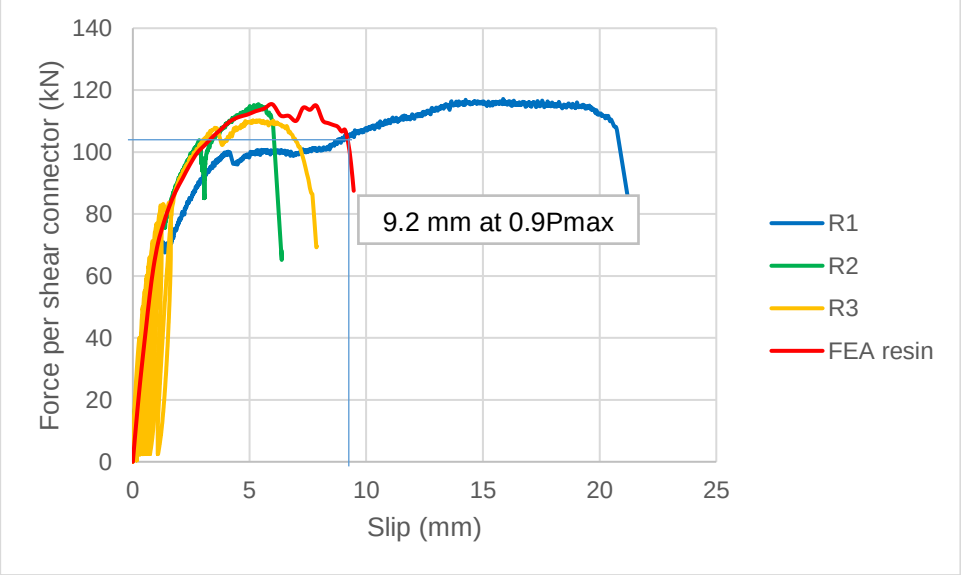

Figure 4.7: Comparison of force-slip curves between FEA resin test and experimental tests

The specimen failed due to shear failure of the bolts. Good matches accomplished in terms of curve shape and maximum force per shear connector. The maximum force per shear connector is 115.5 kN, very close to the maximum average force per shear connector obtained from the experimental tests R1, R2 and R3 which was equal to 114.3 kN. The ratio $P_{ult,FEA}$/ $P_{ult,exp}$ is equal to 1.01 as shown in table 4.2. The slip at 90% of the maximum force is equal to 9.2 mm so the shear connectors behaved in a ductile manner.

Table 4.2: Comparison of shear resistance between FEA resin test and experimental tests

Shear resistance (kN)		
FEA	Experiments	Ratio
$P_{ult,FEA}$	$P_{ult,exp}$	$P_{ult,FEA}/P_{ult,exp}$
115.5	114.3	1.01

The second stiffness of FEA specimen with resin injected bolts is calculated according to Eurocode 4 Annex B [17] and compared with the second stiffness derived from the experiments as shown in figure 4.8.

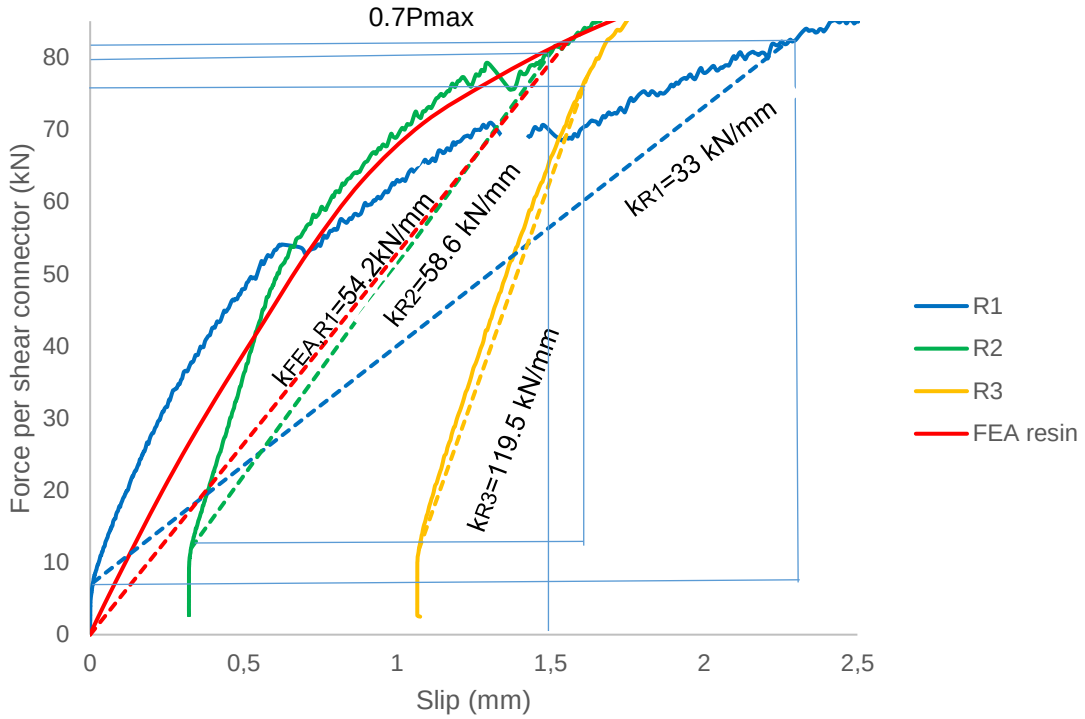

Figure 4.8: Comparison of second stiffness between FEA resin test and experimental tests

Mismatches of experimental results in terms of stiffness are evident. The amount of hydraulic oil that applied to the specimens before the experiments and the leakage of resin after the injection procedure that increased the friction affected the stiffness of the experimental tests. The second stiffness of test FEA resin is very similar to that of test R2.

Deformed shapes of bolts from experiments and FEA are compared in figure 4.9. The deformed bolt from experiments was taken after demounting of the specimens. The deformed bolt from FEA is at the stage before fracture. The deformed shape of the FEA bolts is similar to that of experimental bolts. As it was expected, the maximum von Mises stresses of the bolt occur at the steel section-concrete interface where failure develops.

Concrete damage at the interface layer from experiments and FEA is compared in figure 4.10. The compressive damage of concrete (DAMAGEC) derived from Abaqus software is compared with the damage of the concrete deck derived after demounting of specimens in the lab. As it is obvious from figure 4.10, concrete has been severely damaged in the area around the bolt. Similarities of damaged areas between experimental and FEA results are obvious.

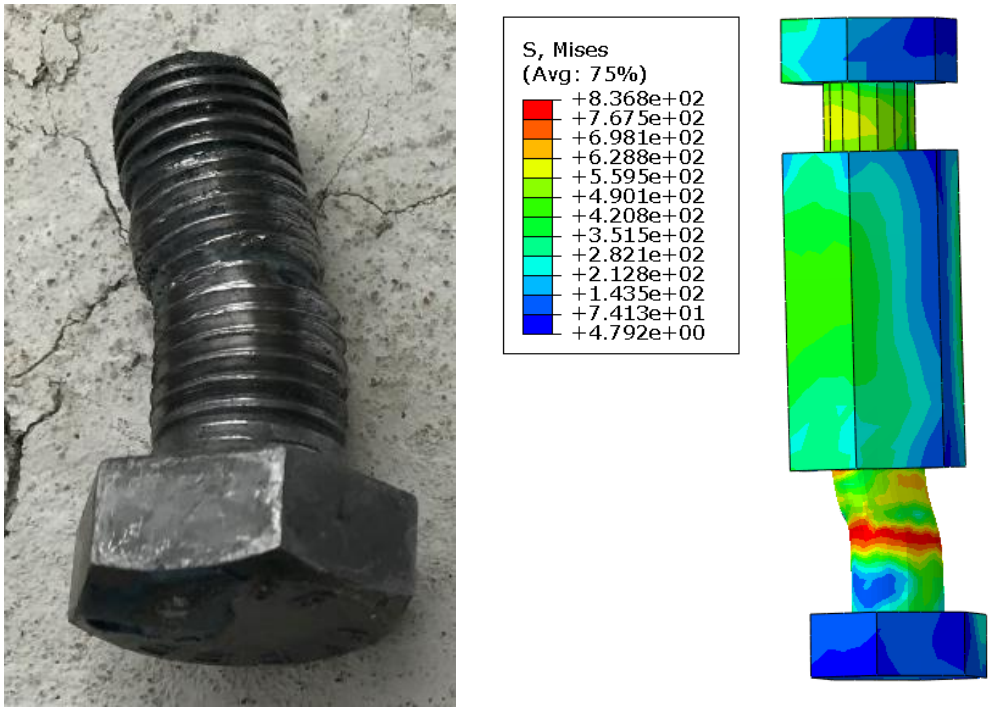

a) Experiments b) FEA

Figure 4.9: Comparison of deformed shape of bolts between FEA resin test and experimental test

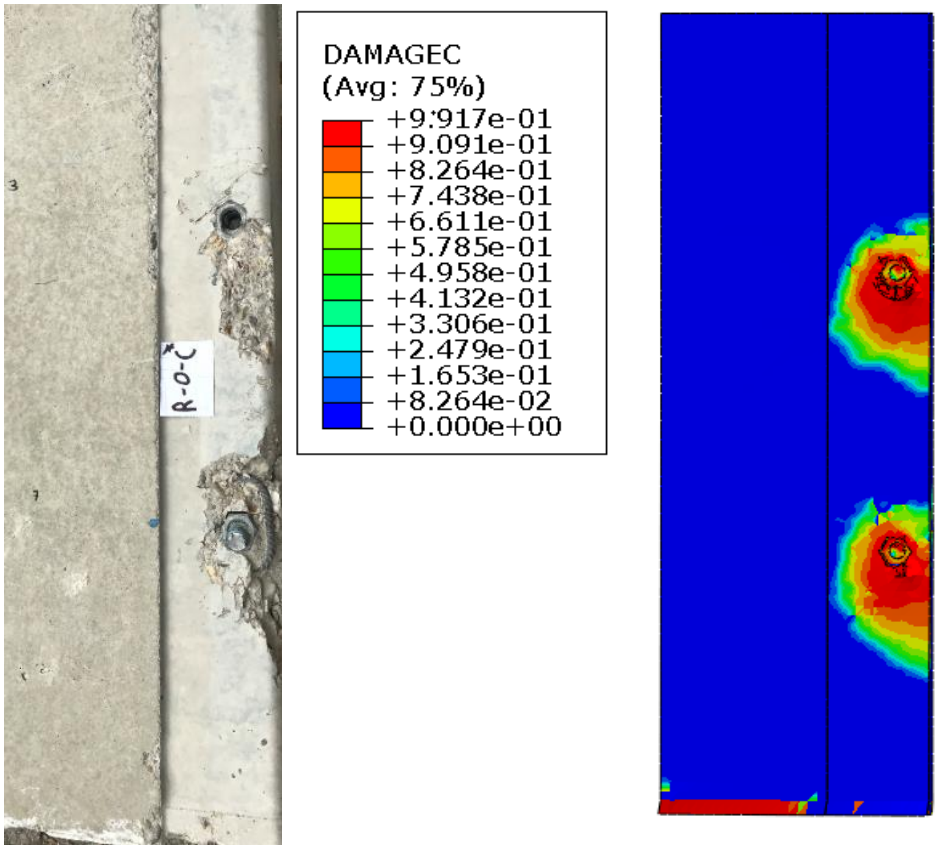

Figure 4.10: Comparison of concrete damage of bolts between FEA resin test and experimental test

4.7.2 Prediction for reinforced resin injected bolts

In figure 4.11, the force per shear connector-slip curve derived from FEA push-out test for reinforced resin injected bolts M20 is presented and compared with the equivalent force-slip curves derived from the experiments.

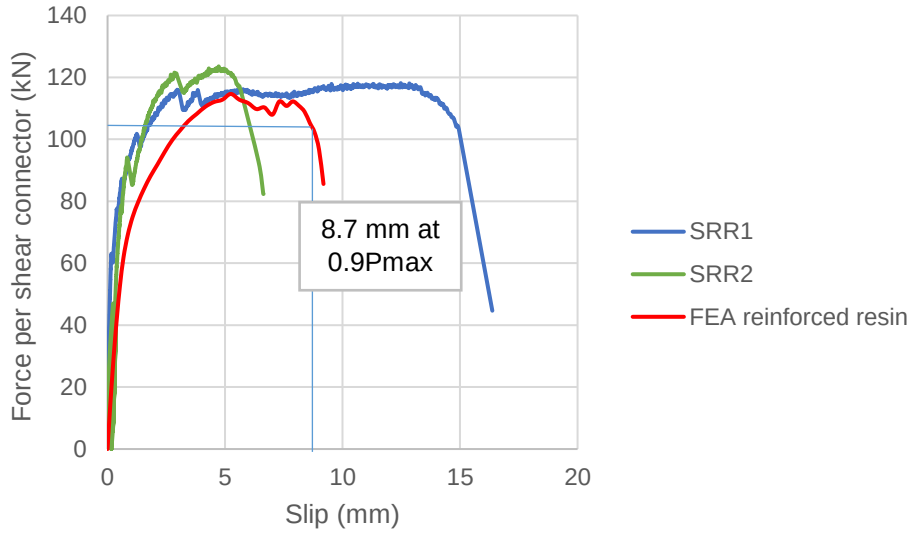

Figure 4.11: Comparison of force-slip curves between FEA reinforced resin test and experimental tests

Good matches accomplished in terms of maximum force per shear connector. The maximum force per shear connector is 114.7 kN, very close to the maximum average force per shear connector obtained from the experimental tests SRR1 and SRR2 which was equal to 120.9 kN. As depicted in table 4.3 P_{ult} from experiments and FEA is matching well with a ratio of 0.95. The specimen failed due to shear failure of the bolts and the slip at 90% of the maximum force is 8.7 mm which indicates a ductile behaviour of the shear connectors.

Table 4.3: Comparison of shear resistance between FEA reinforced resin test and experimental tests

Shear resistance (kN)		
FEA	Experiments	Ratio
$P_{ult,FEA}$	$P_{ult,exp}$	$P_{ult,FEA}/P_{ult,exp}$
114.7	120.9	0.95

The second stiffness of FEA specimen with reinforced resin injected bolts is compared with the second stiffness derived from the experiments as shown in figure 4.12.

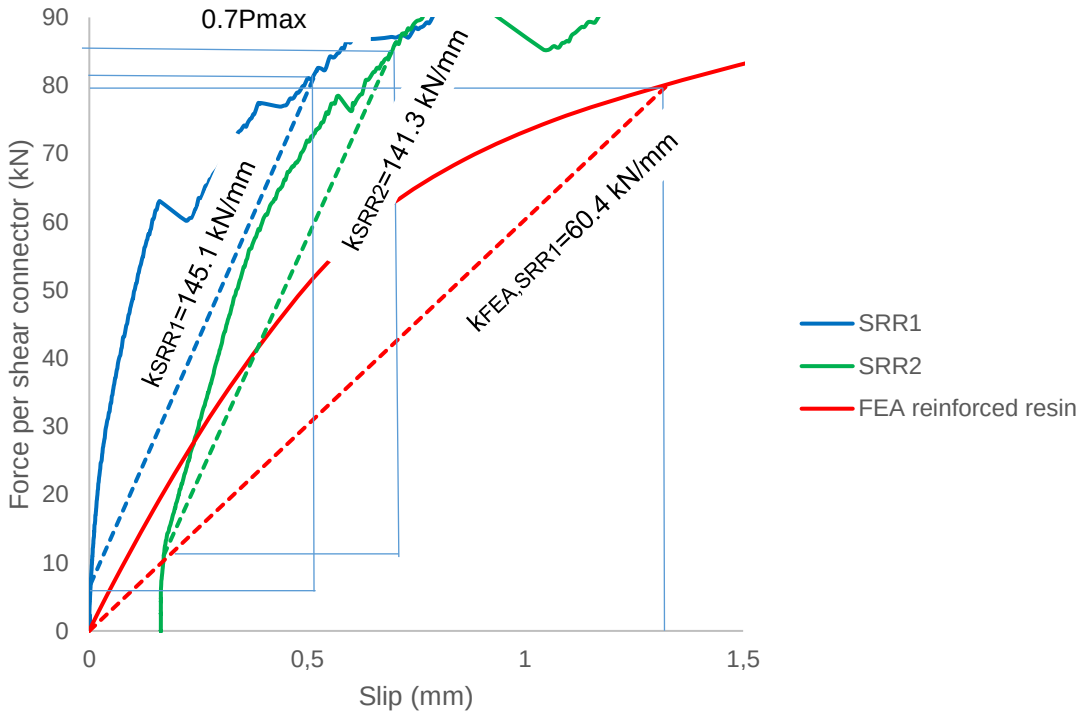

Figure 4.12: Comparison of second stiffness between FEA reinforced resin test and experimental tests

Mismatches of second stiffness between experimental results and FEA are obvious. In experiments the second stiffness is two times higher than in FEA. The increased stiffness derived from experimental results indicates high friction between steel and concrete. This high friction occurred from the leakage of resin around the hole in the steel section during the resin injection procedure.

Deformed shapes of bolts from experiments and FEA are compared in figure 4.13. The deformed shape of the FEA bolts at the stage before failure is similar to that of experimental bolts derived after demounting of the specimens. As in case of resin injected bolts, the maximum von Mises stresses of the bolt occur at the steel section-concrete interface where failure develops.

Concrete damage at the interface layer from experiments and FEA is compared in figure 4.14. Both in the FEA and experimental results concrete has damaged around the holes, but in case of experiments damage of concrete is also observed in the area between the holes. A possible reason is that during demounting of the specimens, when the L-angle profile was removed, concrete must have been damaged.

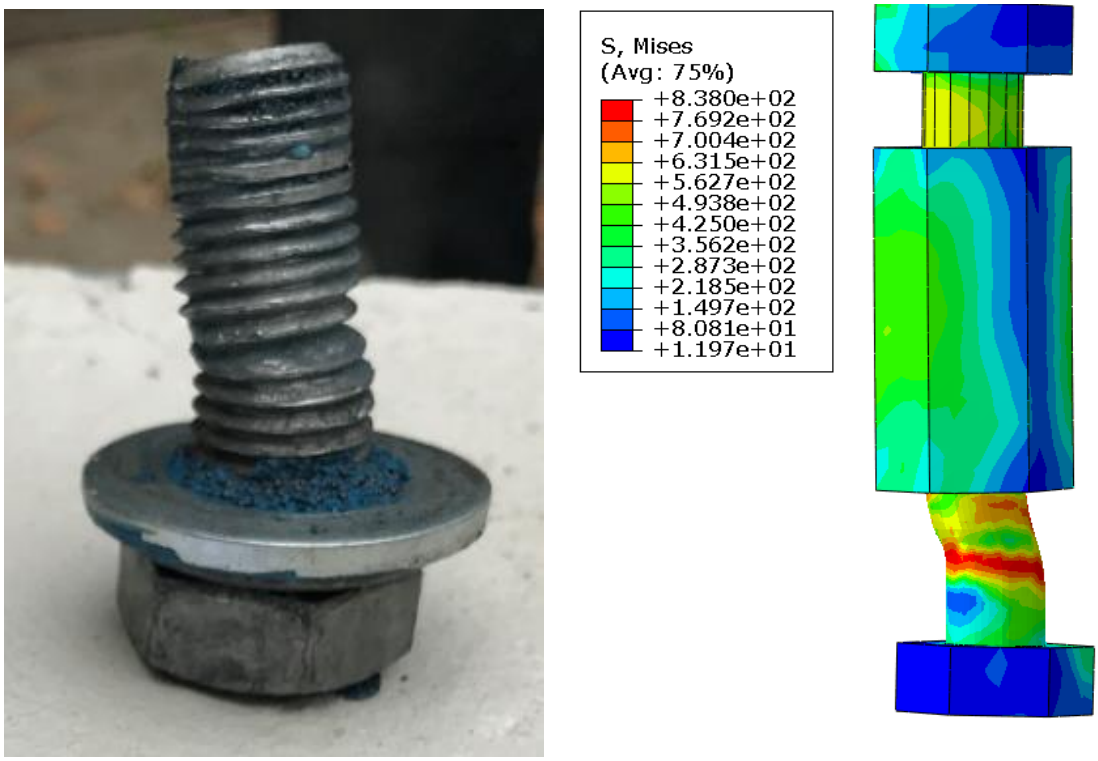

Figure 4.13: Comparison of deformed shape of bolts between FEA reinforced resin test and experimental test

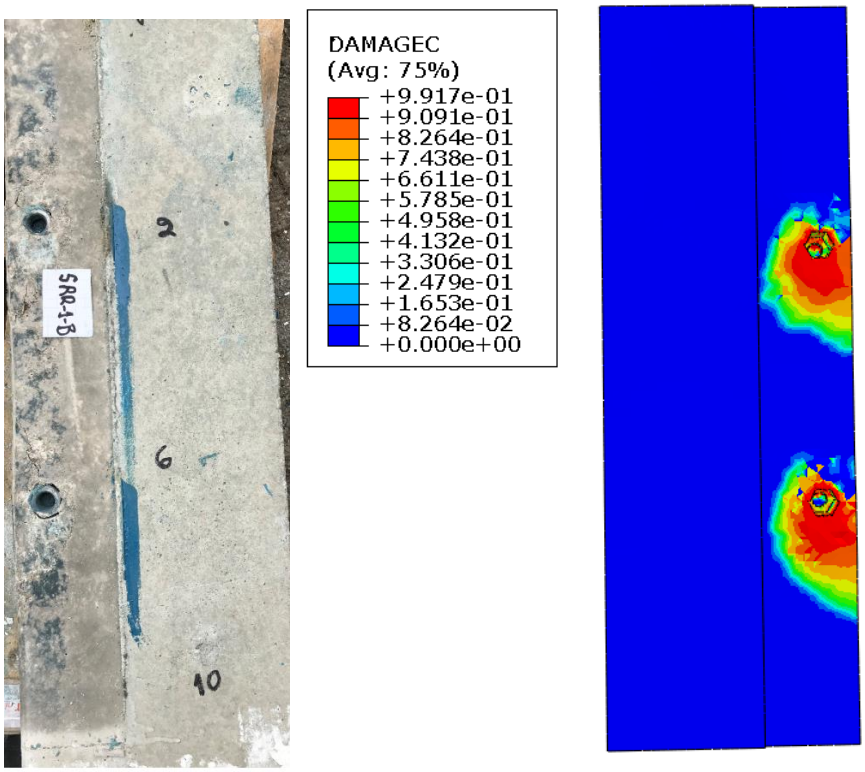

Figure 4.14: Comparison of concrete damage of bolts between FEA reinforced resin test and experimental test

4.8 Comparison between test FEA with resin injected bolts and test FEA with reinforced resin injected bolts

In figure 4.15 the force per shear connector-slip curve derived from FEA push-out test for resin injected bolts M20 is compared with the equivalent force-slip curve derived from FEA push-out test for reinforced resin injected bolts M20. Moreover, a comparison of the second stiffness between model FEA with resin injected bolts and FEA with reinforced resin injected bolts is made and presented in figure 4.16.

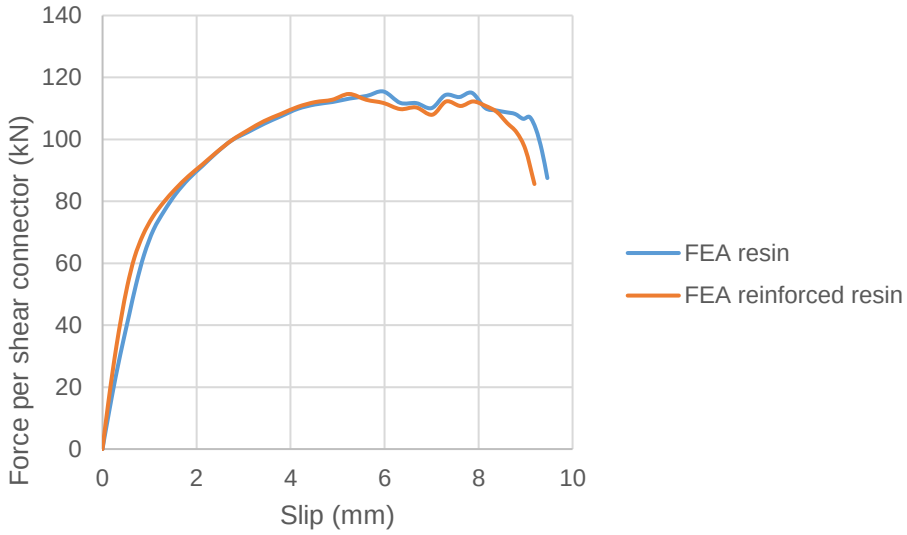

Figure 4.15: Comparison of force-slip curves between FEA resin and FEA reinforced resin test

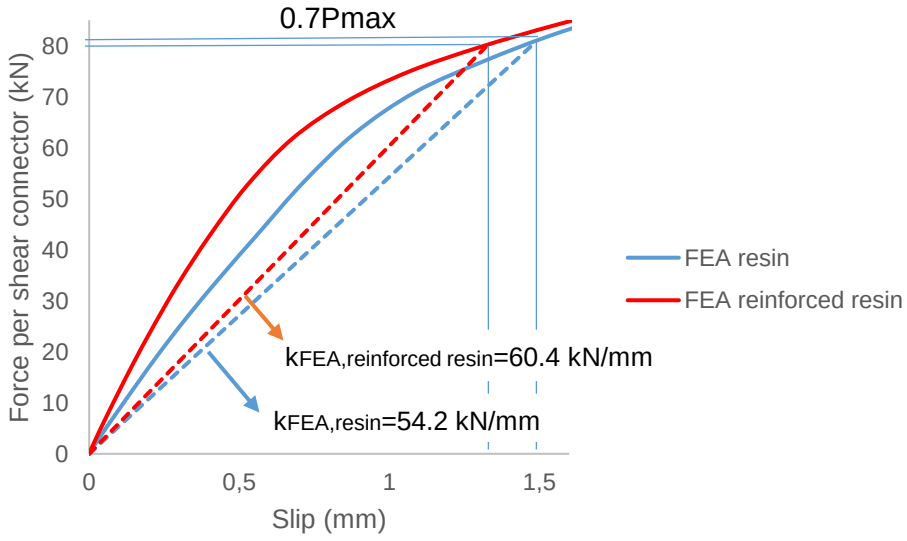

Figure 4.16: Comparison of second stiffness between FEA resin and FEA reinforced resin test

As it is obvious from figure 4.15, the curve shapes are almost the shame, the only difference is the stiffness. The maximum force per shear connector in case of resin injected bolts is 115.5 kN while in case of reinforced resin injected bolts 114.7 kN. The second stiffness in case of resin injected bolts at 70% of the maximum force is equal to 54.2 kN/mm and in case of reinforced resin injected bolts is equal to 60.4 kN/mm, 11.4% higher. In experiments the second stiffness in case of reinforced resin injected bolts was two times that of resin injected bolts. This happened due to the leakage of resin during the injection procedure that increased the friction between steel and concrete and thus the stiffness. Consequently, the reinforcement in resin does not have any effect on the shear resistance but it does affect the stiffness.

4.9 Conclusions

Two FE push-out tests have been conducted, one with resin injected bolts and one with reinforced resin injected bolts. The results are compared with the experimental ones. The following conclusions may be drawn:

1. Results from the experiments and FEA show good accordance in terms of shear capacity with an average ratio of $P_{ult,FEA}/P_{ult,exp}$ equal to 1.01 and 0.95 in case of resin and reinforced resin injected bolts respectively.
2. The leakage of resin that occurred during the resin injection procedure before the execution of the experiments increased the friction between steel and concrete which affected the stiffness. Therefore, the comparison of the second stiffness from experiments with the second stiffness from FEA models is not successful.
3. According to FEA the reinforcement in resin does not affect the shear resistance but it affects the second stiffness, which is 11.4% higher.

5 Parametric study

A variety of parameters were used to examine their effect on the shear capacity and stiffness of the resin injected bolted connections. The parametric study was performed with the use of the ABAQUS software. The same boundary conditions and interactions, finite element mesh, material models and loading step were used as described in chapter 4. The parameters examined and the results of the analysis are presented in this chapter.

5.1 Parameters and ranges

The parameters considered in this study are: the concrete strength class, the bolt strength class, the resin injected bolt diameter class, the embedded bolt height, the steel section hole diameter, detailing of the deck and the injection material. The ranges of the parameters are presented in table 5.1.

Table 5.1: Parameters and ranges considered in FEA parametric study

Parameter	Range
Concrete strength class	C20/25, C30/37,C40/50, C50/60
Bolt diameter class	M16, M20, M24
Bolt strength class	4.6, 8.8, 10.9
Embedded bolt height (mm)	40, 60, 80
Steel section hole diameter (mm)	24, 32, 40
Detailing of the deck - L-angle profile	with, without
Injection material	resin, steel

5.2 Effect of the different parameters on the shear resistance and stiffness of the connection

5.2.1 Concrete strength class

Four FEA models were created in order to investigate the effect of concrete strength class on the behaviour of resin injected bolted shear connections. In all models bolts were M20 with strength class 8.8 but four different concrete strength classes were considered: C20/25, C30/37, C40/50 and C50/60. The force-slip curves obtained from FEA are presented in figure 5.1 and the maximum forces per shear connector derived from the curves are presented in table 5.2.

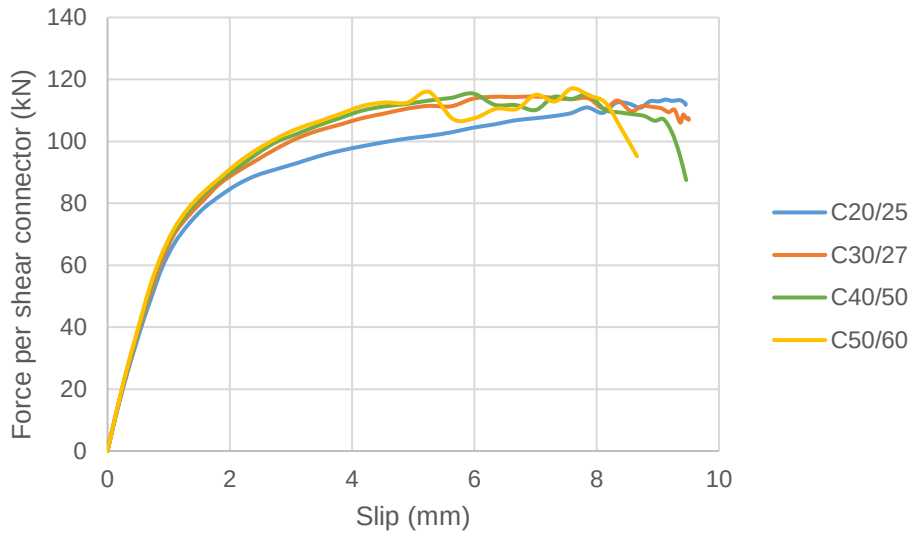

Figure 5.1: Force-slip curves for different concrete strength classes

As it can be seen in figure 5.1, the curve shapes for concrete strength classes C30/37, C40/50 and C50/60 are very similar and only the curve shape for concrete C20/25 differs slightly. The ABAQUS models with concrete strength classes C20/25 and C30/37 failed due to concrete failure while the models with classes C40/50 and C50/60 failed due to shear failure of the bolts. The maximum force per shear connector increases only 3% when the concrete strength class increases from C20/25 to C50/60. Consequently, the concrete strength class does not affect the maximum resistance of the shear connection.

Table 5.2: Shear resistance for different concrete strength classes

Concrete strength class	C20/25	C30/37	C40/50	C50/60
Shear resistance (kN)	113.5	114.5 (1%↑)	115.5 (2%↑)	117.1 (3%↑)

A comparison of the second stiffness of the force per shear connector-slip curves for the different concrete strength classes at 70% of the maximum resistance is made and presented

in figures 5.2 and 5.3. The second stiffness increases 14% when the concrete strength class increases from C20/25 to C50/60. The small increase of initial stiffness was expected as the Young modulus of Elasticity of concrete increases 23% from C20/25 to C50/60.

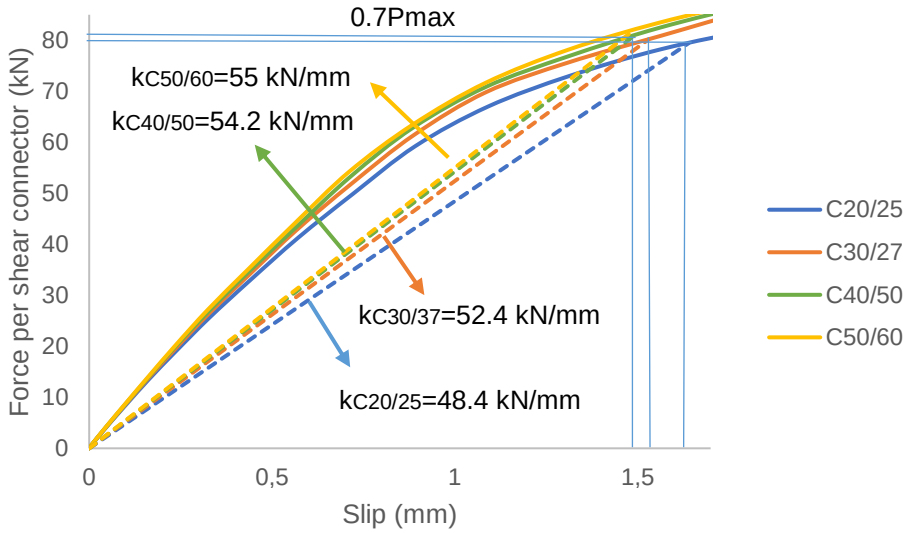

Figure 5.2: Second stiffness for different concrete strength classes

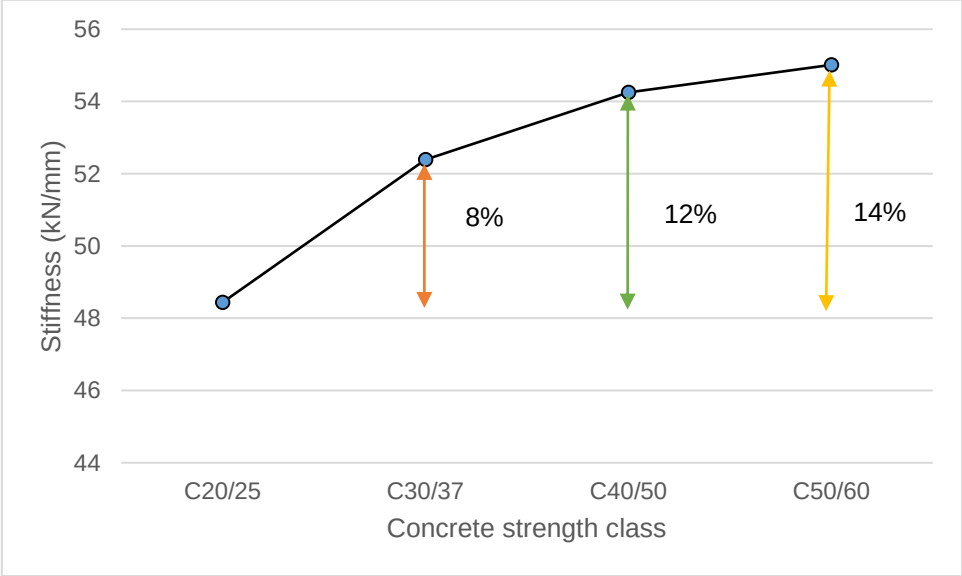

Figure 5.3: Comparison of second stiffness for different concrete strength classes

The stiffness degradation (SDEG) and the concrete compressive damage (DAMAGEC) derived from ABAQUS software are compared for the different concrete strength classes in figures 5.4 and 5.5 respectively. Even though the force per shear connector-slip curves are very similar, both the stiffness degradation and the compressive damage of concrete around the bolt decrease from strength class C20/25 to C50/60.

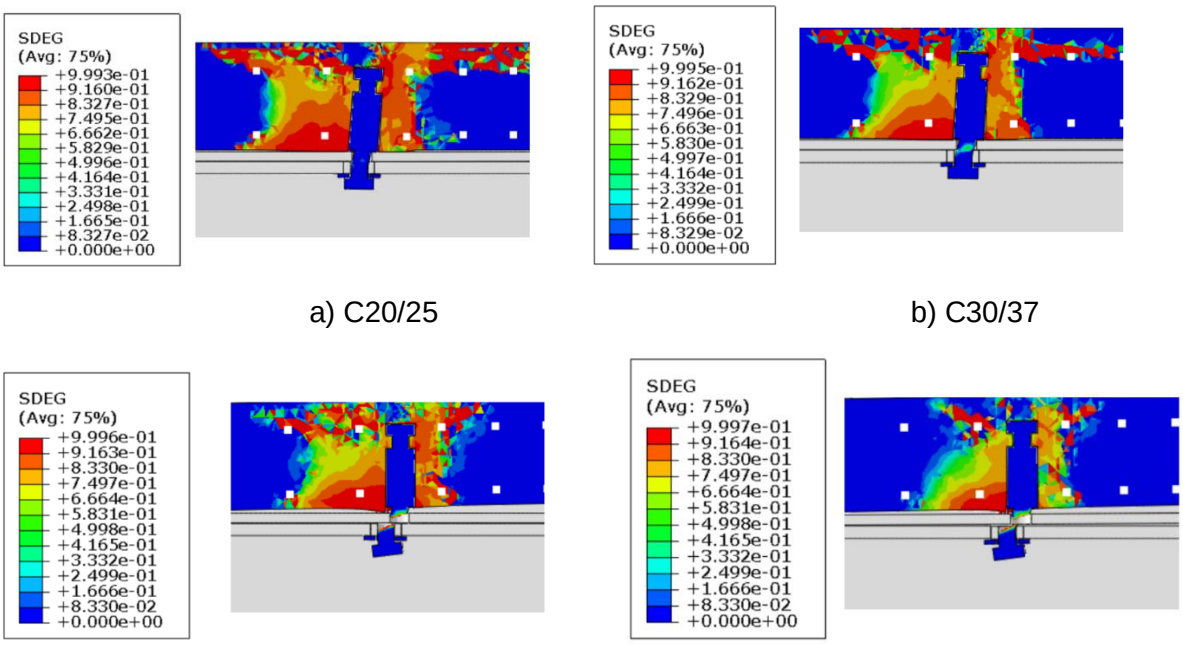

Figure 5.4: Comparison of stiffness degradation for different concrete strength classes

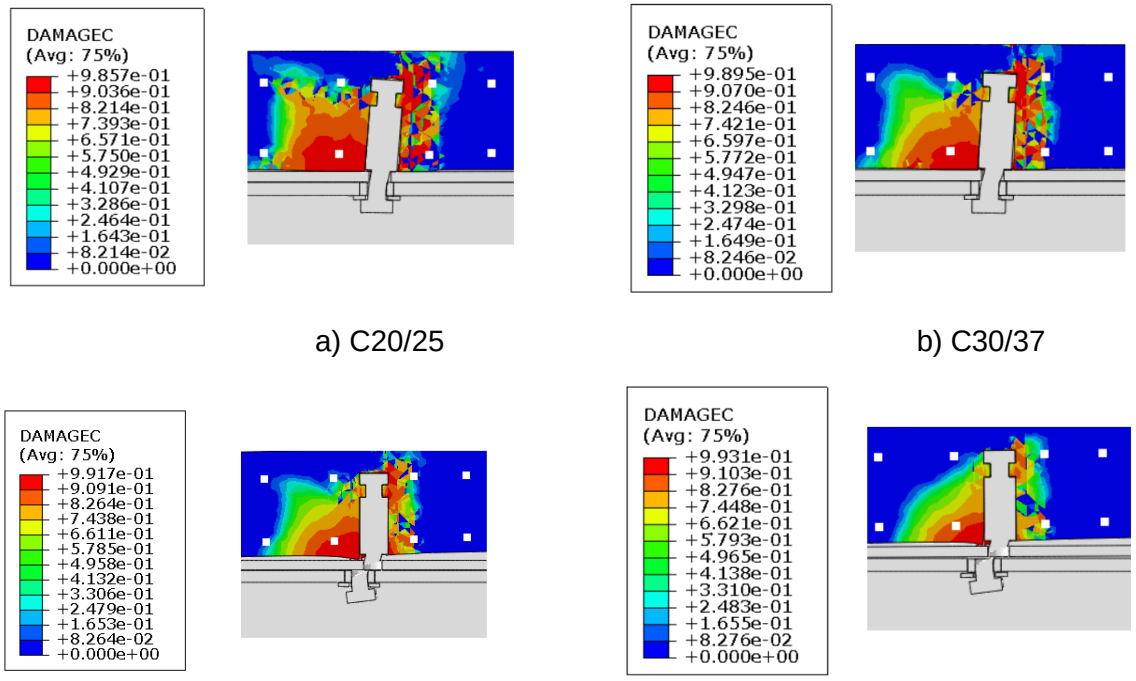

Figure 5.5: Comparison of concrete compressive damage for different concrete strength classes

5.2.2 Bolt diameter

In order to examine the influence of the bolt diameter on the shear resistance of resin injected bolts, three FEA models were created with same concrete strength class C40/50 and bolt strength class 8.8 but with bolts M16, M20 and M24. The threaded part of the bolt was omitted and the diameters of the bolts were 14.14, 17.66 and 21.2 mm for the M16, M20 and M24 bolts respectively based on the net cross section area of the bolt. The dimension of the embedded coupler also changed according to DIN6334. The cross section of the FEA models for the different bolt diameters is presented in figure 5.6. The force per shear connector-slip curves obtained from the FEA are presented in figure 5.6 and the maximum forces per shear connector derived from the curves are presented in table 5.3.

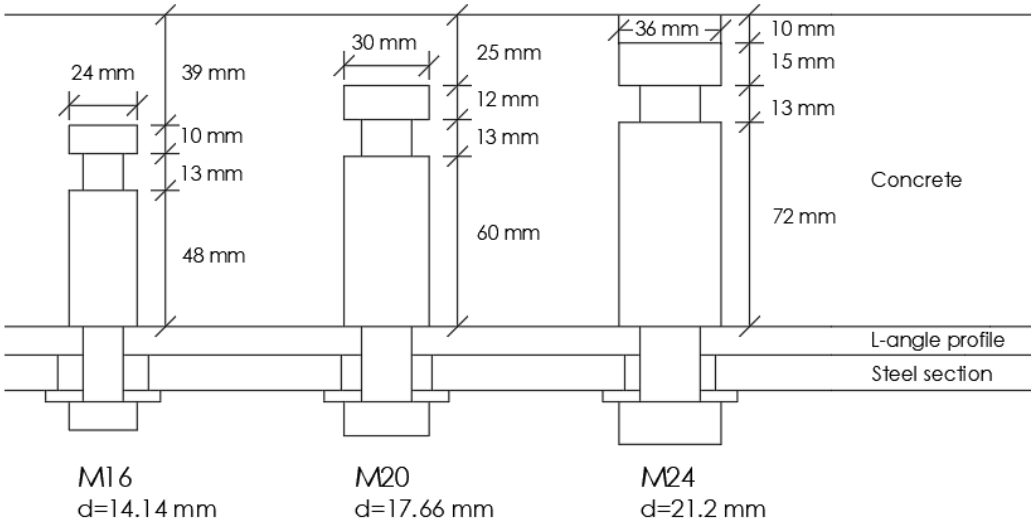

Figure 5.6: Cross section of the FEA models for the different bolt diameters

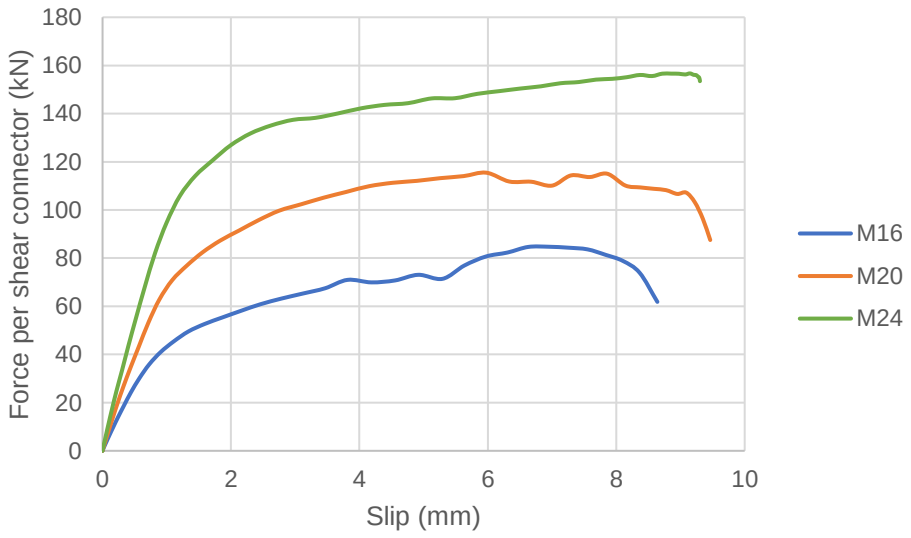

Figure 5.7: Force-slip curves for different bolt diameters

As it can be observed from figure 5.6, the force per shear connector-slip curves differ significantly for the different bolt diameters. The shear resistance increases 36% from bolt M16 to bolt M20 and 85% from bolt M16 to bolt M24. As it was expected, the shear resistance has a large influence on the maximum force per shear connector, the larger the net cross section area of the bolt the larger the maximum resistance. ABAQUS models with bolt diameter M16 and M20 failed due to shear failure of the bolts while the model with diameter M24 failed due to concrete failure.

Table 5.3: Shear resistance for different bolt diameters

Bolt diameter (mm)	16	20	24
Shear resistance (kN)	84.7	115.5 (36%↑)	156.7 (%85↑)

The second stiffness at 70% of the maximum force per shear connector for the different bolt diameters is presented in figure in figure 5.8 and a comparison of the values of the second stiffness between bolts M16, M20 and M24 is presented in figure 5.9. The second stiffness increases 110% and 223% from bolt M16 to bolt M20 and from bolt M16 to bolt M24 respectively. The second stiffness is also affected by the diameter of the bolts, the higher the bolt diameter the higher the second stiffness. The second stiffness increases linearly with the increase of the bolt diameter.

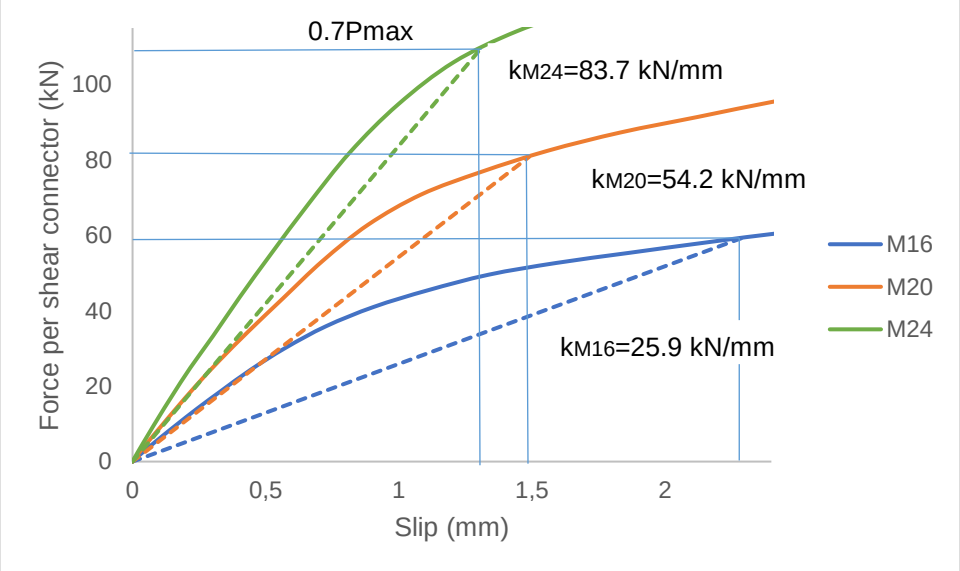

Figure 5.8: Second stiffness for different bolt diameters

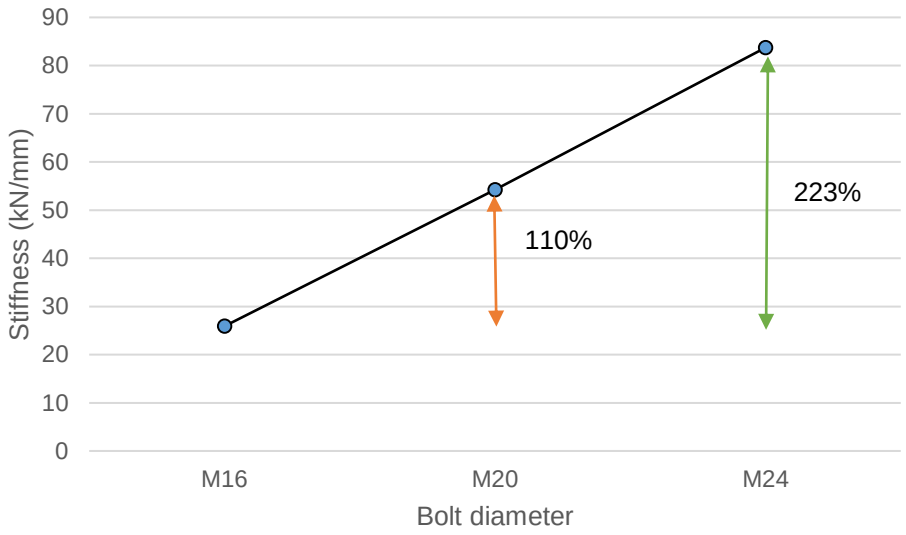

Figure 5.9: Comparison of second stiffness for different bolt diameters

The stiffness degradation (SDEG) and the concrete compressive damage (DAMAGEC) derived from ABAQUS software are compared for the different concrete strength classes in figures 5.10 and 5.11 respectively. Both the stiffness degradation and the compressive damage of concrete around the bolt increase with the increase of the bolt diameter.

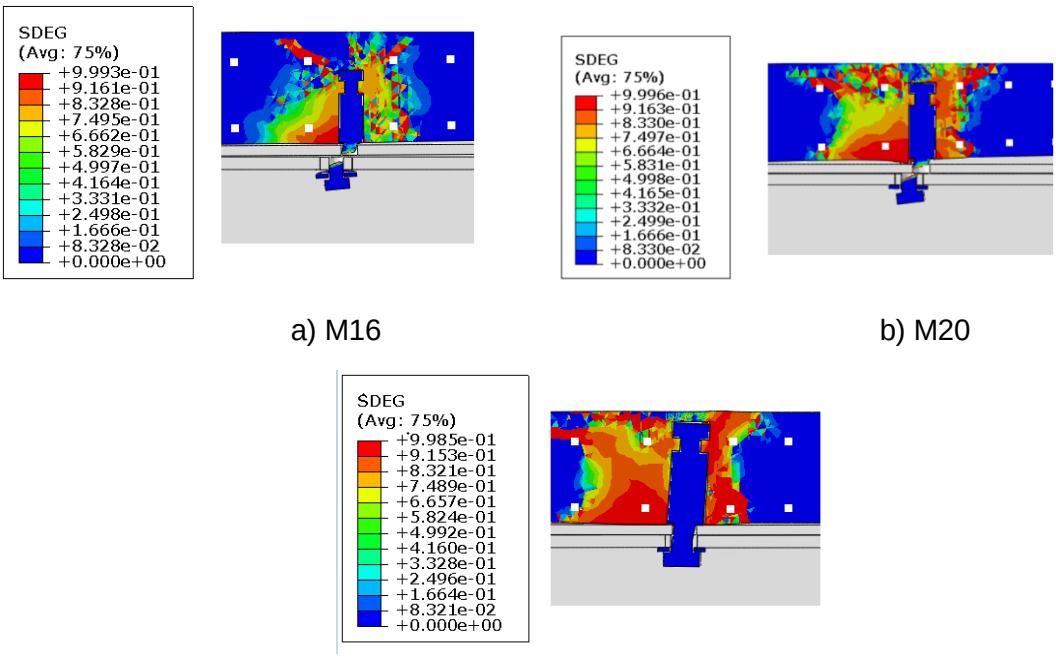

a) M16

b) M20

c) M24

Figure 5.10: Comparison of stiffness degradation for different bolt diameters

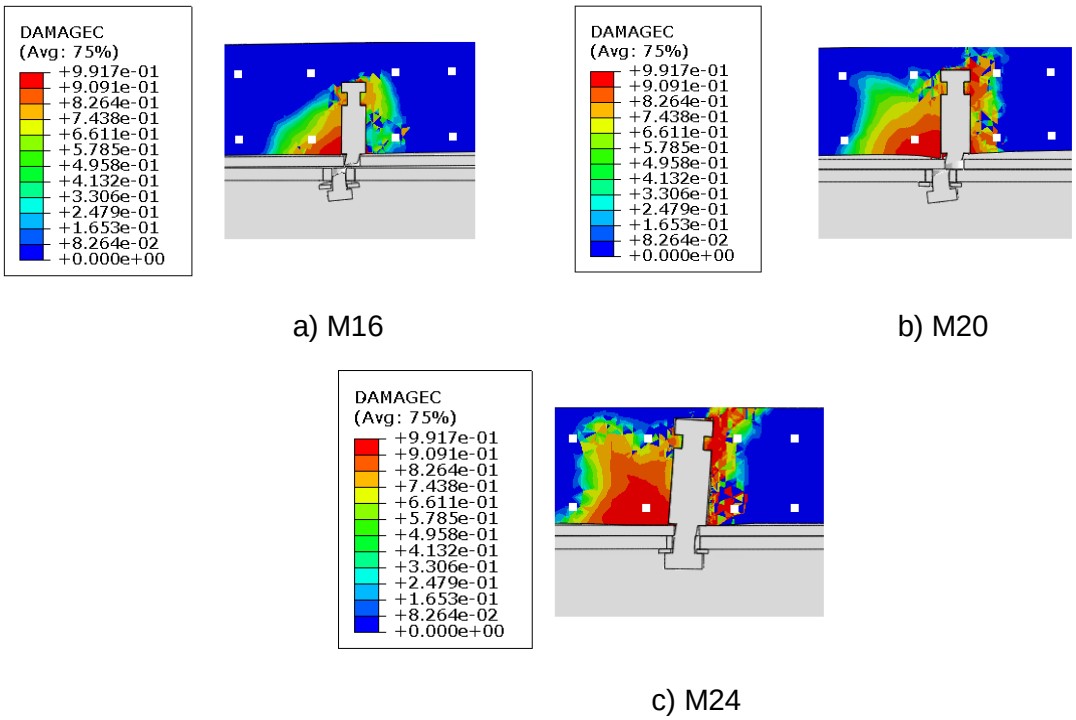

Figure 5.11: Comparison of concrete compressive damage for different bolt diameters

5.2.3 Bolt strength class

Parametric study of bolt strength class has been conducted in order to evaluate its influence on shear resistance of resin injected bolts. Three models with different bolt strength classes 4.6, 8.8 and 10.9 were created. The models have the same bolts M20 and same concrete strength class C40/50. The force per shear connector-slip curves obtained from FEA are presented in figure 5.12 and the maximum values of shear resistance in table 5.4.

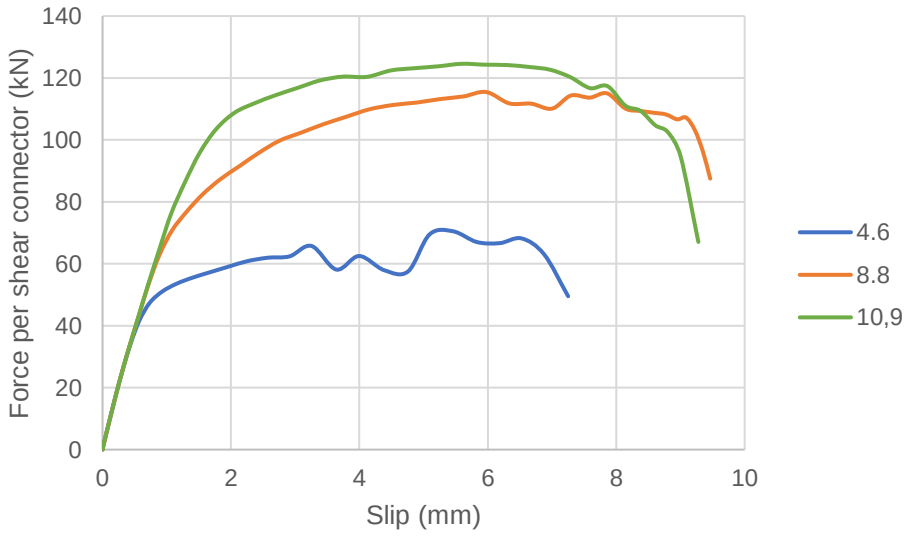

Figure 5.12: Force-slip curves for different bolt strength classes

The bolt strength class influences the shear resistance. The shear resistance increases 64% when the concrete strength class increases from 4.6 to 8.8 and 77% when the concrete strength class increases from 4.6 to 10.9. As a result, increase of bolt strength class leads to increase of shear resistance but in case of strength class 4.6 the maximum shear resistance is much lower than in cases of bolt strength classes 8.8 and 10.9 where the values of resistance do not differ significantly. Moreover, the shear connectors in cases of bolt strength classes 8.8 and 10.9 behaved more ductile compared to case of bolt strength class 4.6. All three models failed due to shear failure of the bolts.

Table 5.4: Shear resistance for different bolt strength classes

Bolt strength class	4.6	8.8	10.9
Shear resistance (kN)	70.5	115.5 (64%↑)	124.6 (77%↑)

In figure 5.13 the calculation of the second stiffness at 70% of the maximum force is presented for the different bolt strength classes while in figure 5.14 the values of second stiffness derived for strength classes 8.8 and 10.9 are compared with the value of second stiffness for strength class 4.6. As it is obvious in figure 5.13, in the beginning the initial stiffness is the same but comparing the second stiffness at 70% of the maximum force the values of the second stiffness differ slightly. By calculating the second stiffness at 70% of the maximum force, it decreases 7.7% from bolt strength class 4.6 to 8.8 which is not valid, so this method of calculating the second stiffness is not applicable on this case. The second stiffness increases 14% from bolt strength class 4.6 to 10.9.

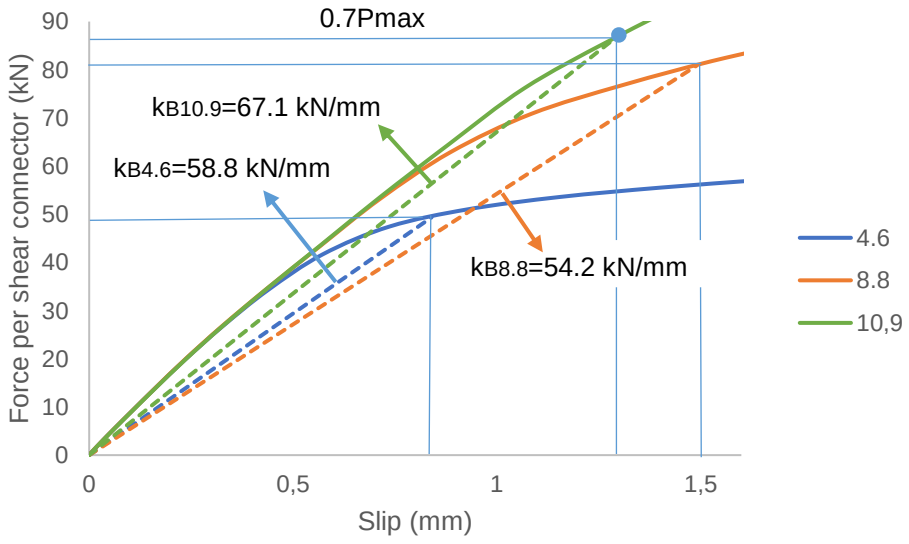

Figure 5.13: Second stiffness for different bolt strength classes

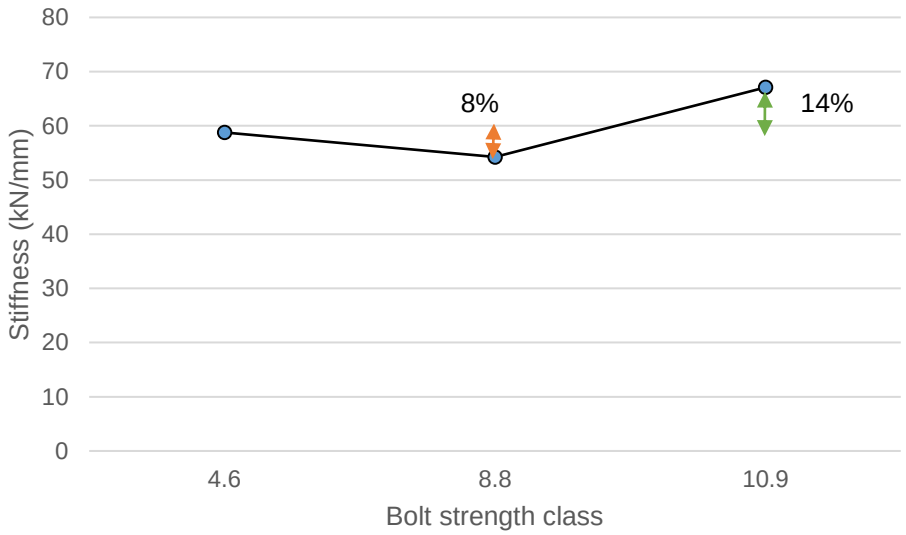

Figure 5.14: Comparison of second stiffness for different bolt strength classes

The stiffness degradation (SDEG) derived from ABAQUS software is compared for the different bolt strength classes in figure 5.15 while the concrete compressive damage (DAMAGEC) in figure 5.16. Both the stiffness degradation and the compressive damage of concrete around the bolt is significant in case of bolt strength classes 8.8 and 10.9 while in case of bolt strength class 4.6 the stiffness degradation and the compressive damage of concrete are barely noticeable.

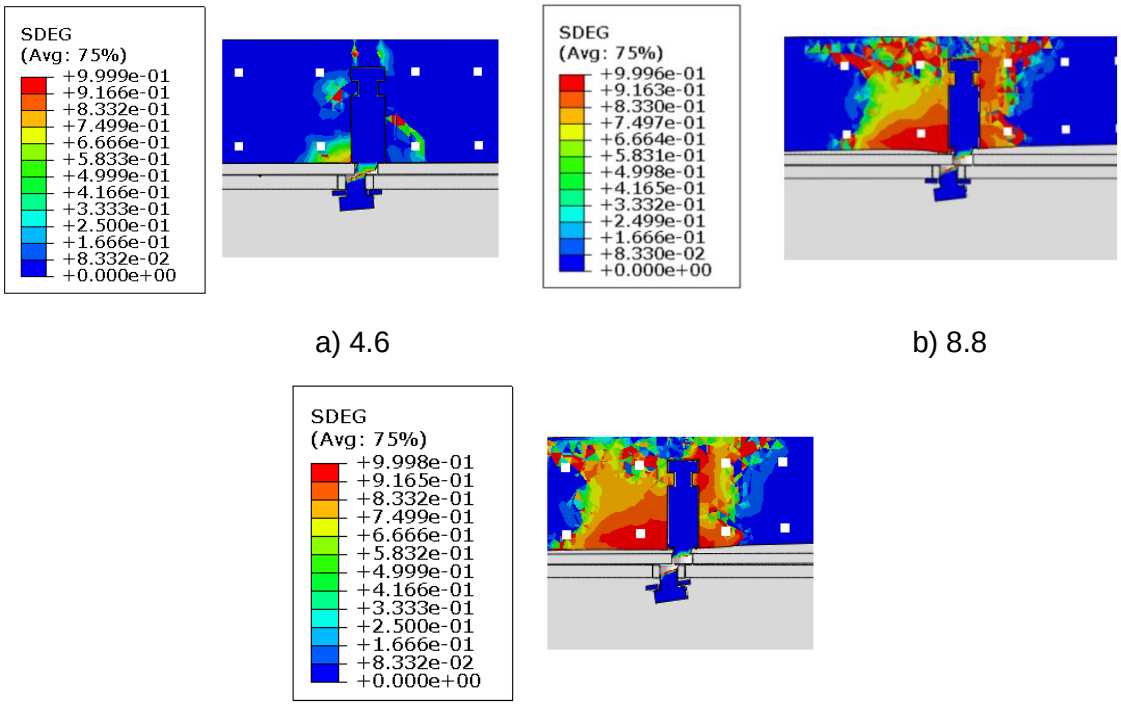

Figure 5.15: Comparison of stiffness degradation for different bolt strength classes

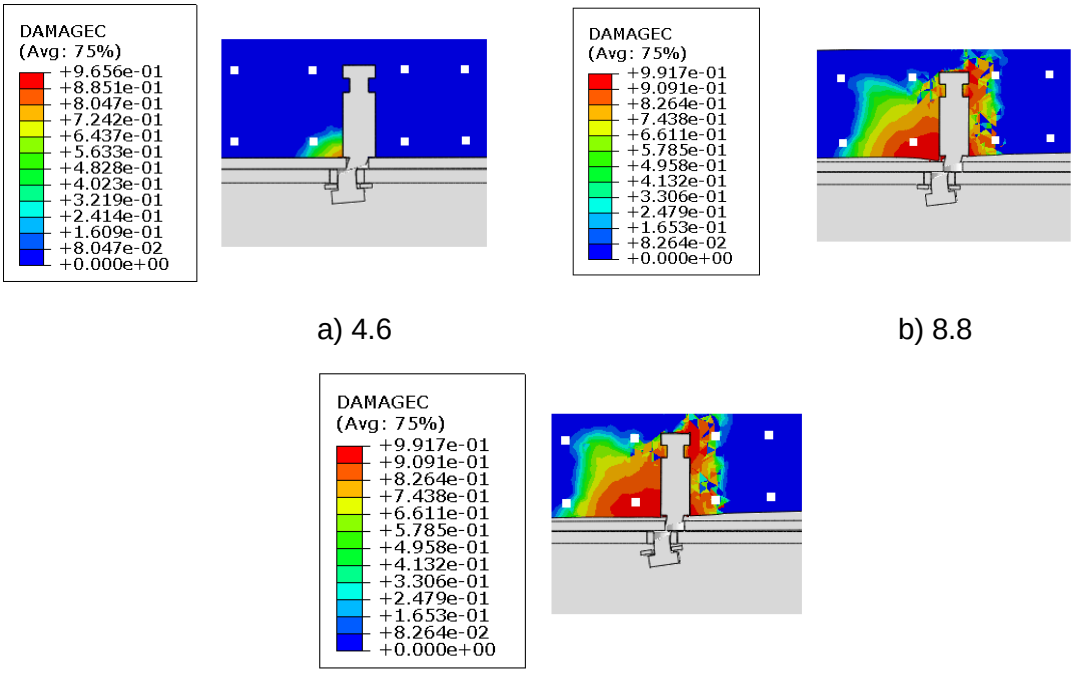

a) 4.6

b) 8.8

c) 10.9

Figure 5.16: Comparison of concrete compressive damage for different bolt strength classes

5.2.4 Embedded bolt height

Three FEA models were created with different height of the embedded bolt in order to examine the influence of the embedded bolt height on the shear resistance of resin injected bolts. The cross section of the models is presented in figure 5.17. The three heights of embedded bolt and concrete used are 40 mm, 60 mm, 80 mm and 120, 140, 160 respectively. All the models have bolts M20, bolt strength class 8.8 and concrete strength class C40/50. The force per shear connector-slip curves obtained from FEA are presented in figure 5.18 and the maximum forces per shear connector derived from the curves are presented in table 5.5.

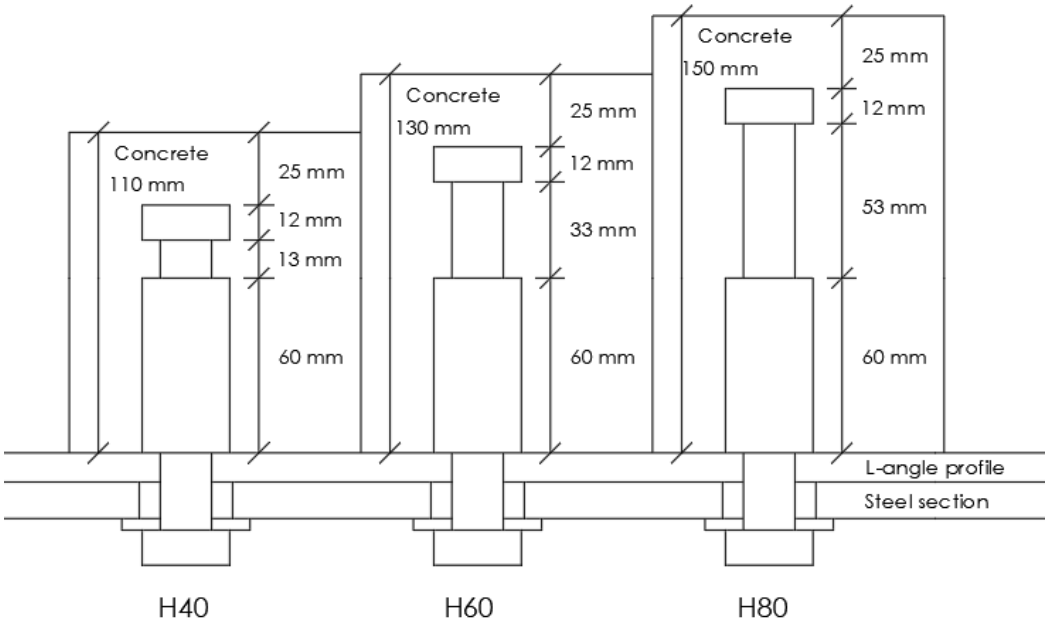

Figure 5.17: Cross section of the FEA models for the different embedded bolt heights

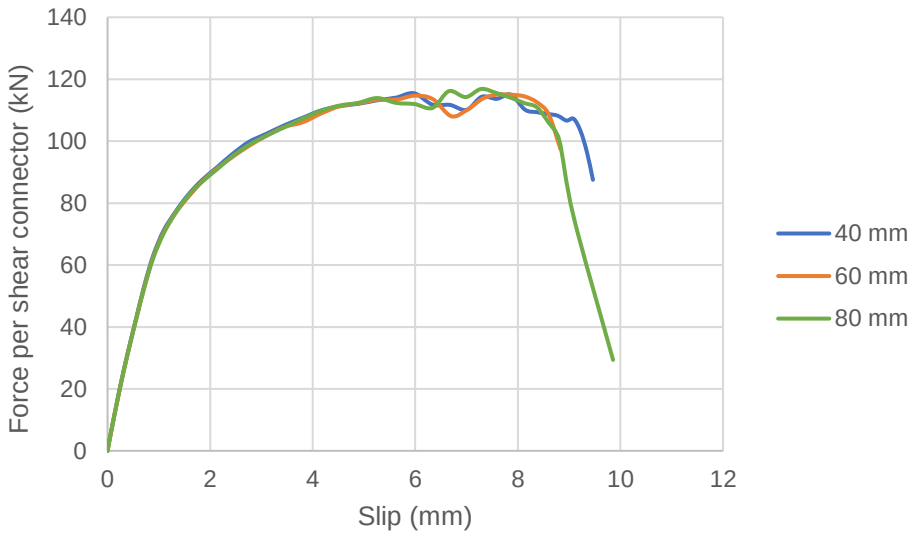

Figure 5.18: Force-slip curves for different embedded bolt heights

As it is obvious from figure 5.18 the embedded bolt height does not influence the maximum force per shear connector, the values of the maximum force remain the same. It was expected that the embedded bolt height would not affect the shear resistance because the embedded bolt is far away from the steel section-concrete area which is the area of interest. It can also be concluded that by increasing the concrete height the shear resistance will not increase, so it will just lead to higher cost due to embedded bolts, concrete and steel section because due to the higher concrete thickness, higher thickness of the flange of the cross section will be required.

Table 5.5: Shear resistance for different embedded bolt heights

Embedded bolt height (mm)	40	60	80
Shear resistance (kN)	115.5	115.1	116.9

In figure 5.19 the calculation of the second stiffness at 70% of the maximum force is presented for the different values of the height of the embedded bolt. The embedded bolt height has no influence on the stiffness.

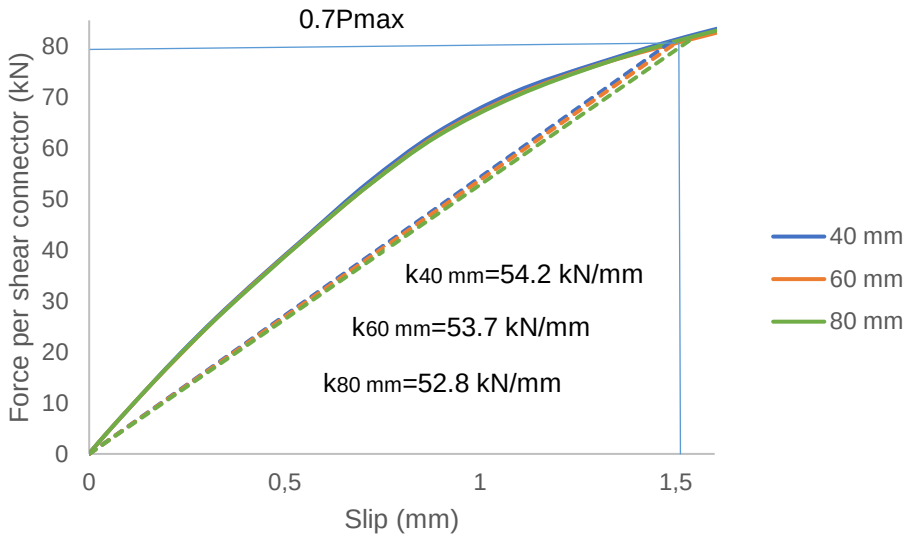

Figure 5.19: Second stiffness for different embedded bolt heights

The stiffness degradation (SDEG) and the concrete compressive damage (DAMAGEC) derived from ABAQUS software are compared for the different embedded bolt heights in figures 5.20 and 5.21 respectively. Both the stiffness degradation and the compressive damage of concrete locally slightly decrease with the increase of the embedded bolt height.

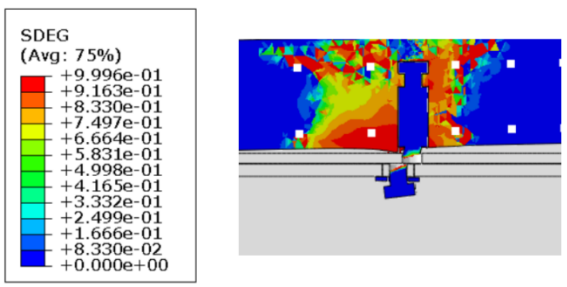

a) 40 mm

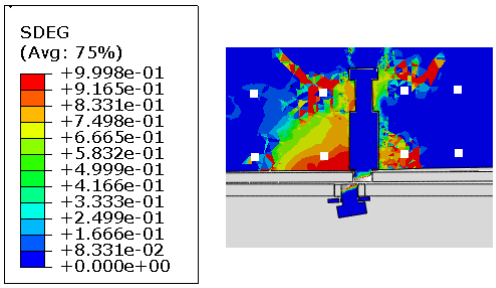

b) 60 mm

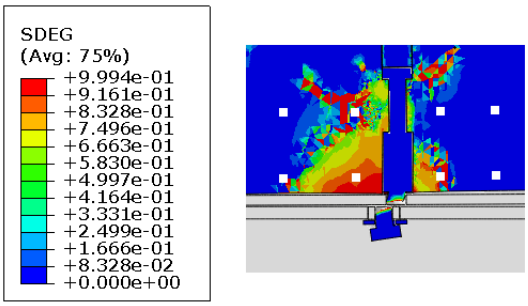

c) 80 mm

Figure 5.20: Comparison of stiffness degradation for different embedded bolt heights

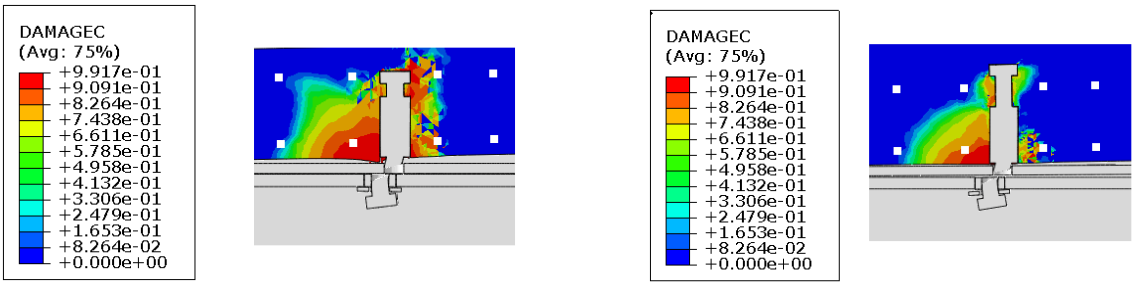

a) 40 mm b) 60 mm

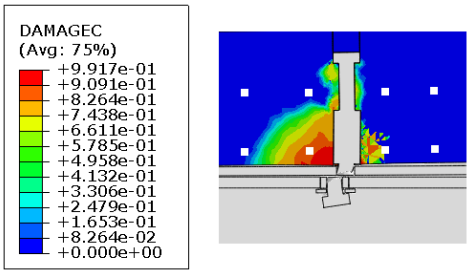

c) 80 mm

Figure 5.21: Comparison of concrete compressive damage for different embedded bolt heights

5.2.5 Steel section hole diameter

In figure 5.22 is depicted the force per shear connector-slip curve of three models with three different diameters of the hole of the steel cross section: 24, 32 and 40 mm. In all specimens M20 bolts were considered, concrete strength class C40/50 and bolt strength class 8.8. The maximum forces per shear connector derived from the curves are presented in table 5.6.

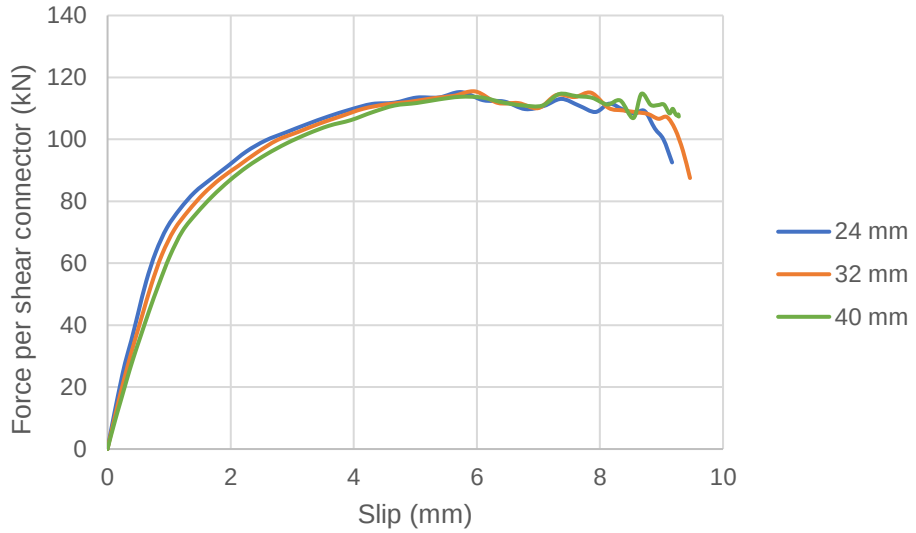

Figure 5.22: Force-slip curves for different steel section hole diameters

The shear resistance remains the same by increasing the diameter of the hole of the steel cross section, so the diameter of the hole of the steel section does not have any effect on the shear resistance. The models with hole diameter of the steel section equal to 24 and 32 mm failed due to shear failure of the bolts while the model with hole diameter of the steel section equal to 40 mm failed due to concrete failure.

Table 5.6: Shear resistance for different steel section hole diameters

Steel section hole diameter (mm)	24	32	40
Shear resistance (kN)	115.3	115.5	114.7

The second stiffness at 70% of the maximum force is presented in figure 5.23 for the different values of the diameter of the hole of the steel section. In figure 5.24 a comparison is made between the different values of the stiffness for the different hole steel section diameters. The second stiffness decreases linearly with the increase of the diameter of the hole of the steel section. The second stiffness decreases 11% when the hole diameter increases from 24 to 32 mm and 20% when it increases from 24 to 40 mm. Hence, the diameter of the steel section hole affects the stiffness. Even though by increasing the hole diameter of the cross section there is a small decrease of the second stiffness, the increase of the hole size allows for an easier assembly process.

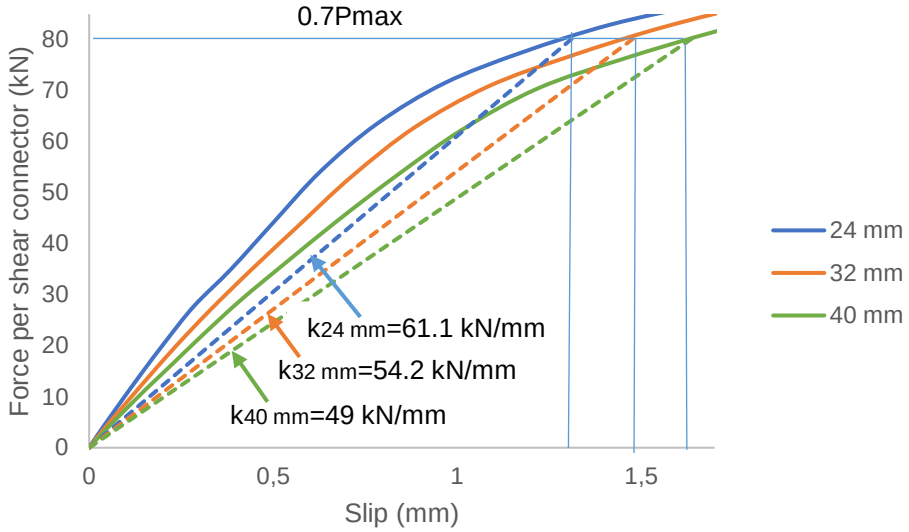

Figure 5.23: Second stiffness for different steel section hole diameters

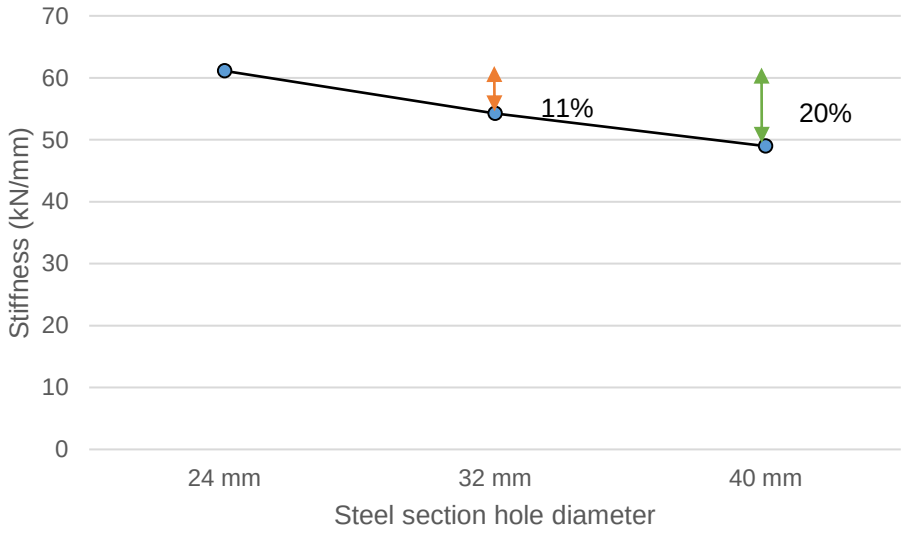

Figure 5.24: Comparison of second stiffness for different steel section hole diameters

The stiffness degradation (SDEG) derived from ABAQUS software is presented in figure 5.25 for the different diameters of the hole of the steel section and the concrete compressive damage (DAMAGEC) in figure 5.26. Both the stiffness degradation and the compressive damage of concrete around the bolt almost remain the same with the increase of the hole diameter of the steel section.

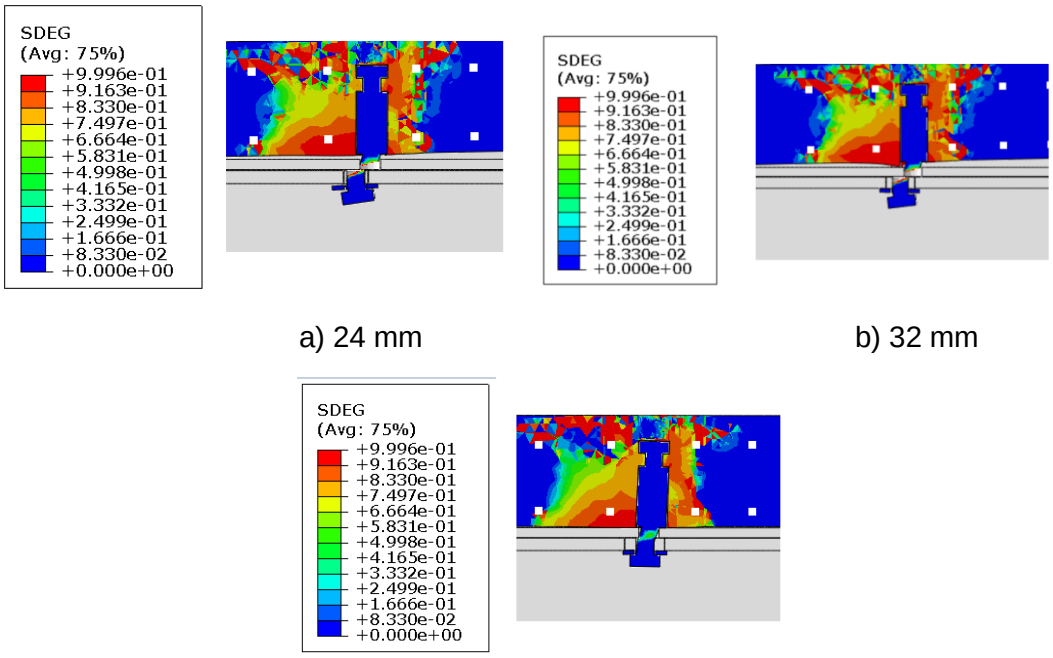

Figure 5.25: Comparison of stiffness degradation for different steel section hole diameters

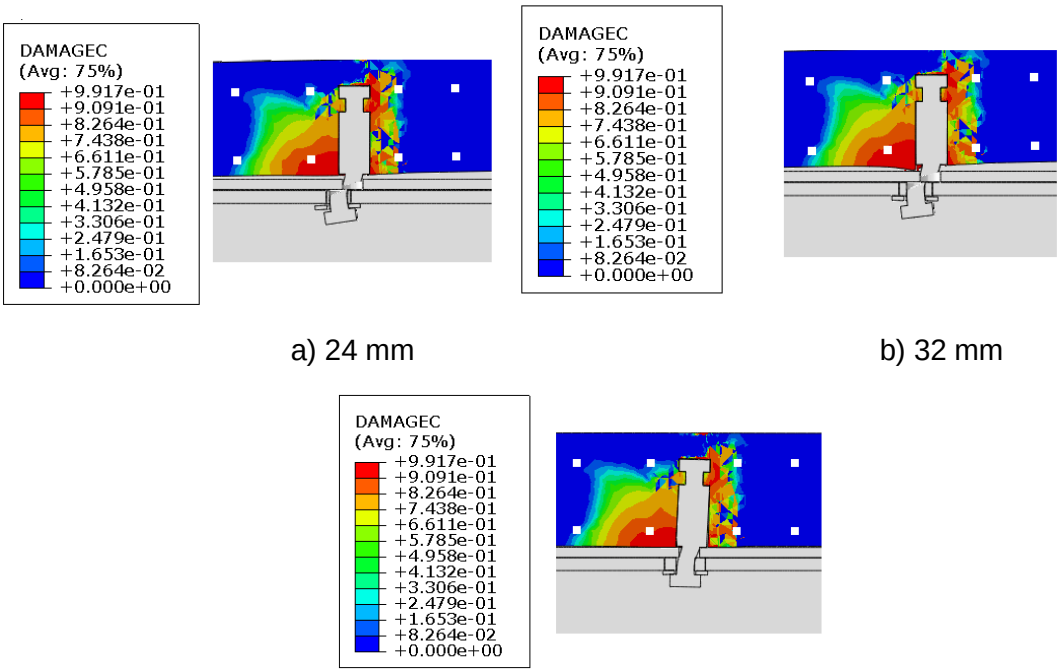

Figure 5.26: Comparison of concrete compressive damage for different steel section hole diameters

5.2.6 Detailing of the deck

A model was run without the L-angle profile in order to investigate whether the existence of the L-angle profile affects or not the shear resistance of resin injected bolted connections. The model has the same bolts M20, concrete strength class C40/50 and bolt strength class 8.8 as the model with the L-angle profile. The cross sections of the models with and without the L-angle profile are presented in figure 5.27. The force per shear connector-slip curves obtained from the FEA are presented in figure 5.28 and the maximum forces per shear connector derived from the curves are presented in table 5.7.

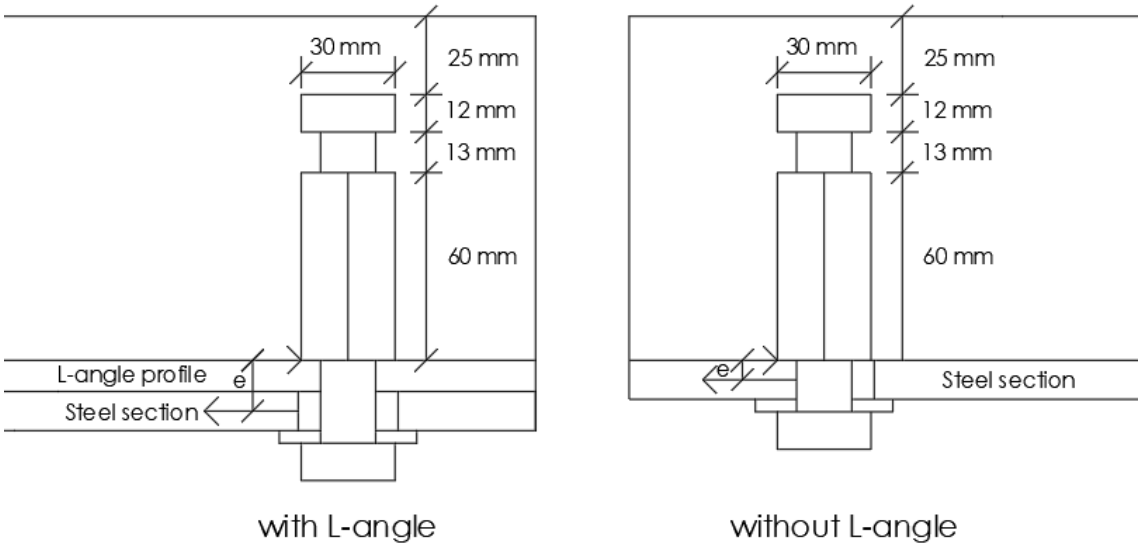

Figure 5.27: Cross section of the FEA models with and without the L-angle profile

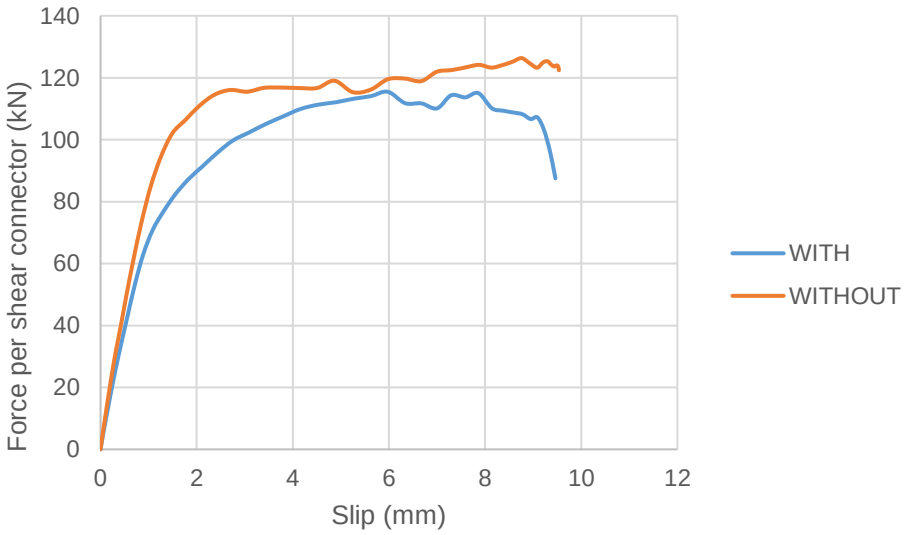

Figure 5.28: Force-slip curves with and without L-angle profile

As it can be seen in figure 5.27, the curve shapes derived from FEA for the models with and without the L-angle profile differ. In case of the model without the L-angle profile, when the shear resistance 119 kN is achieved, the curve reaches a plateau and after that a small increase in the resistance is observed while in case of the model with the L-angle profile when the maximum force is reached then the curve drops. This happens because in case of the existence of the L-angle profile, the lever arm e depicted in figure 5.27 is larger and this leads to higher stresses. For force per shear connector equal to 100 kN, in case of existence of the L-angle profile the maximum von Mises stress in the bolt is 836 MPa while in case of absence of the L-angle is equal to 731 MPa for the same time. The shear resistance of the model without the L-angle profile is 9% higher than the shear resistance of the model with the L-angle profile. The model with the L-angle profile failed due to shear failure of the bolts while the model without the L-angle profile failed due to concrete failure.

Table 5.7: Shear resistance with and without L-angle profile

L-angle	with	without
Shear resistance (kN)	115.5	126.3 (9%↑)

In figure 5.28 the calculation of the second stiffness at 70% of the maximum force is presented for the models with and without the L-angle profile and a comparison is made in figure 5.29. The second stiffness is case of the absence of the L-angle profile is 46% higher than in case of the existence of the L-angle profile. The L-angle profile affects negatively the shear resistance and the stiffness and also the total cost of the structure, so it can be omitted.

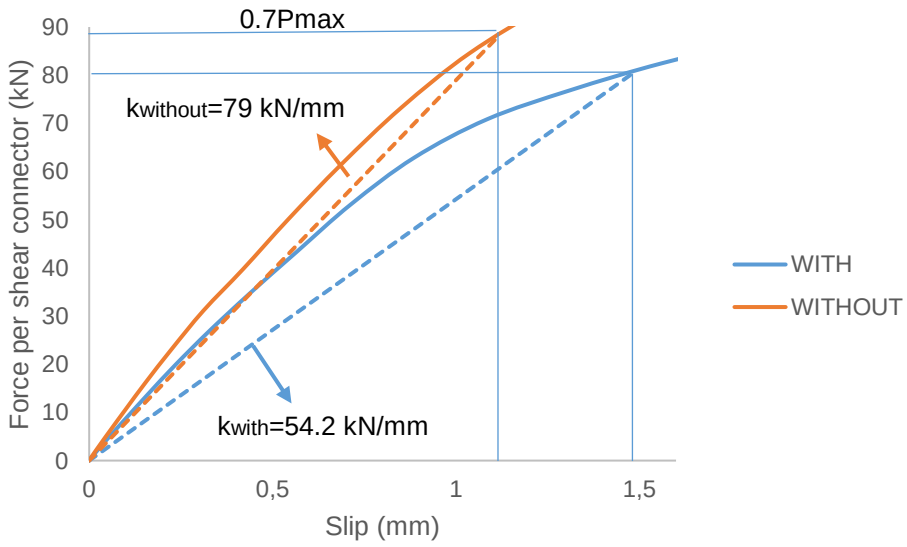

Figure 5.29: Second stiffness with and without L-angle profile

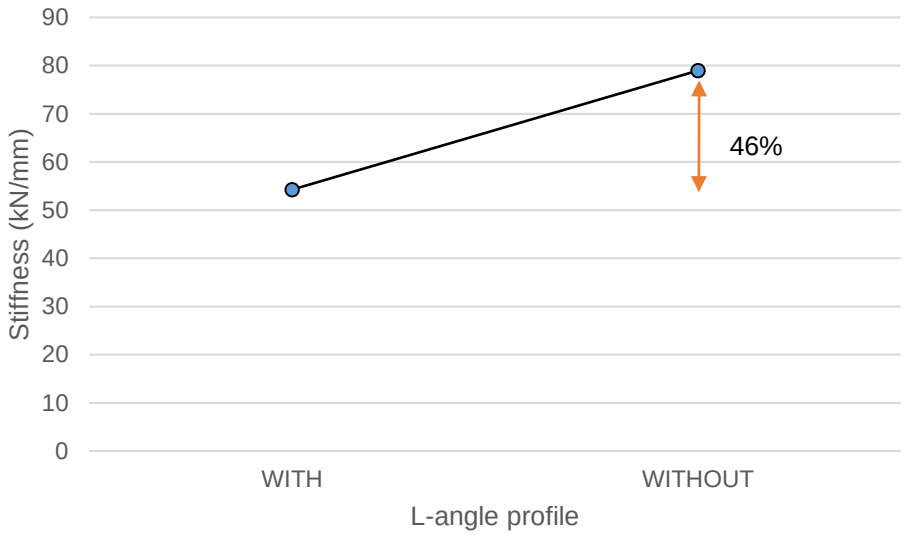

Figure 5.30: Comparison of second stiffness with and without L-angle profile

The stiffness degradation (SDEG) and the concrete compressive damage (DAMAGEC) derived from ABAQUS software for the models with and without the L-angle profile are presented in figures 5.31 and 5.32 respectively. Both the stiffness degradation and the compressive damage of concrete around the bolt decrease significantly when the L-angle profile is absent.

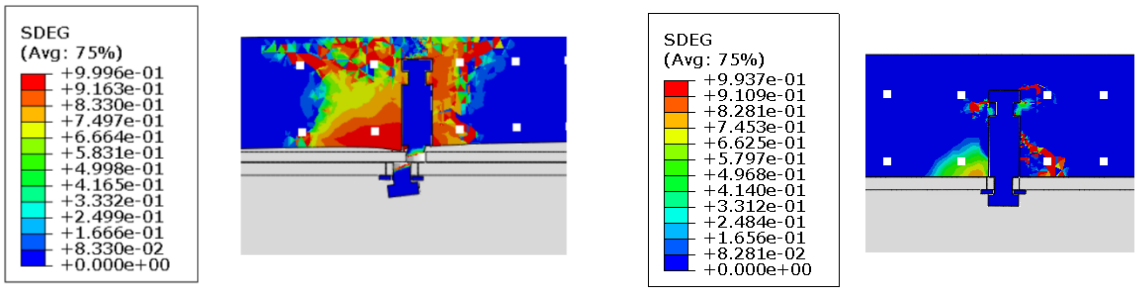

a) with b) without

Figure 5.31: Comparison of stiffness degradation with and without the L-angle profile

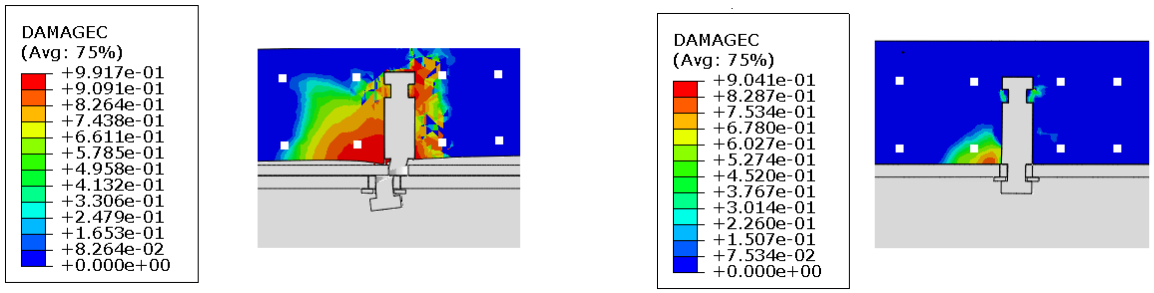

a) with b) without

Figure 5.32: Comparison of concrete compressive damage with and without the L-angle profile

5.2.7 Injection material

A model was run with injection material steel S355 and compared with the model with resin injection material. In reality, this is not feasible but an effort is made to simulate fitted bolts and compare their behaviour with resin injected bolts. The two models have the same bolts M20, concrete strength class C40/50 and bolt strength class 8.8. The force per shear connector-slip curves obtained from FEA are presented in figure 5.33 and the maximum forces per shear connector derived from the curves are presented in table 5.8.

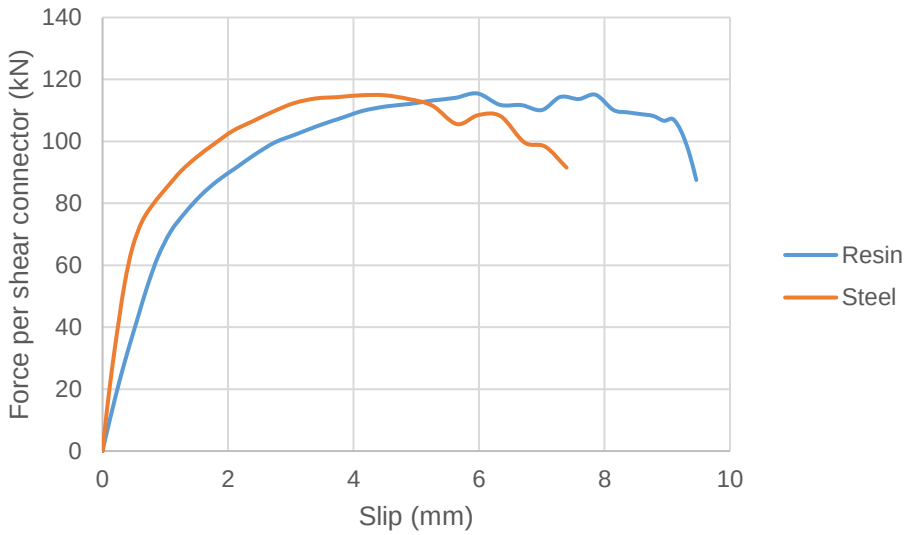

Figure 5.33: Force-slip curves for resin and steel injection material

The maximum force per shear connector as it can be seen in table 5.8 remains the same. By changing the injection material from resin to steel, it does not have any effect on the shear resistance. Both models failed due to shear failure of the bolts but in case of resin injection material the shear connectors behaved more ductile compared to steel injection material.

Table 5.8: Shear resistance for resin and steel injection material

Injection material	Resin	Steel
Shear resistance (kN)	115.5	114.9

The calculation of the second stiffness at 70% of the maximum force for the models with resin and steel injection material is presented in figure 5.34 and a comparison is made in figure 5.35. The second stiffness is case of steel injection material is 79% higher than in case of resin injection material. Even though the second stiffness would increase, demountability and

reusability of the structural parts would not be possible. Another advantage of resin injection material over steel injection material is that the shear connectors behave more ductile.

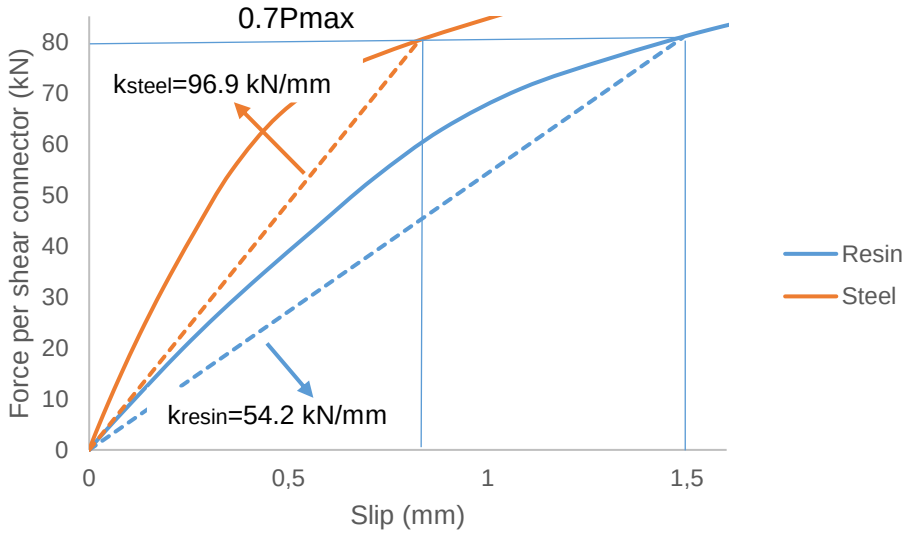

Figure 5.34: Second stiffness for resin and steel injection material

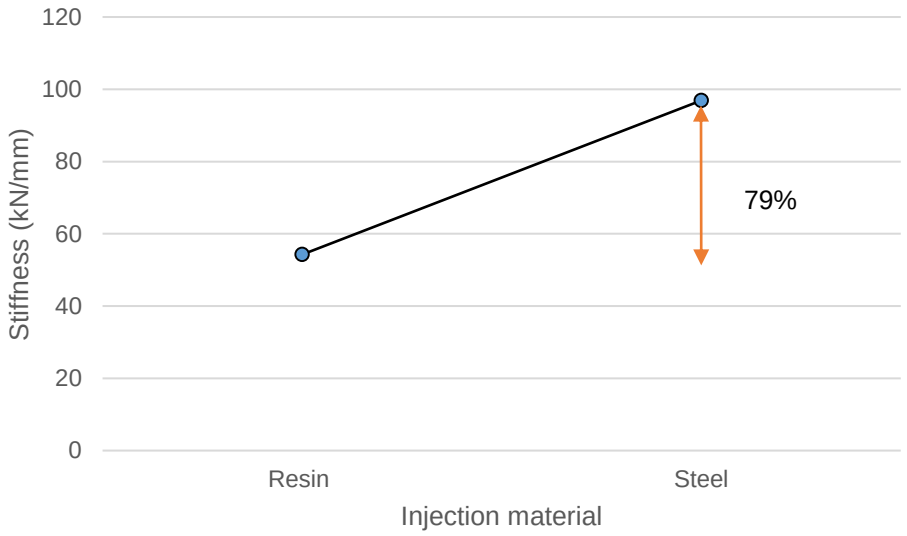

Figure 5.35: Comparison of second stiffness for resin and steel injection material

The stiffness degradation (SDEG) and the concrete compressive damage (DAMAGEC) derived from ABAQUS software for the models with resin and steel injection material are presented in figures 5.36 and 5.37 respectively. Both the stiffness degradation and the compressive damage of concrete around the bolt remain the same by changing the injection material from resin to steel.

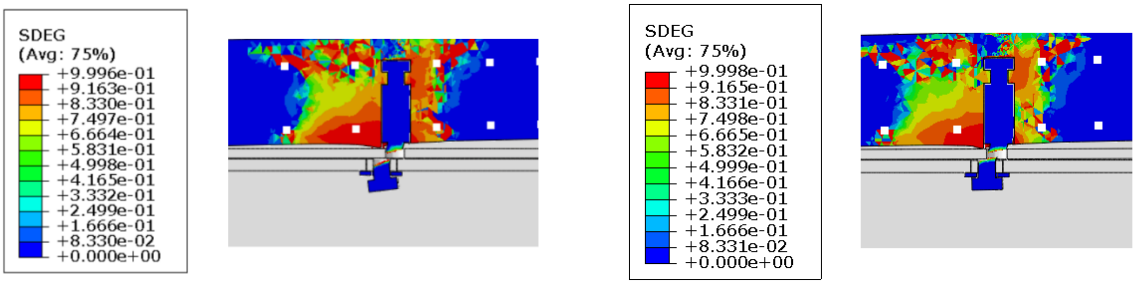

a) resin b) steel

Figure 5.36: Comparison of stiffness degradation for resin and steel injection material

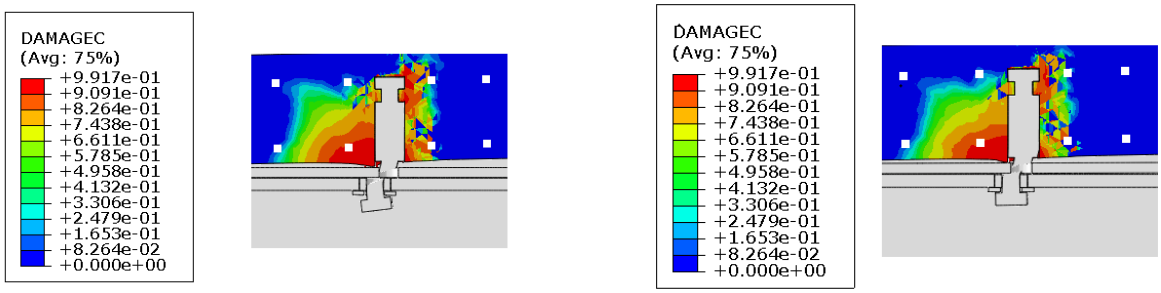

a) resin b) steel

Figure 5.37: Comparison of concrete compressive damage for resin and steel injection material

5.3 Conclusions

1. The parameters that affect significantly the resistance of the shear connection with resin injected bolts are the bolt diameter and the bolt strength class. The shear resistance increase 85% from bolt M16 to bolt M24 and 77% from bolt strength class 4.6 to bolt strength class 10.9.
2. The parameter that affects significantly the stiffness of the shear connection with resin injected bolts is the bolt diameter. The second stiffness increases 223% from bolt M16 to bolt M24.
3. The increase of the embedded bolt height and consequently of the concrete height does not have any influence neither on the shear resistance nor on the stiffness, which was expected as the embedded bolt is away from the steel-concrete interface. Hence, the increase of the embedded bolt height and the concrete height is not economically desirable.
4. The concrete strength class and the diameter of the hole of the steel section does not affect the shear resistance but they affect the stiffness. The second stiffness increases 14% from concrete strength class C20/25 to concrete strength class C50/60 which was expected as the Young modulus of Elasticity of concrete increases 23% from C20/25 to C50/60. Moreover, the second stiffness decreases 20% when the diameter of the steel section increases from 24 to 40 mm. However, the increase of the hole size allows for an easier assembly process.
5. In case of absence of the L-angle profile, both the shear resistance and the second stiffness increase 9% and 45% respectively. Consequently, the L-angle profile should be omitted because it affects negatively both the shear resistance and the stiffness and is not economically desirable.
6. Theoretically, if steel injection material was steel instead of resin, the shear resistance would remain the same but the second stiffness would increase 79%. But in this case the demountability and reusability of the structural components would be impossible. Moreover, the ductility would decrease if steel injection material was used instead of resin.

6 Conclusions and future work

6.1 Conclusions

The behaviour of an innovative type of shear connectors, resin injected bolts, in steel-concrete composite structures was investigated in terms of shear capacity and stiffness. Based on the literature review, the experimental work, the Finite Element Analysis and parametric study the following conclusion may be drawn:

1. According to push-out tests that conducted in the lab, the maximum shear resistance that can be achieved with resin injected bolts as shear connectors is 116.9 kN. This value was validated using Finite Element Analysis.

2. According to experimental work, two failure modes were observed: concrete failure and shear failure of the bolts. In tests that were loaded until failure, concrete failure preceded shear failure of the bolts while tests under cyclic loading failed due to shear failure of the bolts and no cracks were observed in concrete. The type of loading influenced the failure mode, in case of cyclic loading steady openings of cracks occur and the energy is not released which has as a result the absence of cracks in concrete.

3. In the specimens that failed due to concrete failure, the shear connectors behaved very ductile. In the specimens that failed due to shear failure of the bolts, the shear connectors behaved either ductile according to Eurocode as the slip was higher than 6 mm which is the limit for a ductile behaviour or brittle but the slip was close to the limit for a ductile behaviour.

4. The resin injection procedure, during the preparation of the specimens, affected the initial stiffness. In the specimens with reinforced resin injected bolts, the resin was injected downwards while in the specimens with resin injected bolts the resin was injected upwards. In both cases, especially in case of reinforced resin injected bolts, leakage of resin around the hole in the steel section was observed after demounting of the specimens. This leakage increased the friction between steel and concrete and consequently the stiffness.

5. After the performance of the push-out tests, the specimens were demounted with the use of the suitable equipment and the steel section was used in other experiments which proves that demountability and reusability of the structure is possible.

6. The reinforcement in resin does not affect the maximum shear resistance but leads to higher stiffness. According to FEA, the second stiffness increases 11.4% if reinforcement is used in resin.

7. Compared to other types of demountable shear connectors, resin injected bolts have 82% and 65% of the friction grip bolts' and single embedded nut bolts' maximum force per shear connector respectively and lower stiffness. Bolts without embedded nut and welded headed suds have almost the same maximum force per shear connector which is 80% of that of resin injected bolts. However, welded headed studs have a slightly higher initial stiffness than resin injected bolts while bolts without embedded nut have lower stiffness.

8. The parameters that have the larger influence on the resistance of the shear connection with resin injected bolts are the bolt diameter and the bolt strength class while the parameter

that has the larger influence on the stiffness is the bolt diameter. The shear resistance increases 85% from bolt M16 to bolt M24 and 77% from bolt strength class 4.6 to bolt strength class 10.9 while the second stiffness increases 223% from bolt M16 to bolt M24.

9. The concrete strength class and the diameter of the hole of the steel section does not affect the shear resistance but they affect the stiffness. The second stiffness increases 14% from concrete strength class C20/25 to concrete strength class C50/60 which is consistent with the increase of Young's modulus of Elasticity of concrete 23% from C20/25 to C50/60. Moreover, the second stiffness decreases 20% when the diameter of the steel section increases from 24 to 40 mm. However, the increase of the hole size allows for an easier assembly process.

10. The increase of the embedded bolt height and consequently of the concrete height does not have any influence neither on the shear resistance nor on the stiffness, which was expected as the embedded bolt is away from the steel-concrete interface. Hence, the increase of the embedded bolt height and the concrete height is not economically desirable.

11. In case of absence of the L-angle profile, both the shear resistance and the second stiffness increase 9% and 45% respectively. Consequently, the L-angle profile should be omitted because it affects negatively both the shear resistance and the stiffness and is not economically desirable.

12. Theoretically, if steel injection material was steel instead of resin, the shear resistance would remain the same but the second stiffness would increase 79%. But in this case the demountability and reusability of the structural components would be impossible. Moreover, the ductility would decrease if steel injection material was used instead of resin.

6.2 Future work

Based on the conclusions drawn above, the following recommendations for future work are proposed:

1. More push-out test should be performed in the lab. Attention should be paid on the resin injection procedure in order leakage of resin during the injection procedure to be avoided.

2. Finite Element models, in which the threaded part of the bolt will be included, should be created for more accurate results.

3. Other parameters like the number of shear connectors and their longitudinal distance should be checked if they affect the shear resistance and initial stiffness or not.

4. In the experimental work performed, the specimens were loaded under static loading. They should also be checked under fatigue loading. Resin injected bolts are used as shear connectors in bridge decks and car parks, structures which are subjected to repeatedly applied loads due to the vehicles. Consequently, fatigue check is crucial.

7 Bibliography

[1] ABAQUS User Manual, Version 6.14, Dassault Systémes, 2014

[2] ABAQUS/Explicit: Advanced Topics, Lecture Presentations, 2005

[3] Akanbi L. A., Oyedele L. O., Akinade O. O., Ajayi A. O., Delgado M. D., Bilal M., Bello S. A., Salvaging building materials in a circular economy: A BIM-based whole-life performance estimator, Conservation and Recycling 129, p.175-186, 2018

[4] Allan R. N., Fisher J.W., Behaviour of bolted joints with oversize or slotted holes, Fritz Laboratory Report No. 318.3, 1967

[5] Allwood J. M., Cullen J. M., Milford R. L., Options for achieving a 50% cut in industrial carbon emissions by 2050, Environmental Science and Technology 44, p.1888-1894, 2010

[6] Arnim M.von, Demountable composite steel-concrete flooring system for reuse, Master Thesis, Karlsruhe Institute of Technology, 2017

[7] Ataei A., Bradford M. A., Liu X., Sustainable composite beams and joints with decostructable bolted shear connectors, 23rd Australasian Conference on the Mechanics of Structures and Materials, Australia, 2014

[8] Bjorhovde R., Colson A., Zandonini R., Connections in steel structures III: Behaviour, strength and design, p.77-87, Oxford, 1996

[9] Clark C., Jambeck J., Townsend T., A Review of Construction and Demolition Debris Regulations in the United States, Critical Reviews in Environmental Science and Technology, 36(2) p.141-86, 2006

[10] Dai X. D., Lam D., Saveri E., Effect of Concrete Strength and Stud Collar Size to Shear Capacity of Demountable Shear Connectors, Journal of Structural Engineering, 141(11): 04015025, 2015

[11] Dallam L.N.: Push-out tests with high strength bolt shear connectors, ACI Journal, Proceeding (No 9): p.767-769, 1968

[12] Dedic D,J., Klaiber W.F.: High-Strength Bolts as Shear Connectors in Rehabilitation Work, Concrete international, 6(7) p.41-46, 1984

[13] Ellen Macarthur Foundation, Towards the circular economy, 2013

[14] EN1090-2: Execution of steel structures and aluminium structures - Part 2: Technical requirements for steel structures, Brussels, Belgium: European Committee for Standardization (CEN), 2011

[15] EN1993-1-1: Eurocode 3: Design of steel structures - Part 1-1: General rules and rules for buildings, Brussels, Belgium: European Committee for Standardization (CEN), 2010

[16] EN1993-1-8: Eurocode 3: Design of steel structures - Part 1-8: Design of joints, Brussels, Belgium: European Committee for Standardization (CEN), 2010

[17] EN1994-1-1: Eurocode 4: Design of composite steel and concrete structures - Part 1-1: General rules and rules for buildings, Brussels, Belgium: European Committee for Standardization (CEN), 2010

[18] Gresnigt A. M., Sedlacek G., Paschen M., Injection bolts to repair old bridges, p.349-460, 2012

[19] Girbacea A., Assessment of demountable steel-concrete composite flooring systems, Master Thesis, Delft University of Technology, 2018

[20] Gritsenko A., Towards a demountable composite slab floor system, Master Thesis, Delft University of Technology, 2018

[21] Huovila P., Buildings and Climate Change: Status, Challenges and Opportunities, UNEP/Earthprint, France, 2007

[22] Kolstein H., Li J., Koper A., Gard W., Nijgh M., Veljkovic M., Behaviour of double shear connections with injection bolts, Steel Construction-Design and research, 10(4) p.287-294, 2017

[23] Koper A., Assessment of Epoxy Resins for Injected Bolted Shear Connections, Master Thesis, Delft University of Technology, 2017

[24] Kortis J., The numerical solution of the bolted connection with the low-quality injected bolts, Proceedings of the 9th International Conference on New Trends in Statics and Dynamics of Buildings, Bratislava, 2011

[25] Kourmpanis B., Papadopoulos A., Moustakas K., Stylianou M., Haralambous K. J., Loizidou M., Preliminary study for the management of construction and demolition waste, Waste Management and Research, 26(3) p.267-275, 2008

[26] Kozma A., Odenbreit C., Braun M.V., Veljkovic M., Nijgh M.P., Push-out tests on demountable shear connectors of steel-concrete composite structures, 12th International Conference on Advances in Steel-Concrete Composite structures, Valencia, 2018

[27] Kwon G., Engelhardt M.D., Klingner R.E.: Behaviour of post-installed shear connectors under static and fatigue loading, Journal of Constructional Steel Research, 66(4) p. 532- 541, 2010

[28] Lam D., Dai X.: Demountable Shear Connectors for Sustainable Composite Construction, The 2013 World Congress on Advances in Structural Engineering and Mechanics, Korea, 2013

[29] Lam D., Dai X., Ashour A., Rahman N., Recent research on composite beams with demountable shear connectors, Steel Construction 10(2), 2017

[30] Lam D., Ellobody E., Behaviour of Headed Stud Shear Connectors in Composite Beam, Journal of Structural Engineering, 131(1), 2015

[31] Lee S.M., Bradford M.A.: Sustainable composite beam behaviour with deconstructable bolted shear connectors, The 2013 World Congress on Advances in Structural Engineering and Mechanics, Korea, 2013

[32] Mahmoud A. M., Finite element modelling of steel concrete beam considering double composite action, Ain Shams Engineering Journal 7, p.73-88, 2016

[33] Marshall W.T., Nelson H.M., Banerjee H.K.: An experimental study of the use of high-strength friction-grip bolts as shear connectors in composite beams, The structural engineer, 49(4) p. 171-178, 1971

[34] Moynihan M. C., Allwood J. M., Viability and performance of demountable composite connectors, Journal of Constructional steel research 99, p.47-56, 2014

[35] Nijgh M., New materials for injected bolted connections: A feasibility study for demountable connections, Master Thesis, Delft University of Technology, 2017

[36] Nijgh M., Arnim M. von, Pavlovic M., Veljkovic M., Preliminary Assessment of a Composite Flooring System for Reuse, 8th International Conference on Composite Construction in Steel and Concrete, Jackson, 2017

[37] Nijgh M., Xin, H., Veljkovic, M., Non-linear hybrid homogenization method for steel-reinforced resin, Construction and Building Materials 182, p.324-333, 2018

[38] Ollgaard J.G., Slutter R.G., Fisher J.W., Shear strength of stud connectors in lightweight and normal weight concrete, Engineering Journal-American Institute of Steel Construction, AISC.8(2): p.55-64, 1971

[39] Pallares L., Hajjar J.F., Headed Steel Stud Anchors in Composite Structures: Part I-Shear, Journal of Constructional Steel Research, 66(2): p.198-212, 2010

[40] Pathirana S.W., Use of innovative shear connectors in construction and rehabilitation of steel-concrete composite beams, Doctoral Dissertation, The University of New Wales, Australia, 2017

[41] Pathirana S.W., Uy B,. Mirza O., Zhu X., Flexural behaviour of composite steel-cocrete beams utilising blind bolt shear connectors, Engineering Structures 114, p.181-194, 2016

[42] Pavlovic M., Resistance of bolted shear connectors in prefabricated steel-concrete composite decks, Doctoral Dissertation, University of Belgrade, Faculty of Civil Engineering, Serbia, 2013

[43] Pavlovic M., Markovic Z., Veljkovic M., Budevac D., Bolted shear connectors vs. headed studs behaviour in push-out tests, Journal of Constructional Steel Research, 88(0) p.134-149, 2013

[44] Pavlovic M., Veljkovic M., FE validation of push-out tests, Steel Construction, 10(2) p.135-144, 2017

[45] Qureshi J., Mottram J. T., Resin injected bolted connections: A step towards achieving slip-resistant joints in FRP bridge engineering, FRP Bridges 2012, United Kingdom, 2012

[46] Rehman N., Behaviour of demountable shear connectors in composite structures, Doctoral Dissertation, University of Bradford, 2017

[47] Shariati A., RamliSulong N.H., Shariati M., Various types of shear connectors in composite structures: A review, International Journal of Physical Sciences, 7(22) p.2876-2890, 2012

[48] Suwaed A., Development of Novel Demountable Shear Connectors for Precast Steel-Concrete Composite Bridges, Doctoral Dissertation, University of Warwick, Structural Engineering Group, England, 2017

[49] Suwaed A., Karavasilis T. L., Experimental evaluation of a novel demountable shear connector for accelerated repair or replacement of precast steel-concrete composite bridges, Eurosteel, 1 (2-3) p.4163-4172, 2017

[50] Zafari B., Qureshi J., Mottram T., Rusev R., Static and fatigue performance of resin injected bolts for a slip and fatigue resistant connection in FRP bridge engineering, Structures, no.7, p.71-84, 2016

A Annex - Input data for ABAQUS

In chapters 4 and 5 in Finite Element Analysis, detailed material models were used. The input data for the ABAQUS material models were obtained from [40].

A.1 Concrete

Concrete C20/25

Table A.1: Density and Elastic for C20/25

Density:	2.5e-006
Elastic:	
Young's modulus	Poisson's ratio
30000	0.2

Table A.2: Concrete Damaged Plasticity for C20/25

Dilation angle	Eccentricity	fb0/fc0	K	Viscocity parameter
36	0.1	1.2	0.59	0

Table A.3: Concrete Compression Hardening for C20/25

Yield Stress	Inelastic Strain
11.2	0
19.8	0.00049
25.5	0.00098
27.8	0.00146
28	0.00163
27.5	0.00193
26.1	0.00223
23.8	0.00253
20.8	0.00283
17	0.00313
15	0.00335
13	0.00402
11.06	0.00513
9.24	0.00668
7.55	0.00868
6.04	0.01112
4.72	0.01401
3.62	0.01734
2.77	0.02112
2.18	0.02534

1.87	0.03
0.4	0.1

Table A.4: Concrete Tension Stiffening for C20/25

Yield Stress	Cracking Strain
2.2	0
1.87	0.0001
1.54	0.0002
1.23	0.0003
0.95	0.0004
0.7	0.0005
0.49	0.0006
0.32	0.0007
0.2	0.0008
0.13	0.0009
0.11	0.001

Table A.5: Concrete Compression Damage for C20/25

Damage Parameter	Inelastic Strain
0	0
0	0.0002
0	0.0005
0	0.00091
0	0.00107
0.0175	0.00138
0.0679	0.00173
0.1486	0.00211
0.2571	0.00251
0.3913	0.00293
0.4642	0.00322
0.5359	0.00396
0.6049	0.00513
0.6701	0.00675
0.7303	0.0088
0.7845	0.01129
0.8315	0.01423
0.8706	0.01759
0.9009	0.0214
0.922	0.02564
0.9333	0.03031
0.9857	0.10036

Table A.6: Concrete Tension Damage for C20/25

Damage Parameter	Cracking Strain
0	0
0.1514	0.00011
0.299	0.00022
0.439	0.00033
0.5678	0.00044
0.6821	0.00055
0.779	0.00066
0.856	0.00076
0.9111	0.00087
0.9427	0.00097
0.95	0.00107

Concrete C30/37

Table A.7: Density and Elastic for C30/37

Density:	2.5e-006
Elastic:	
Young's modulus	Poisson's ratio
33000	0.2

Table A.8: Concrete Damaged Plasticity for C30/37

Dilation angle	Eccentricity	fb0/fc0	K	Viscocity parameter
36	0.1	1.2	0.59	0

Table A.9: Concrete Compression Hardening for C30/37

Yield Stress	Inelastic Strain
15.2	0
26.4	0.00052
34.2	0.00104
37.8	0.00157
38	0.00174
37.5	0.002
35.9	0.00226
33.3	0.00252
29.6	0.00278
24.9	0.00304
21.86	0.00326
18.92	0.00393

16.08	0.00504
13.4	0.0066
10.93	0.00861
8.7	0.01106
6.76	0.01396
5.15	0.0173
3.89	0.02109
3.01	0.02532
2.53	0.03
0.4	0.1

Table A.10: Concrete Tension Stiffening for C30/37

Yield Stress	Cracking Strain
2.9	0
2.46	0.0001
2.03	0.0002
1.63	0.0003
1.25	0.0004
0.92	0.0005
0.64	0.0006
0.42	0.0007
0.26	0.0008
0.17	0.0009
0.15	0.001

Table A.11: Concrete Compression Damage for C30/37

Damage Parameter	Inelastic Strain
0	0
0	0.00018
0	0.00047
0	0.00088
0	0.00105
0.0139	0.00132
0.0555	0.00163
0.1247	0.00197
0.2215	0.00234
0.3458	0.00275
0.4247	0.00306
0.5021	0.00382
0.5767	0.00502
0.6473	0.00666
0.7124	0.00874
0.7711	0.01126
0.8221	0.01421

0.8645	0.0176
0.8976	0.02143
0.9207	0.02569
0.9333	0.03038
0.9895	0.10045

Table A.12: Concrete Tension Damage for C30/37

Damage Parameter	Cracking Strain
0	0
0.1514	0.00011
0.299	0.00023
0.439	0.00034
0.5678	0.00045
0.6821	0.00056
0.779	0.00067
0.856	0.00078
0.9111	0.00088
0.9427	0.00098
0.95	0.00108

Concrete C40/50

Table A.13: Density and Elastic for C40/50

Density:	2.5e-006
Elastic:	
Young's modulus	Poisson's ratio
35000	0.2

Table A.14: Concrete Damaged Plasticity for C40/50

Dilation angle	Eccentricity	fb0/fc0	K	Viscocity parameter
36	0.1	1.2	0.59	0

Table A.15: Concrete Compression Hardening for C40/50

Yield Stress	Inelastic Strain
19.2	0
32.6	0.00053
42.7	0.00105
47.6	0.00158
48	0.00175
47.3	0.00199
45.1	0.00223
41.1	0.00247

35.4	0.00271
27.5	0.00295
24.19	0.00317
20.98	0.00385
17.88	0.00496
14.95	0.00653
12.25	0.00854
9.83	0.011
7.72	0.0139
5.98	0.01726
4.63	0.02106
3.69	0.02531
3.2	0.03
0.4	0.1

Table A.16: Concrete Tension Stiffening for C40/50

Yield Stress	Cracking Strain
3.5	0
2.97	0.0001
2.45	0.0002
1.96	0.0003
1.51	0.0004
1.11	0.0005
0.77	0.0006
0.5	0.0007
0.31	0.0008
0.2	0.0009
0.18	0.001

Table A.17: Concrete Compression Damage for C40/50

Damage Parameter	Inelastic Strain
0	0
0	0.00014
0	0.00038
0	0.00076
0	0.00093
0.0148	0.00119
0.0613	0.00149
0.1428	0.00184
0.2635	0.00225
0.4279	0.00272
0.496	0.00303
0.563	0.00379
0.6275	0.005

0.6885	0.00665
0.7447	0.00874
0.7952	0.01127
0.8391	0.01423
0.8754	0.01764
0.9036	0.02147
0.9231	0.02575
0.9333	0.03046
0.9917	0.10054

Table A.18: Concrete Tension Damage for C40/50

Damage Parameter	Cracking Strain
0	0
0.1514	0.00011
0.299	0.00022
0.439	0.00033
0.5678	0.00044
0.6821	0.00055
0.779	0.00066
0.856	0.00076
0.9111	0.00087
0.9427	0.00097
0.95	0.00107

Concrete C50/60

Table A.19: Density and Elastic for C50/60

Density:	2.5e-006
Elastic:	
Young's modulus	Poisson's ratio
37000	0.2

Table A.20: Concrete Damaged Plasticity for C50/60

Dilation angle	Eccentricity	fb0/fc0	K	Viscocity parameter
36	0.1	1.2	0.59	0

Table A.21: Concrete Compression Hardening for C50/60

Yield Stress	Inelastic Strain
23.2	0
39	0.00055
51.1	0.00109
57.5	0.00164

58	0.00182
57.3	0.00203
55.1	0.00224
51	0.00245
44.8	0.00266
36.1	0.00287
31.8	0.00294
27.54	0.00326
23.43	0.00393
19.55	0.00504
15.97	0.00665
12.75	0.00883
9.95	0.01164
7.62	0.01511
5.81	0.0193
4.55	0.02425
3.87	0.03
0.4	0.1

Table A.22: Concrete Tension Stiffening for C50/60

Yield Stress	Cracking Strain
4.1	0
3.48	0.0001
2.87	0.0002
2.3	0.0003
1.77	0.0004
1.3	0.0005
0.91	0.0006
0.59	0.0007
0.36	0.0008
0.23	0.0009
0.21	0.001

Table A.23: Concrete Compression Damage for C50/60

Damage Parameter	Inelastic Strain
0	0
0	0.00012
0	0.00034
0	0.00071
0	0.00088
0.012	0.00111
0.0507	0.00138
0.1205	0.0017
0.2269	0.00208

0.377	0.00252
0.4517	0.00271
0.5252	0.00314
0.596	0.00392
0.6629	0.00513
0.7247	0.00685
0.7802	0.00912
0.8285	0.01199
0.8687	0.01553
0.8999	0.01977
0.9216	0.02475
0.9333	0.03052
0.9931	0.10062

Table A.24: Concrete Tension Damage for C50/60

Damage Parameter	Cracking Strain
0	0
0.1514	0.00012
0.299	0.00023
0.439	0.00035
0.5678	0.00046
0.6821	0.00058
0.779	0.00069
0.856	0.00079
0.9111	0.0009
0.9427	0.001
0.95	0.00111

A.2 Bolt

Bolt 4.6

Table A.25: Density and Elastic for bolt 4.6

Density:	7.8e-006
Elastic:	
Young's modulus	Poisson's ratio
210000	0.3

Table A.26: Plastic for bolt 4.6

Yield Stress	Plastic strain
325.7	0

370.4	0.0015
391.5	0.0054
422.2	0.0341
451	0.0686
465.2	0.0985
475.3	0.1199
497	0.1646
523.2	0.216
546.5	0.2596
582.8	0.3239
636	0.4113
639.2	0.4162

Table A.27: Ductile Damage for bolt 4.6

Fracture Strain	Stress Triaxiality	Strain Rate
0.7278	-1	1
0.2678	-0.33333	1
0.1624	0	1
0.1398	0.1	1
0.1203	0.2	1
0.0985	0.33333	1
0.0767	0.5	1
0.0362	1	1
0.0081	2	1

Table A.28: Ductile Damage Evolution for bolt 4.6

Damage Variable	Displacement
0	0
0.008	0.0492
0.063	0.1521
0.155	0.2702
0.238	0.3704
0.354	0.5185
0.492	0.7194
1	0.7308

Damage evolution:

Type: Displacement

Softening: Tabular

Degradation: Multiplicative

Table A.29: Shear Damage for bolt 4.6

Fracture strain	Shear Stress Ratio	Strain Rate
0.08	1.732	0.1

Table A.30: Shear Damage Evolution for bolt 4.6

Displacement at Failure	Exponential Low Parameter
0.3	0.7

Damage evolution:

Type: Displacement

Softening: Exponential

Degradation: Multiplicative

Bolt 8.8

Table A.31: Density and Elastic for bolt 8.8

Density:	7.8e-006
Elastic:	
Young's modulus	Poisson's ratio
210000	0.3

Table A.32: Plastic for bolt 8.8

Yield Stress	Plastic strain
522.3	0
555.6	0.0004
577.7	0.0013
600.1	0.0028
605.1	0.0071
621.3	0.0085
631.1	0.0099
701.6	0.0217
772.1	0.037
815	0.0524
840.8	0.0684
850.9	0.0782

860.8	0.0897
877.5	0.109
899.8	0.134
927.5	0.1643
954.9	0.1934
977.6	0.217
1016.2	0.2556
1048.4	0.2868
1103.5	0.3381
1152.9	0.3819
1194.2	0.4171
1237.6	0.4527
1255.1	0.4668
1349.2	0.5391
1462.2	0.6195
1597.7	0.7081
1760.3	0.8051

Table A.33: Ductile Damage for bolt 8.8

Fracture Strain	Stress Triaxiality	Strain Rate
0.576346376	-1	0.001
0.210968499	-0.33	0.001
0.128600259	0	0.001
0.110687269	0.1	0.001
0.095269415	0.2	0.001
0.078390977	0.33	0.001
0.060746461	0.5	0.001
0.028694596	1	0.001
0.00640263	2	0.001

Table A.34: Ductile Damage Evolution for bolt 8.8

Damage Variable	Displacement
0	0
0.003868732	0.010939512
0.018244087	0.029193182
0.052035813	0.05294263
0.101076212	0.081689973
0.150682639	0.109233105
0.192597112	0.131578862
0.265688945	0.168214796
0.330250189	0.197788987
0.415201923	0.246409513
0.499208493	0.287943624
0.564363408	0.32130321
0.63088974	0.355096151

1	0.36844966

Damage evolution:

Type: Displacement

Softening: Tabular

Degradation: Multiplicative

Table A.35: Shear Damage for bolt 8.8

Fracture strain	Shear Stress Ratio	Strain Rate
0.08	1.732	0.1

Table A.36: Shear Damage Evolution for bolt 8.8

Displacement at Failure	Exponential Low Parameter
0.3	0.7

Damage evolution:

Type: Displacement

Softening: Exponential

Degradation: Multiplicative

Bolt 10.9

Table A.37: Density and Elastic for bolt 10.9

Density:	7.8e-006
Elastic:	
Young's modulus	Poisson's ratio
210000	0.3

Table A.38: Plastic for bolt 10.9

Yield Stress	Plastic strain
830.7	0
854.8	0.0029
876.4	0.0071
900.7	0.016
916.7	0.0237
924.5	0.0296

932	0.0378
971.2	0.0789
1017.7	0.1257
1076.3	0.1816
1169.7	0.2649
1262.2	0.341
1314.6	0.3817
1358.7	0.4147
1372.1	0.4245
1467.8	0.4919
1582.7	0.5673
1720.5	0.6508
1885.9	0.7426

Table A.39: Ductile Damage for bolt 10.9

Fracture Strain	Stress Triaxiality	Strain Rate
0.218716061	-1	0.001
0.080059841	-0.33	0.001
0.04880215	0	0.001
0.042004399	0.1	0.001
0.036153522	0.2	0.001
0.029748371	0.33	0.001
0.023052503	0.5	0.001
0.010889231	1	0.001
0.002429716	2	0.001

Table A.40: Ductile Damage Evolution for bolt 10.9

Damage Variable	Displacement
0	0
0.012701875	0.007735262
0.113651705	0.046718408
0.224367849	0.09106526
0.346109048	0.144145557
0.484544727	0.223025848
0.598475276	0.295203328
0.663526631	0.333760516
0.716722007	0.365063056
1	0.374363878

Damage evolution:

Type: Displacement

Softening: Tabular

Degradation: Multiplicative

Table A.41: Shear Damage for bolt 10.9

Fracture strain	Shear Stress Ratio	Strain Rate
0.08	1.732	0.1

Table A.42: Shear Damage Evolution for bolt 10.9

Displacement at Failure	Exponential Low Parameter
0.3	0.7

Damage evolution:

Type: Displacement

Softening: Exponential

Degradation: Multiplicative

A.3 Resin and reinforced resin

Resin

Table A.43: Density and Elastic for resin

Density:	1.8E-006
Elastic:	
Young's modulus	Poisson's ratio
5640	0.3

Table A.44: Plastic for resin

Yield Stress	Plastic Strain
500	0

Reinforced resin

Table A.45: Density and Elastic for reinforced resin

Density:	1.8E-006
Elastic:	
Young's modulus	Poisson's ratio
15200	0.22

Table A.46: Drucker Prager for reinforced resin

Angle of Friction	FlowStress Ratio	Dilation Angle
52.04	1	0

Table A.47: Drucker Prager Hardening for reinforced resin

Yield Stress	Abs Plastic Strain
124	0
123.7	0.00634
50.1	0.032
12.96	0.04
4.09	0.045